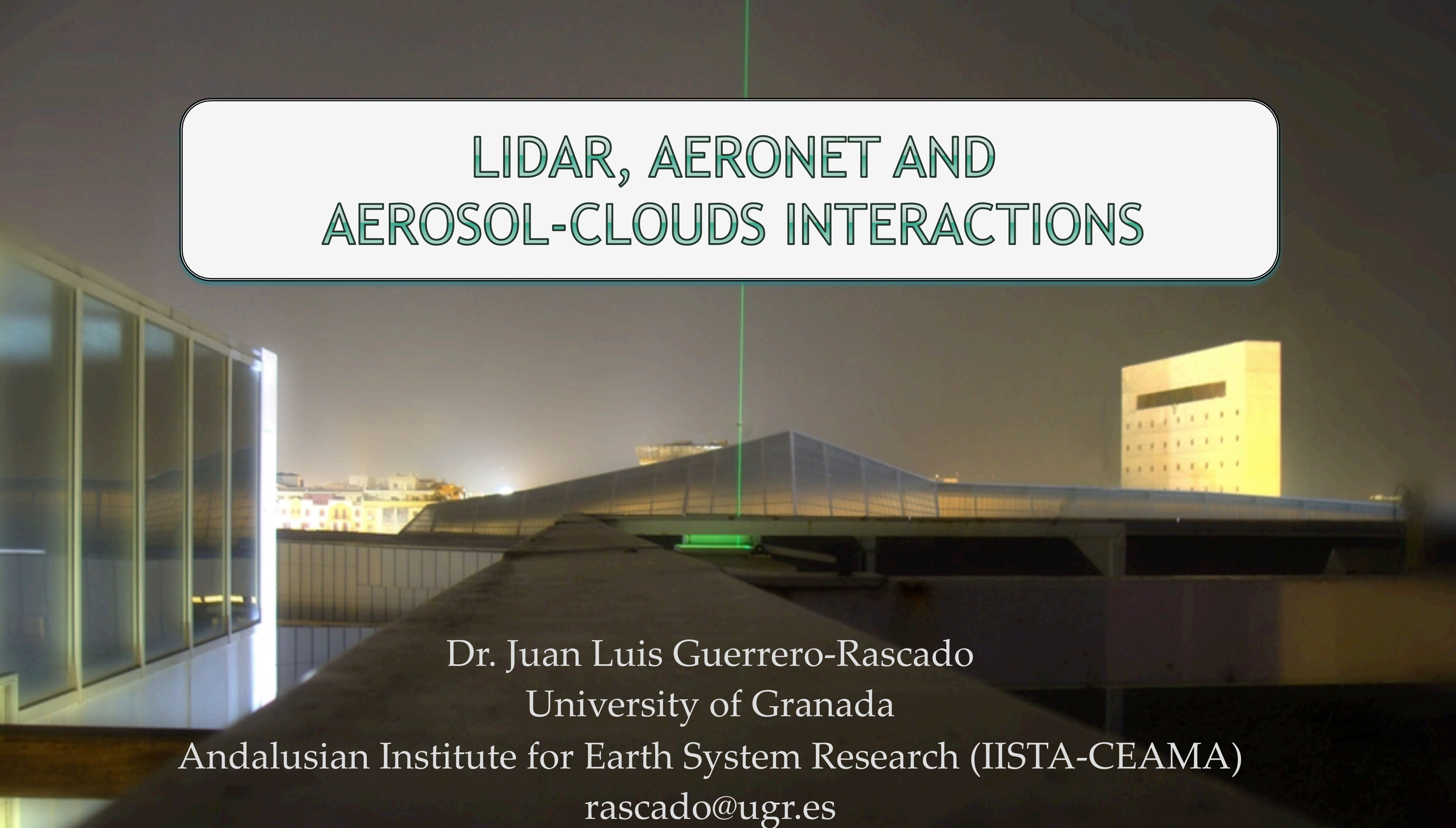

LIDAR, AERONET AND AEROSOL-CLOUDS INTERACTIONS

Dr. Juan Luis Guerrero-Rascado
University of Granada
Andalusian Institute for Earth System Research (IISTA-CEAMA)
rascado@ugr.es

IISTA
Instituto Interuniversitario de Investigación del Sistema Tierra en Andalucía

USP

IFUSP
Instituto de Física da USP

ASCENDING OUTLINE

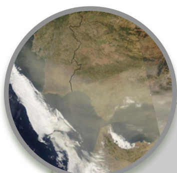

Introduction

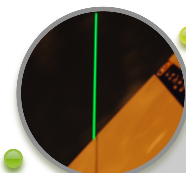

Fundamentals

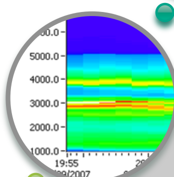

Geometrical properties

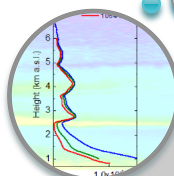

Optical properties

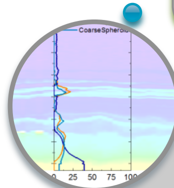

Microphysical properties

Instrumental tests

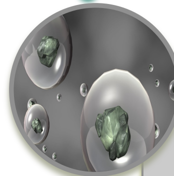

Aerosol-cloud interactions

ASCENDING OUTLINE

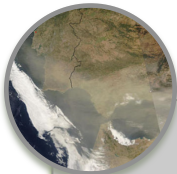

- Introduction

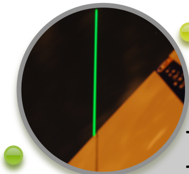

- Fundamentals

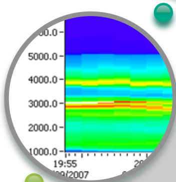

- Geometrical properties

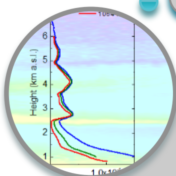

- Optical properties

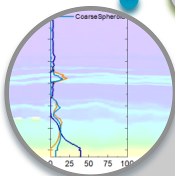

- Microphysical properties

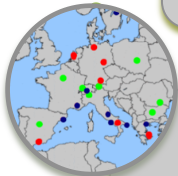

- Instrumental tests

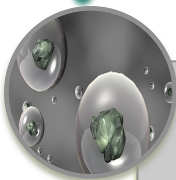

- Aerosol-cloud interactions

INTRODUCTION

WHAT IS REMOTE SENSING?

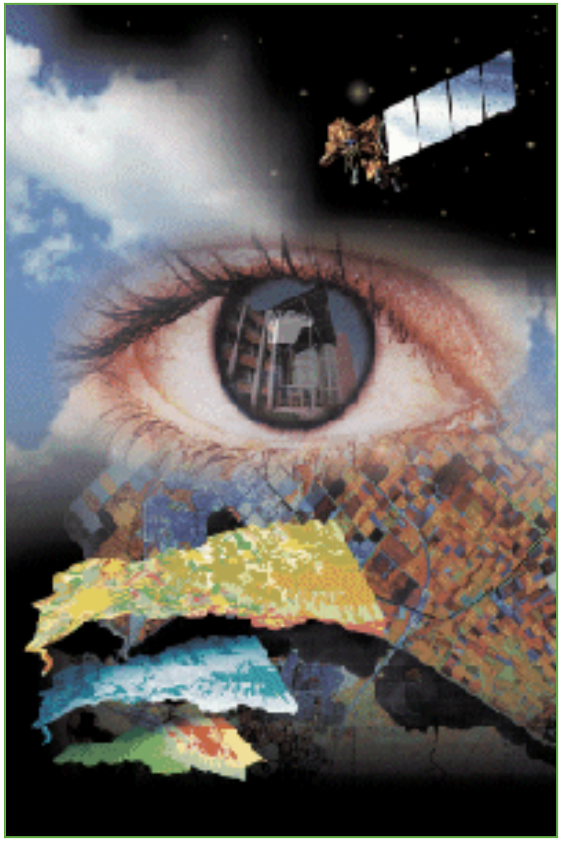

Process of obtaining information about properties of a target without contact.

This information is propagated by means of electromagnetic radiation interacting with the target.

INTRODUCTION

Passive remote sensing

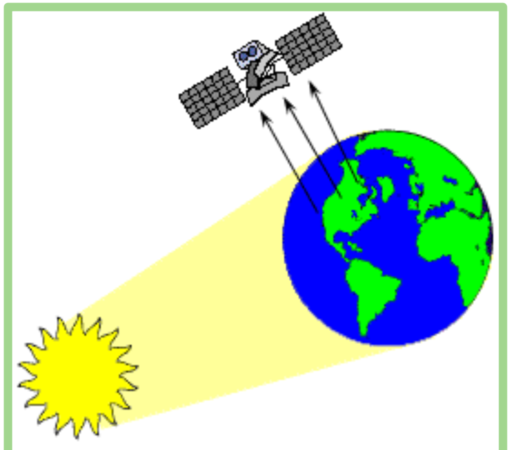

Based on "uncontroled illumination":

- Sun
- terrestrial emission

Passive methods:

- extinction
- scattering
- longwave emission

Active remote sensing

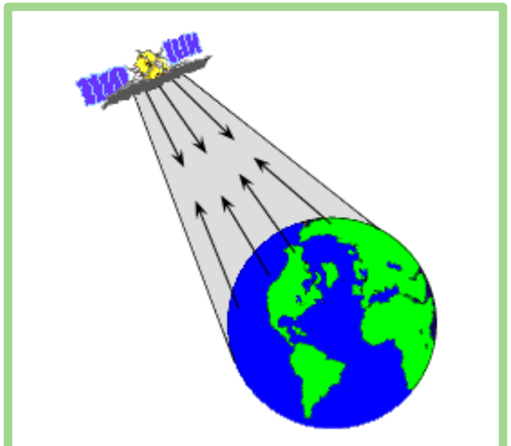

Based on "controled illumination" and measurement of backscattering

Active methods:

- lidar
- radar

Lidar (light detection and ranging) is an active remote sensing technology that measures distance by illuminating a target with a laser and analyzing the reflected light

INTRODUCTION

There are a wide variety of fields of applications for lidar:

* Geology
* Archaeology
* Biology (vegetation)
* Architecture (cultural heritage)
* Astronomy
* Atmosphere

INTRODUCTION

Geology: In geophysics and tectonics, a combination of aircraft-based lidar and GPS has evolved into an important tool for detecting faults and for measuring uplift. The output of the two technologies can produce extremely accurate elevation models for terrain and enables surveys to be taken of the coastline. It is also used extensively to monitor glaciers and perform coastal change analysis

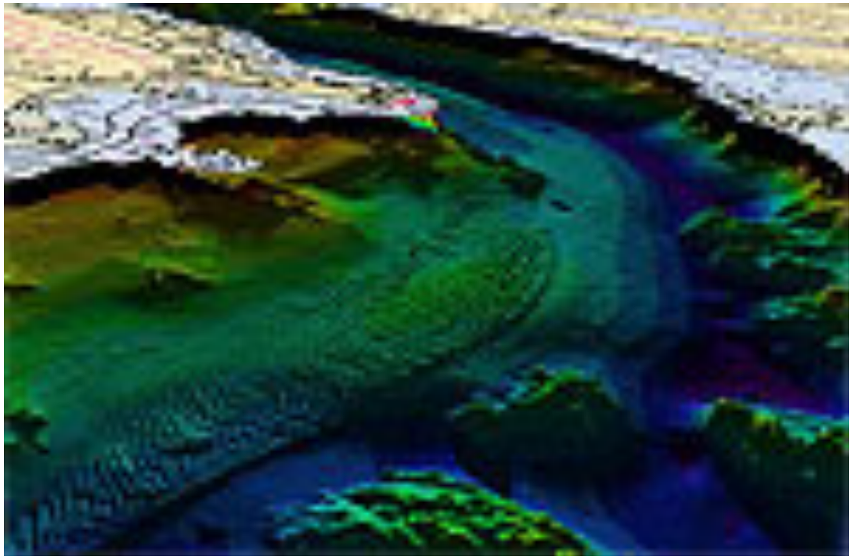

INTRODUCTION

Archaeology: aiding in the planning of field campaigns, mapping features beneath forest canopy, and providing an overview of broad, continuous features that may be indistinguishable on the ground, creating high-resolution digital elevation models (DEMs) of archaeological sites that can reveal micro-topography that are otherwise hidden by vegetation

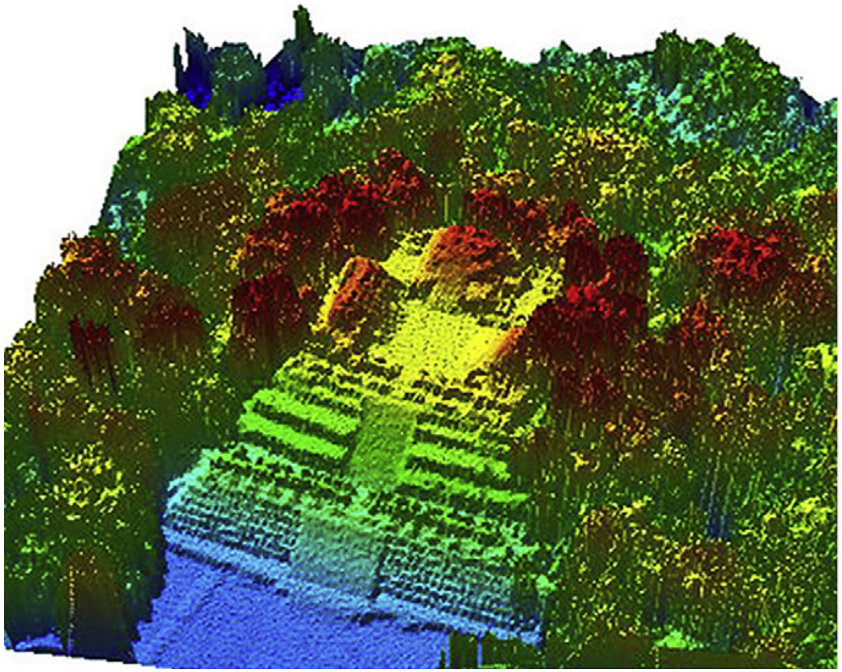

Image taken from: Chase et al., 2011, Journal of Archeological Science, 38, 387-398

Maya Site of Caracol (Belize)

INTRODUCTION

Biology (vegetation): lidar has also found many applications in forestry. Canopy height and biomass measurements can be all be studied using airborne lidar systems. Tree height strongly correlated to other properties (as woody biomass, age, etc)

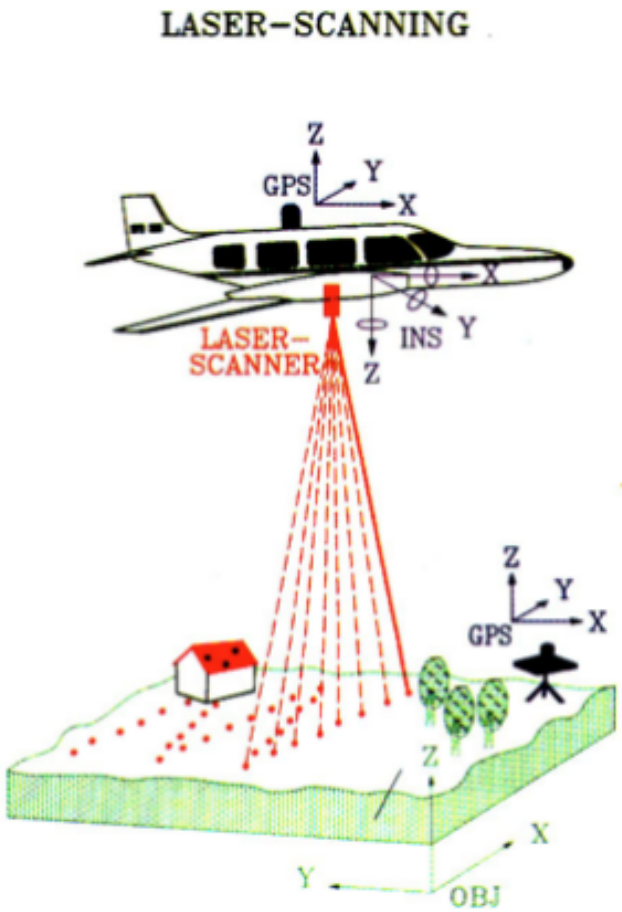

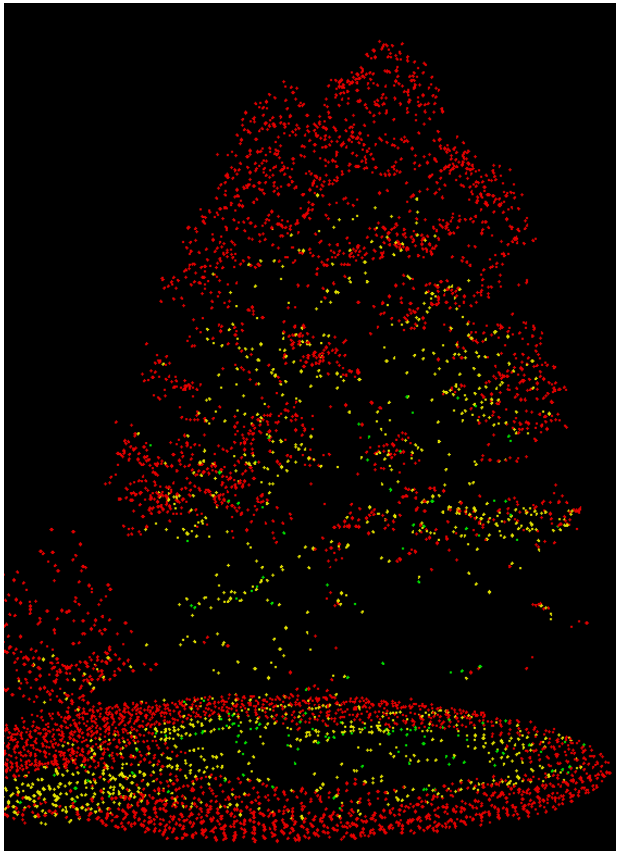

INTRODUCTION

Architecture (cultural heritage): fluorescence lidar technique has been applied to the investigation of the cultural heritage only quite recently: remote diagnostics of monuments, providing helpful information for the assessment of the conservation status of monuments in the outdoor and for the characterization of the materials employed in their construction. Main applications include the detection and characterization of different stones, mortars and other construction materials, of protective treatments, of biodeteriogens and the study of the effects of biocide treatments.

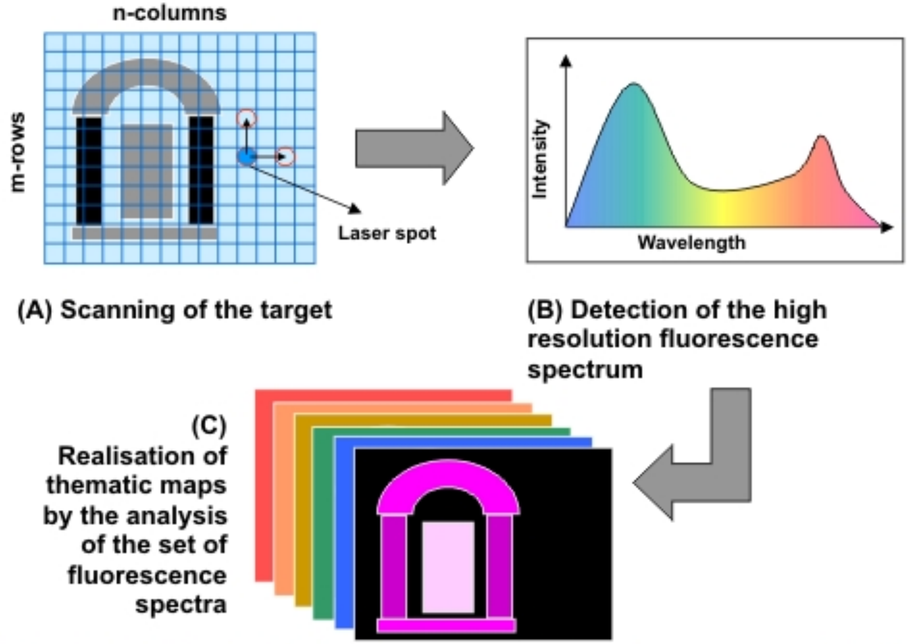

Figure 3.6.3: Basic principles of lidar hyper-spectral imaging on monuments [17].

INTRODUCTION

- Aerosol particles: liquid or solid particles suspended in a gaseous medium (several types)
- Atmospheric aerosols play an important role in the Earth's climate system:

1. they interact with solar and thermal radiation, modulating the Earth radiation budget
2. they modify clouds microphysical properties by acting as cloud condensation nuclei and ice forming nuclei




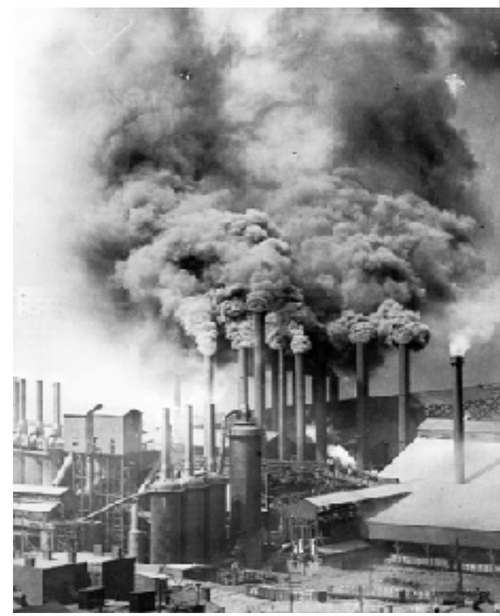

INTRODUCTION

- Aerosol particles: cooling/warming effect
  depending on vertical distribution and types (among other factors)

- Classification:
  - ✓ Mineral particles
  - ✓ Marine particles
  - ✓ Carbon particles
  - ✓ Sulfates, nitrates and organic compounds

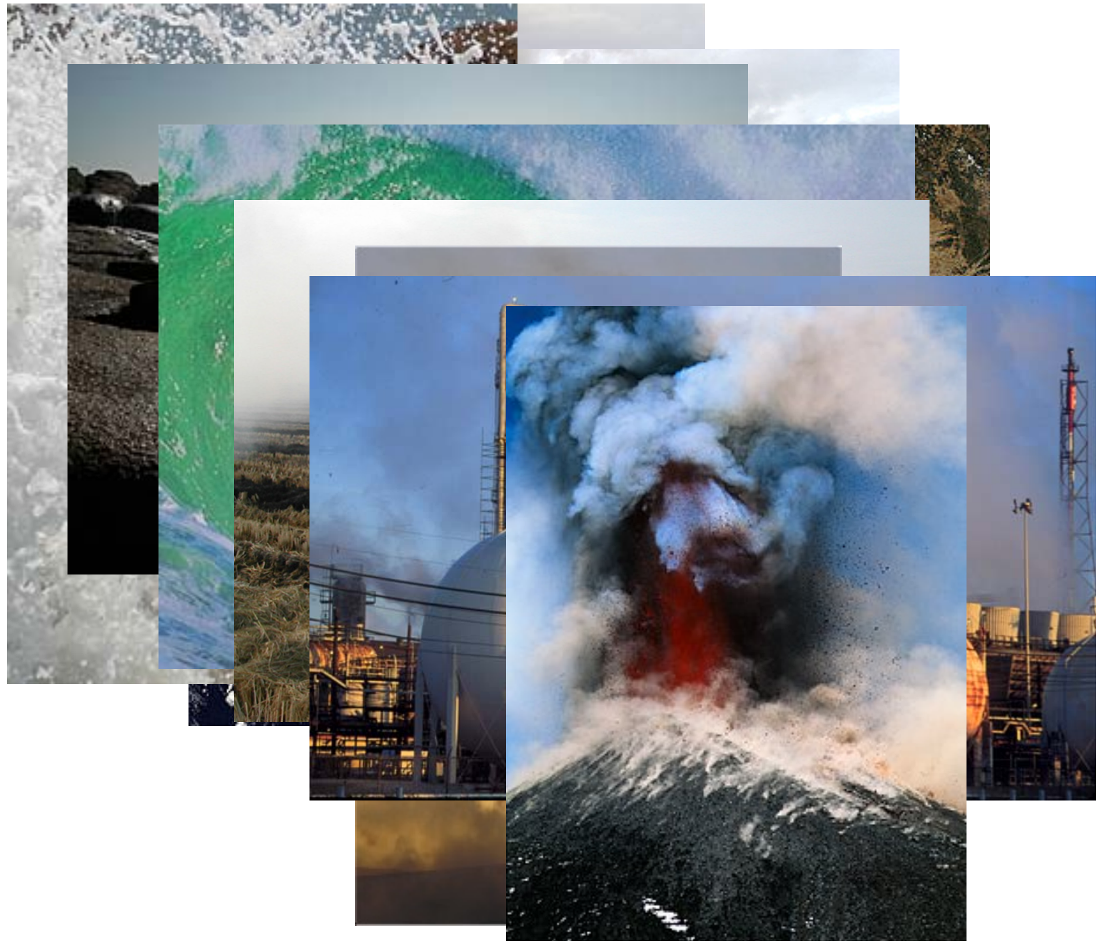

Soil particles or desert (particles) are created by wind erosion of soil and transported from local or remote sources

Anthropogenic origin (pollution) and natural origin (vulcanism)

origin and natural (biomass burning)

INTRODUCTION

Radiative forcing by components

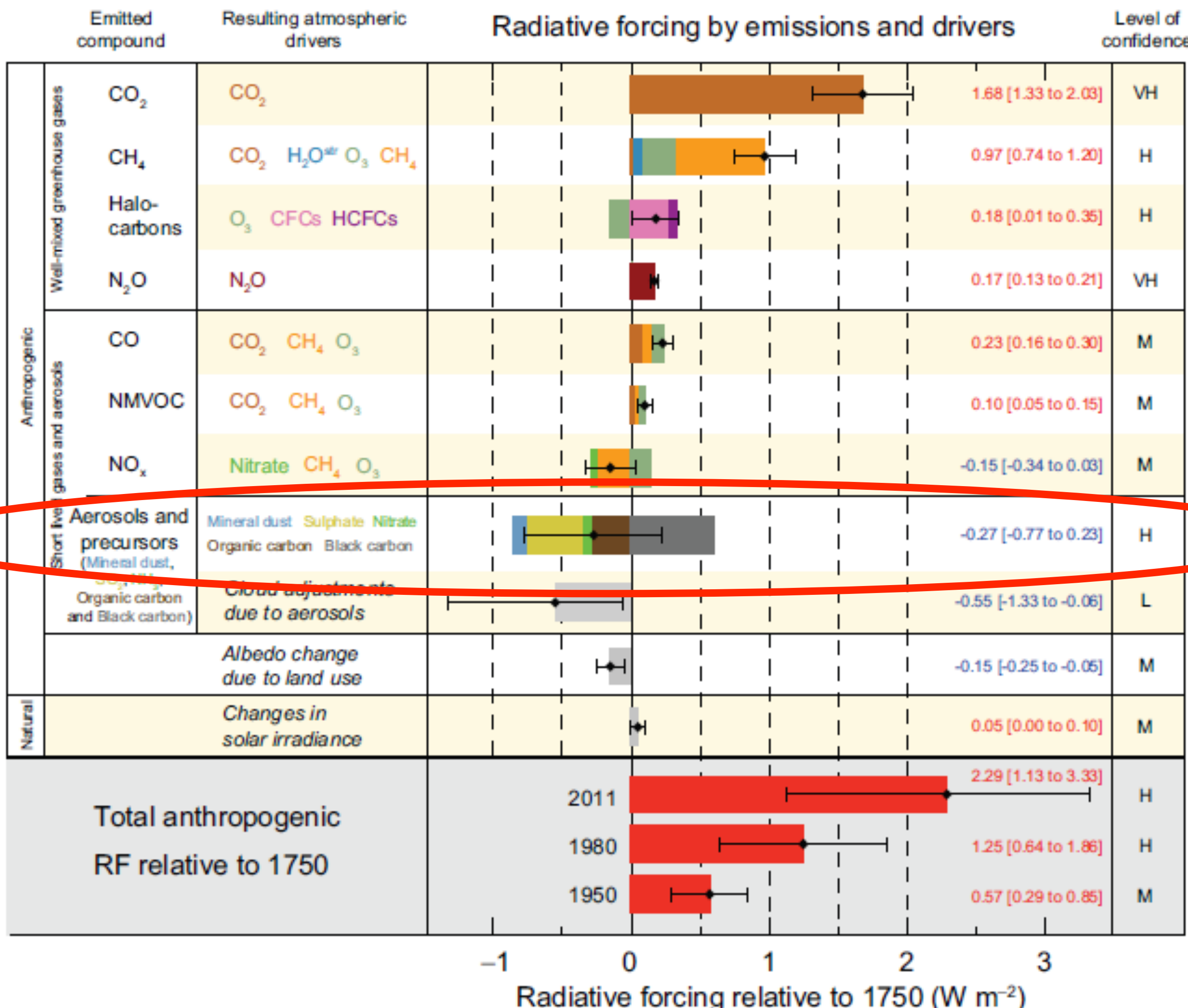

IPCC (2013)

ASCENDING OUTLINE

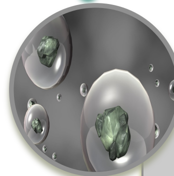

Aerosol-cloud interactions

Instrumental tests

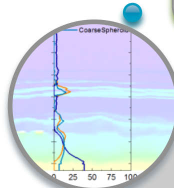

Microphysical properties

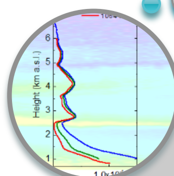

Optical properties

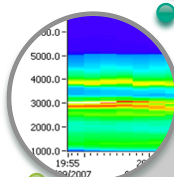

Geometrical properties

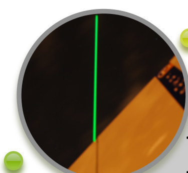

Fundamentals

Introduction

LIDAR TECHNIQUE

Lidar: Light detection and ranging

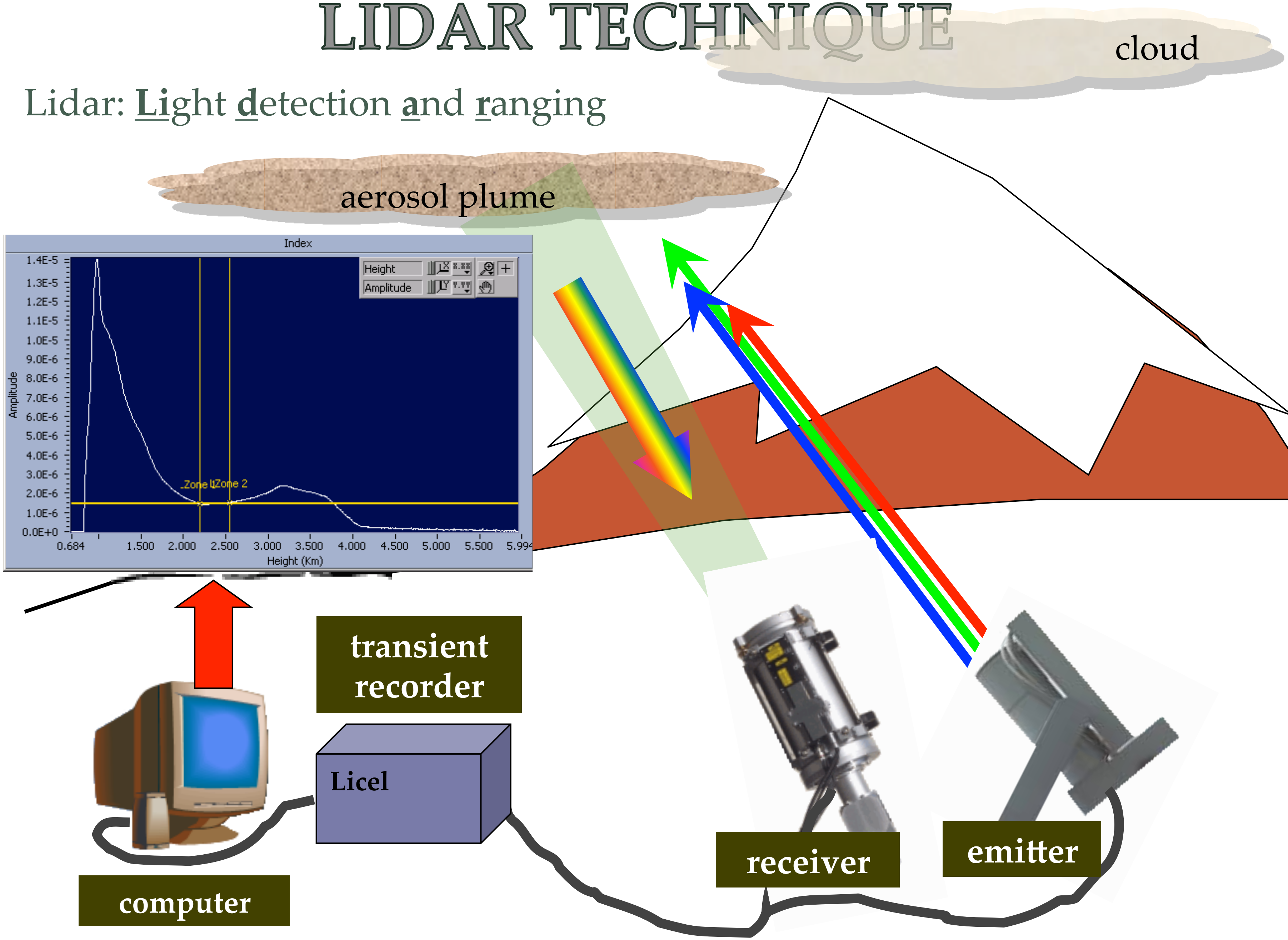

IISTA
USP
IFUSP

LIDAR TECHNIQUE

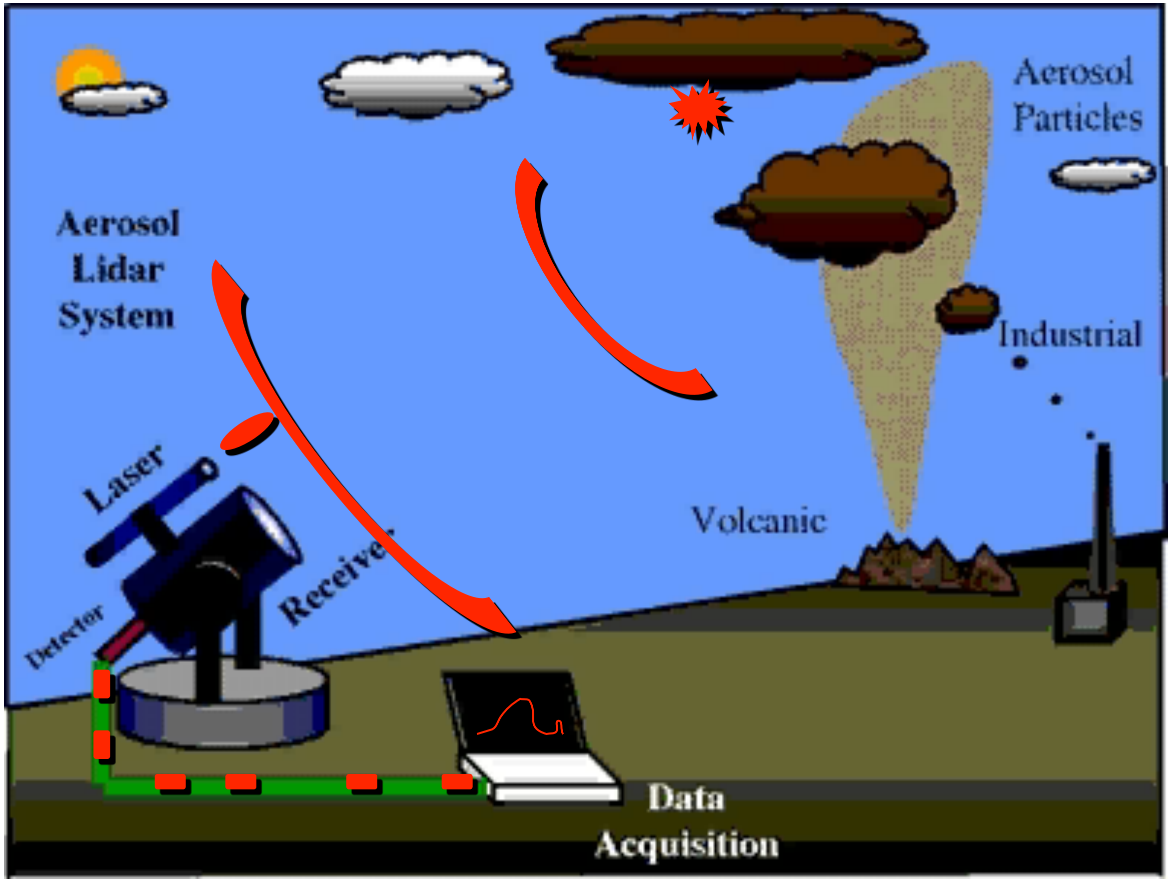

The key of this technique is the use of **pulsed lasers**, which allow for obtaining range-resolved information from the delay between emitted and received pulses

RANGING (BASED ON TIMING)

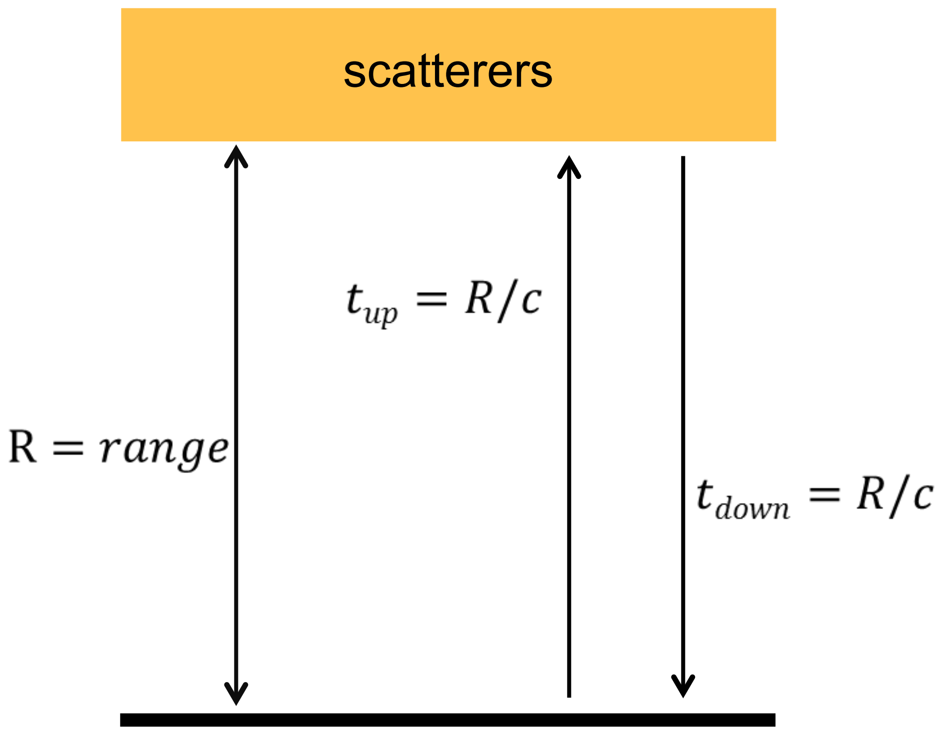

$$t_{total} = t_{up} + t_{down} = 2\,R/c$$

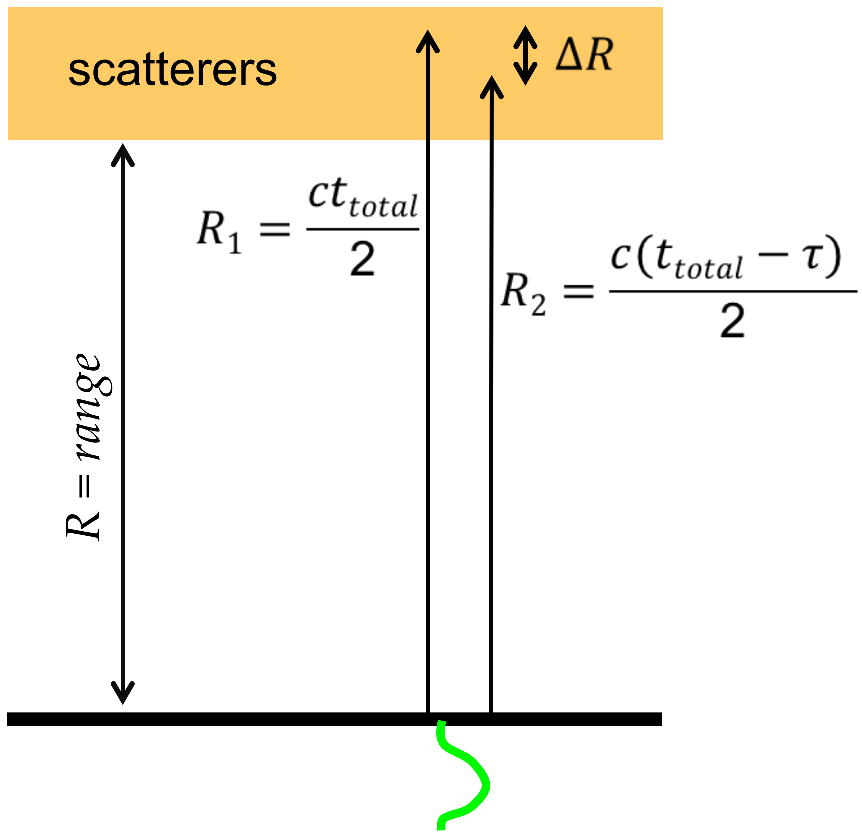

“temporal pulse length” τ

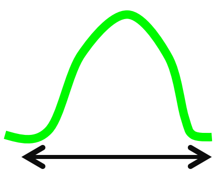

$$\Delta R = R_1 - R_2 = \frac{c\tau}{2}$$

“effective (spatial) pulse length”

RANGING (BASED ON TIMING)

$$\Delta R = R_1 - R_2 = \frac{c\tau}{2}$$

"effective (spatial) pulse length"

(**potential** spatial lidar resolution)

Spatial resolution example:

Nd:YAG Laser (1064 nm)
Q-switch pulsed: τ~ 10 ns

$$\Delta R \approx 1.5 \text{ m}$$

In practice there are additional limitations like the sampling frequency of the acquisition system …

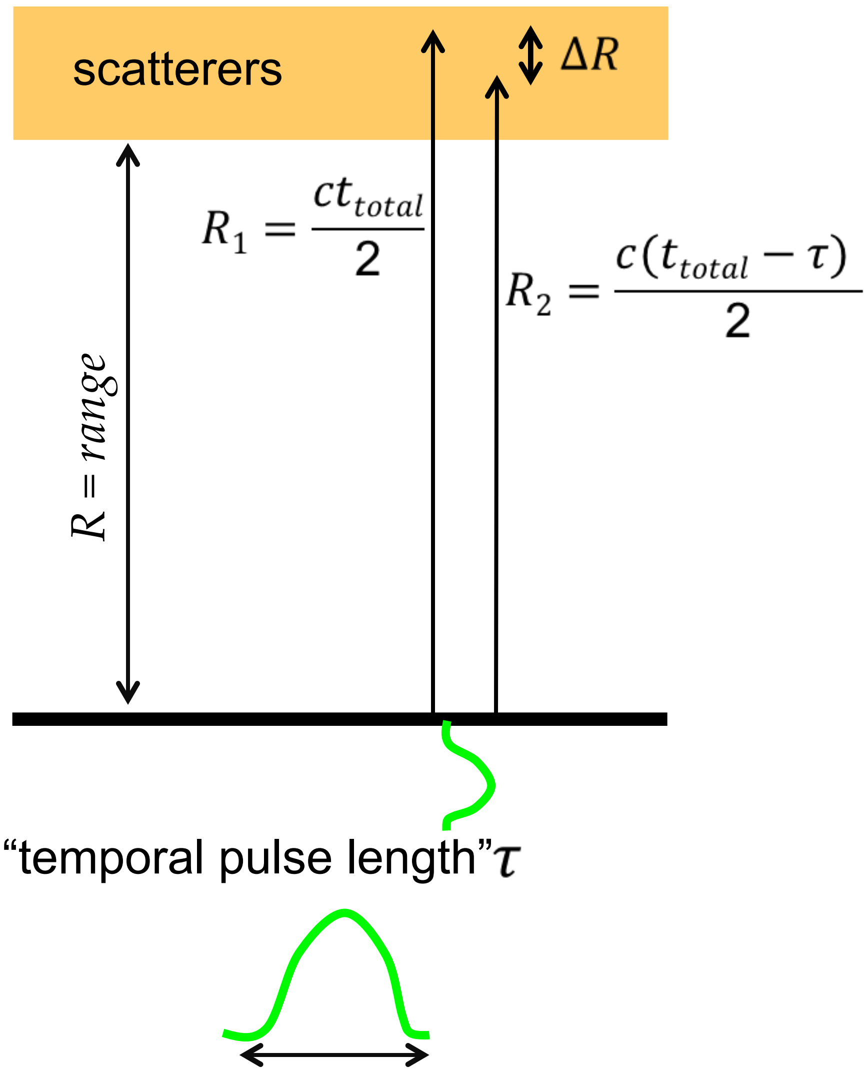

LIDAR SETUP

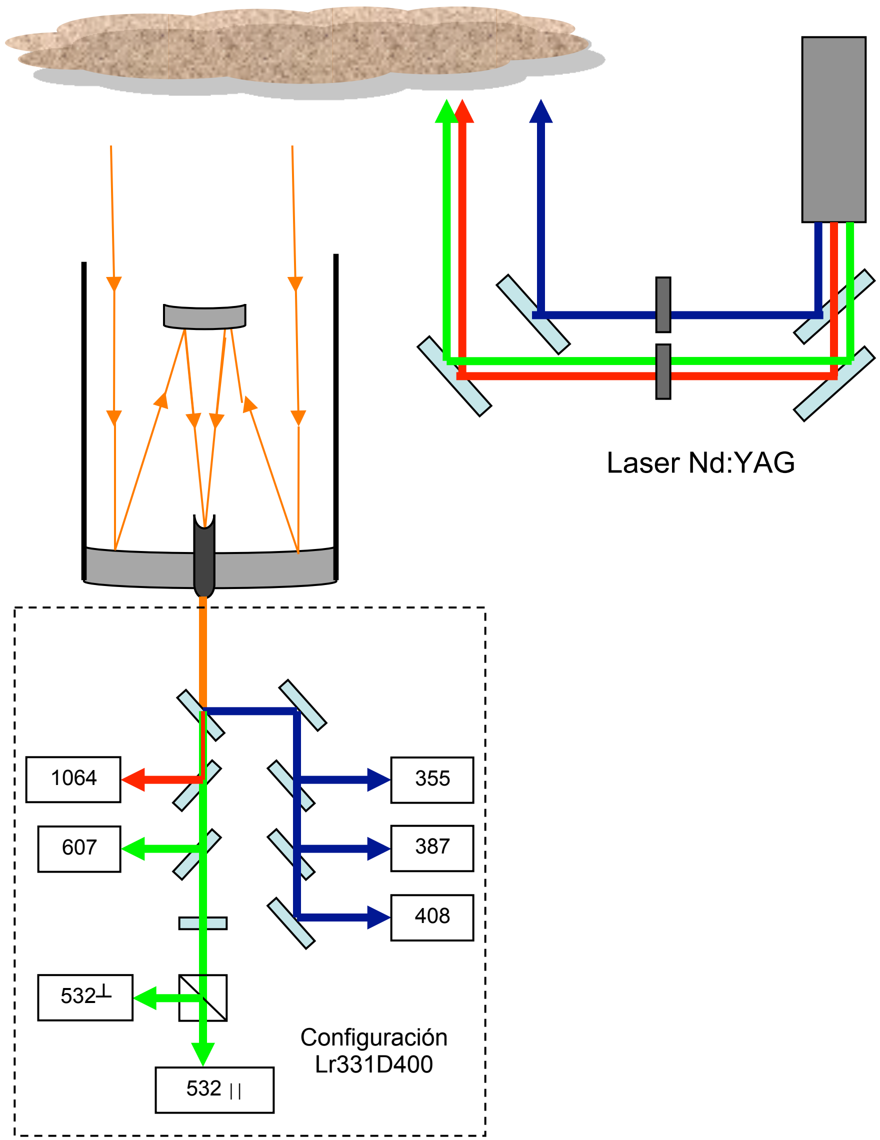

- Transmitter system
- Receiver system

LIDAR SETUP: LASER SOURCE

- 1960's: nitrogen laser (337 nm) and ruby laser (694nm→347nm): relatively low average power, limited to 2 km
- 1980's: pulsed lasers with high average power as UV excimer laser (XeCl at 308nm and XeF at 351 nm) and Nd:YAG laser
- currently Nd:YAG (Neodymiun-doped Yttrium Aluminum Garnet):
  1064 nm → 532 nm → 355 nm
  repetition frequency : 1-50 Hz
  energy/pulse: 100 mJ to 1.5 J (at 1064 nm)

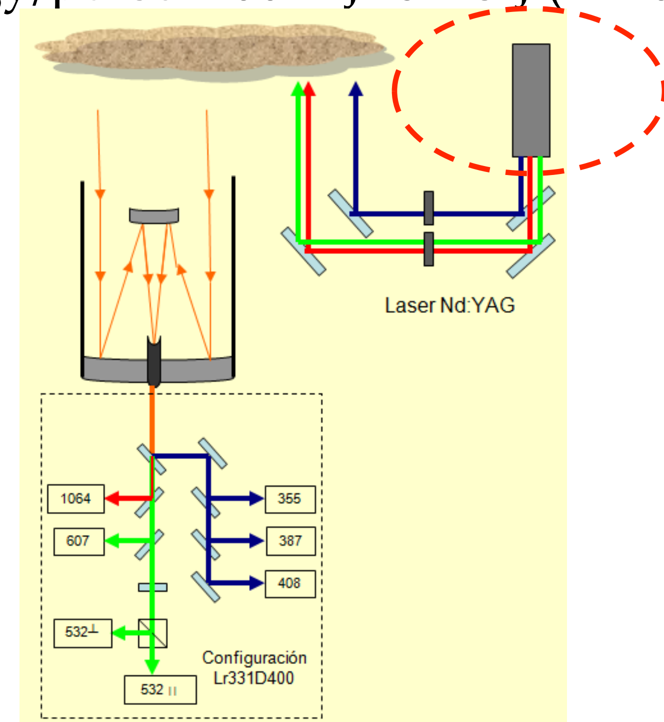

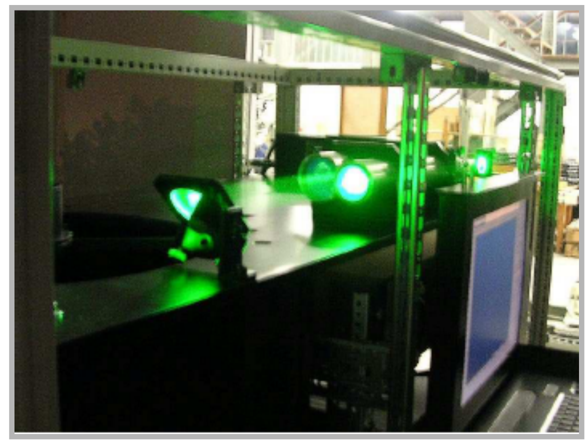

LIDAR SETUP: TRANSMITTER OPTICS

- Mirrors to transmit the laser beam (high reflectivity / high transmissivity)
- Beam expander made of lenses (anti-reflection coated) allows for:
  - a beam expansion by a factor ~ x4 - x10
  - reducing background light
  - increasing SNR
  - reducing divergence (~1mrad)

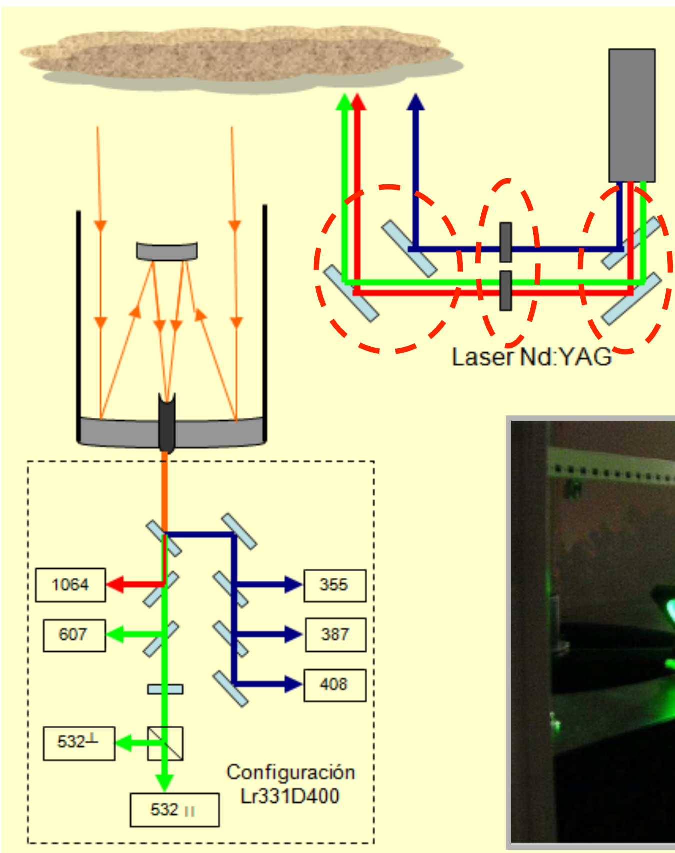

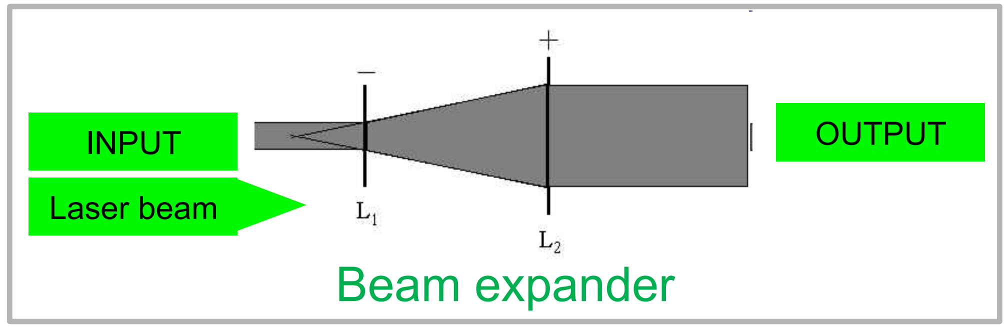

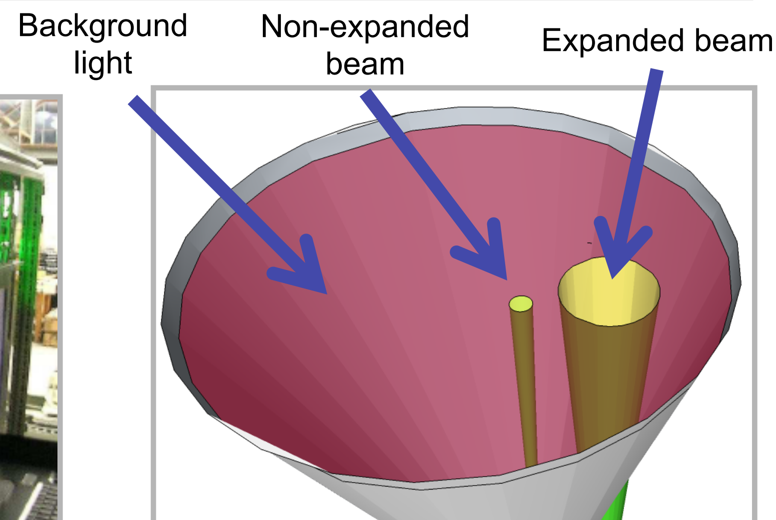

LIDAR SETUP: RECEIVER OPTICS

- $\varphi_{primary}$: 30 cm – 1 m and $\varphi_{secondary}$: ~ 1cm
- compromise between a small FOV necessary for high background supression and a large FOV for a sufficient signal intensity from short distances (FOV a factor of ~2-10 larger than the laser divergence)
- receiver optics behind telescope must be optimized for high transmission of the Raman signals
- dichroic beam splitters: reflect light of a certain λ an transmit others
- interference filters: typically FWHM <0.5 nm, suppresion factor 10^8-10^{10}

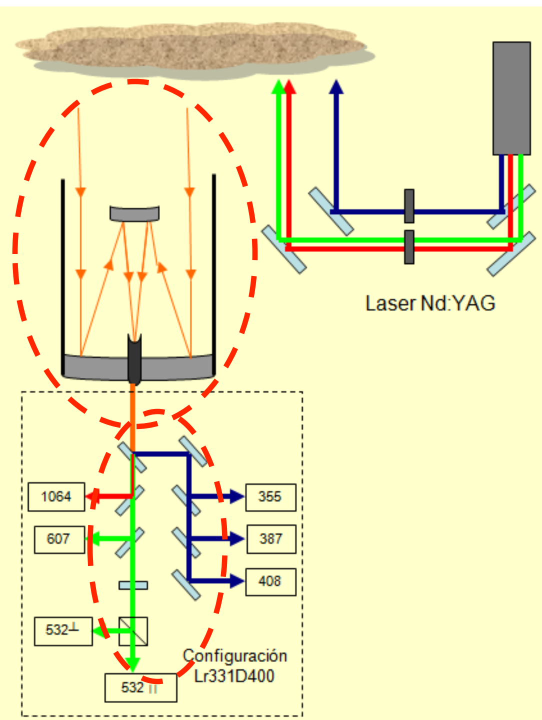

Telescopes

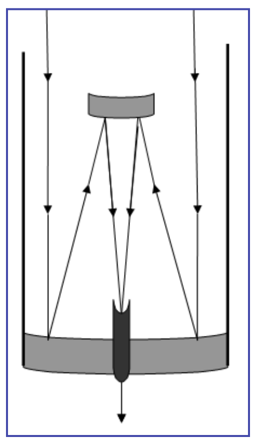

Cassegranian

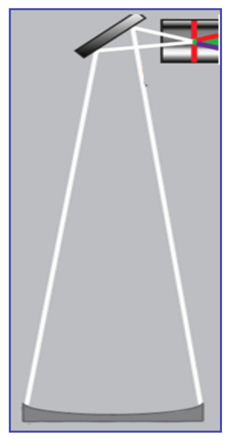

Newtonian

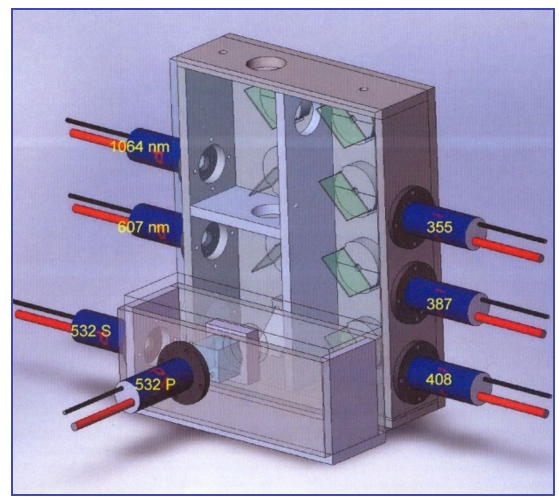

LIDAR SETUP: DETECTORS AND DATA ACQUISITION

- photomultipliers in An and PC mode are typically used (PMTs)
- high quantum efficiency (in UV ~ 25%) and low noise
- detector outputs can be preamplified before registration
- time resolution (or window length) is ~ 100 ns, (7.5 – 15 m)
- averaging time for the raw signals is 10- 60 s
- signals are usually further averaged in time and space during data evaluation

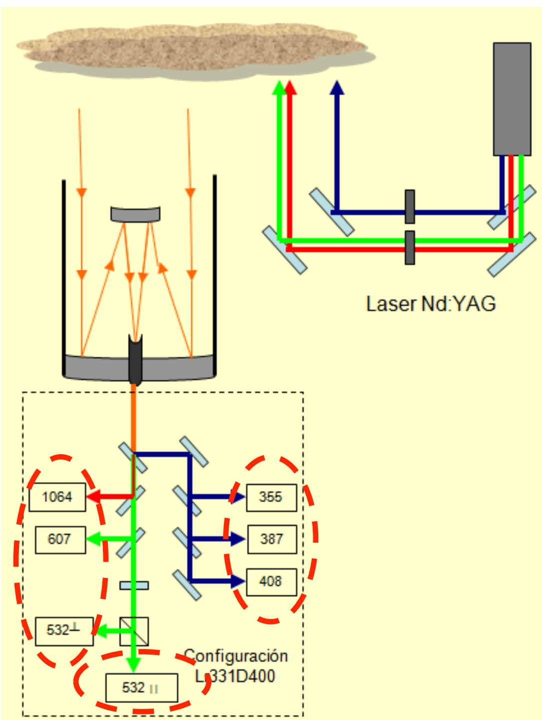

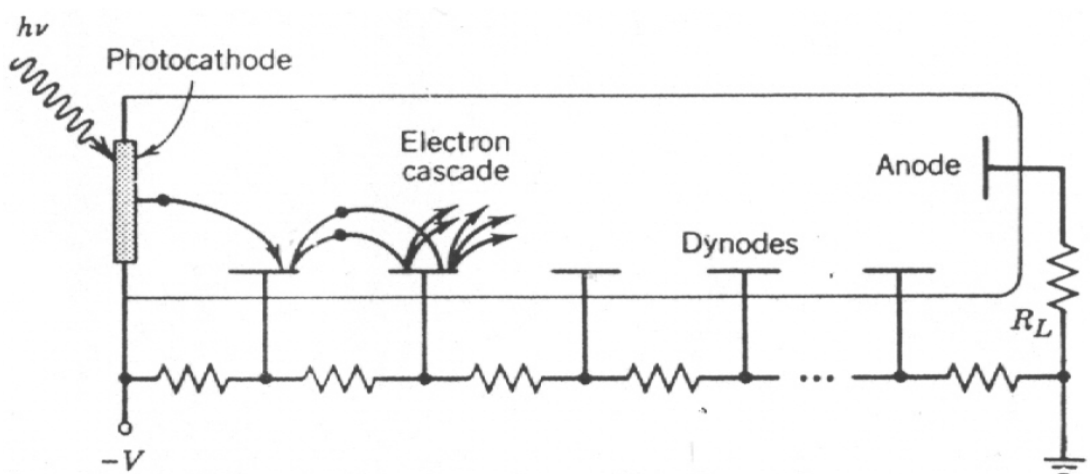

ELASTIC LIDAR FOR AEROSOLS

Generally consists of a non-tunable high-power pulsed laser and intensity of the received signal is measured

A narrow beam is transmitted into the atmosphere and backscattered by the atmosphere to a receiver telescope and detector

The nature of the backscattering is determined by the properties of the volume of the atmosphere that contains the Rayleigh (molecules) and Mie (particles) scatterers

The combination of the short laser pulse (~10 ns) and the small beam divergence (~10^{-3} to 10^{-4} radians) results in volumes of a few cubic meters at ranges of tens of km

The primary properties measured are the intensity and polarization of the signal, and these are used to retrieve particle properties

LIDAR EQUATION

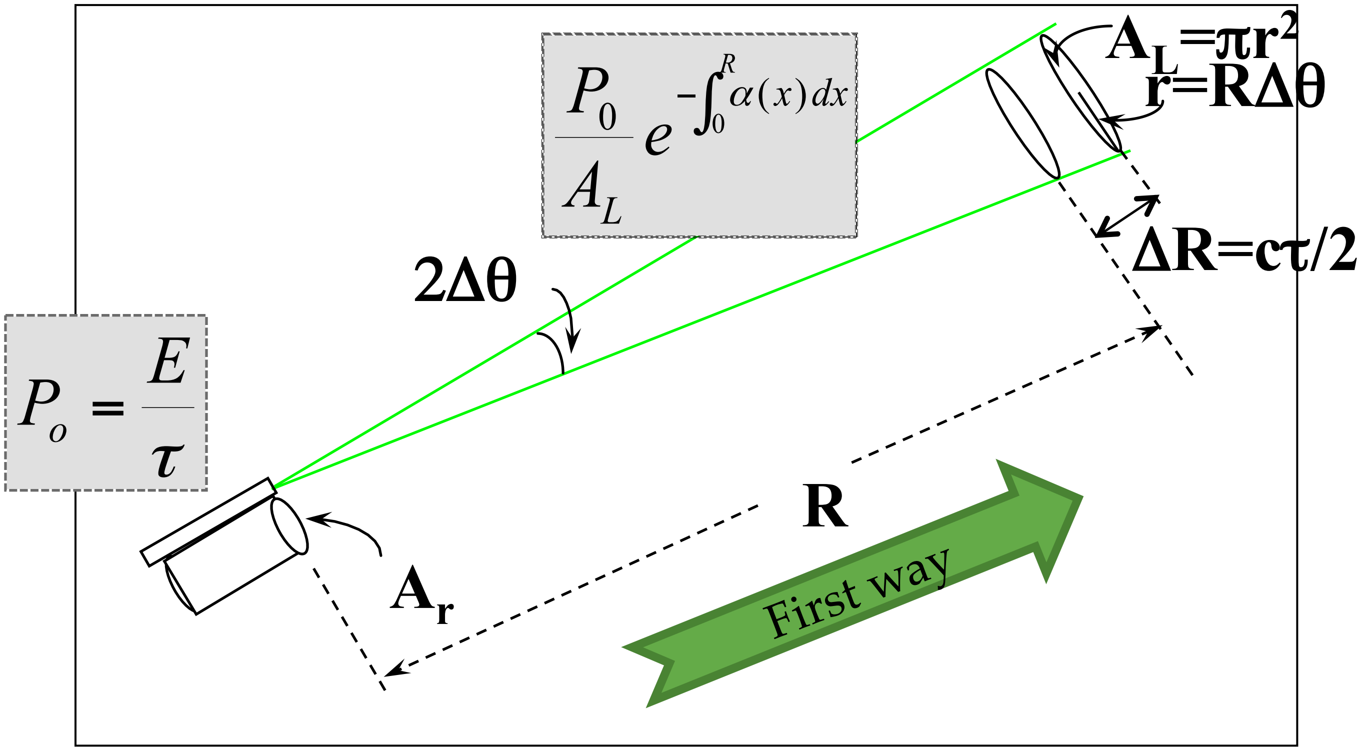

P_o average power of single laser pulse, τ temporal pulse length
$E_o=P_o\tau$ pulse energy
The propagation through distance R implies an attenuation $e^{-\int_0^R \alpha(x)dx}$
and $(P_o/A_L)e^{-\int_0^R \alpha(x)dx}$ represent the power per unit area that illuminates a volume of atmosphere at distance R

LIDAR EQUATION

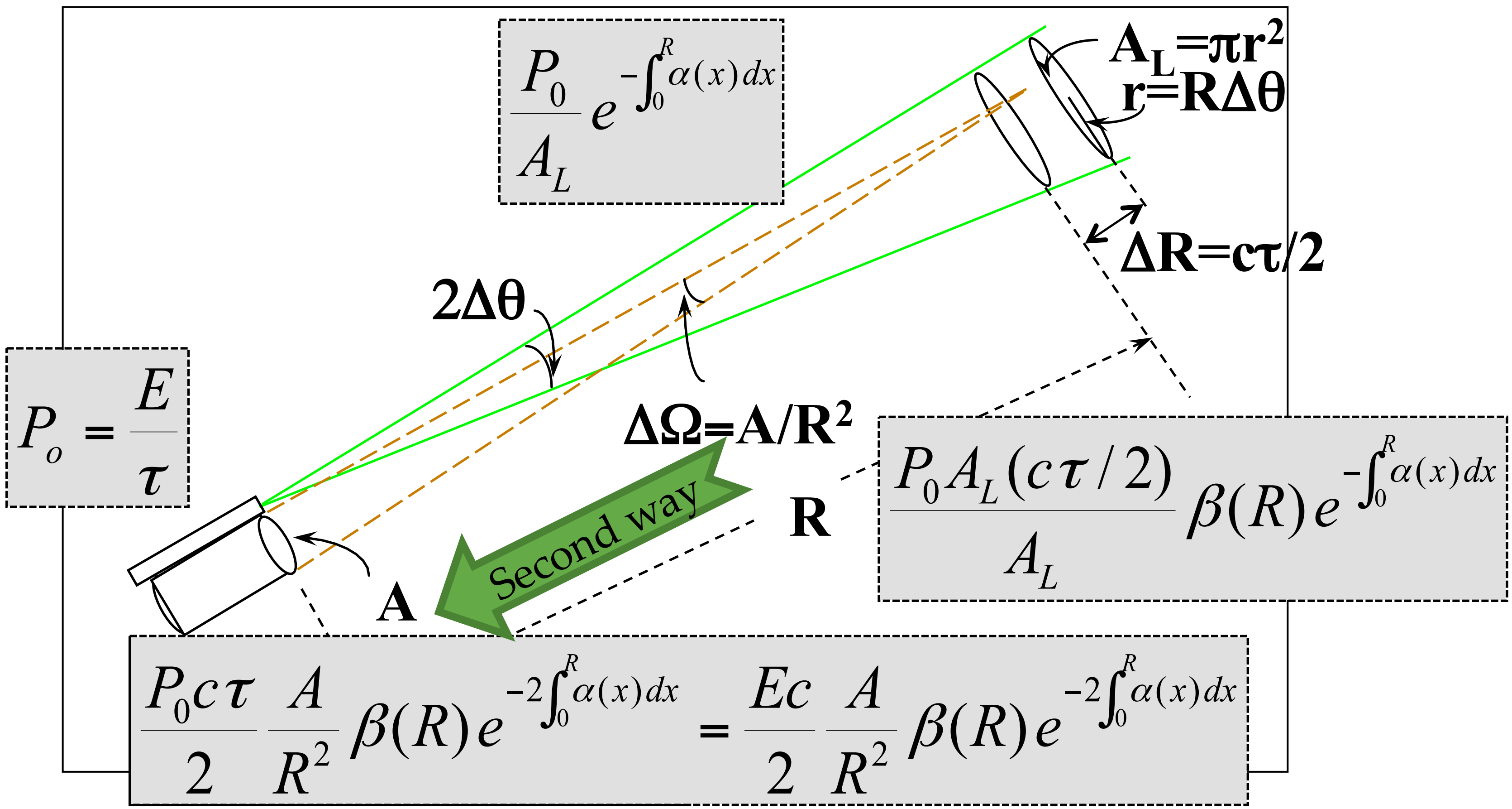

The illuminated volume $c(\tau/2)A_L$ produces a backscattered signal proportional to the backscatter coefficient

This signal travels back to the detector suffering an additional attenuation and thus the signal collected by the detector system of surface A is:

$$\frac{P_0 c\tau}{2} \frac{A}{R^2} \beta(R) e^{-2\int_0^R \alpha(x)dx}$$

LIDAR EQUATION

$$P(R,\lambda) = P_o(\lambda)\frac{C}{R^2}\beta(R,\lambda)e^{-2\int_0^R \alpha(x,\lambda)dx} = P_o(\lambda)\frac{C}{R^2}\beta(R,\lambda)T(R,\lambda)^2$$

P(R,λ) = power received by the system after backscattering from range R

$P_o(\lambda)$= power transmitted

C = lidar calibration constant

β(R, λ) = backscatter coeff. (length^{-1}sr^{-1})

α(R, λ) = volume extinction coeff. (length^{-1})

The term β(R, λ) is the backscatter coefficient at distance R, it stands for the ability of the atmosphere to scatter light back into the direction from which it comes

T(R, λ) is the transmission term and describes how much light gets lost on the way from the lidar to distance R and back

Most of the information about atmospheric properties derived from backscatter lidar measurements is based on extinction, α(R, λ), and backscatter coefficients, β(R, λ)

... MORE ON LIDAR EQUATION

Overlap function O(R):
geometrical overlap between laser beam and telescope field of view

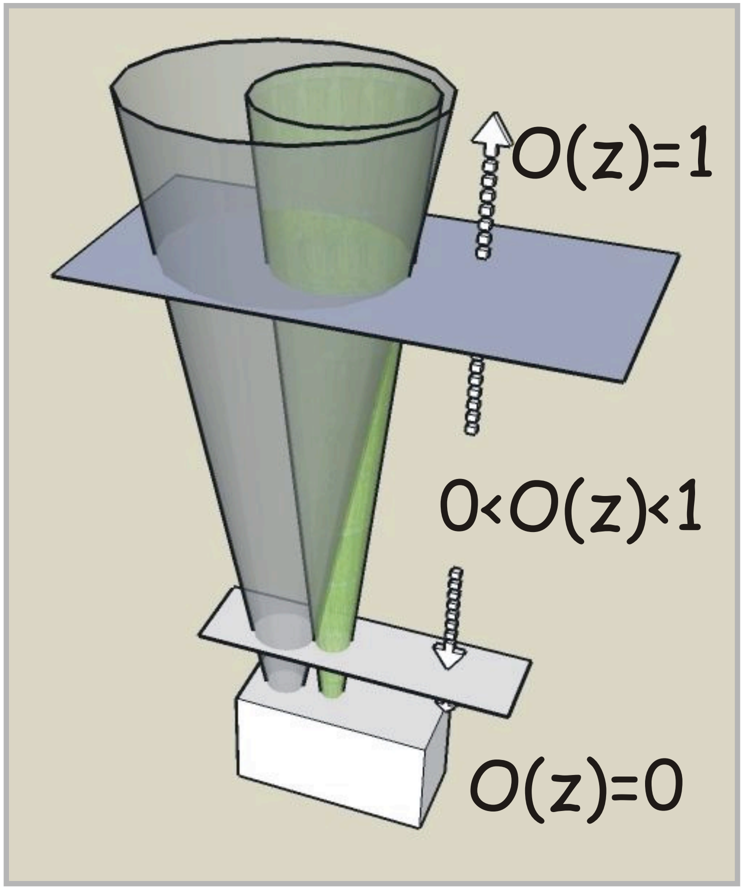

O(R) accounts for the partial overlap in the near height-range and tends to estabilize (ideally to 1) in the far height-range

Elastic lidar equation including overlap:

$$P(R,\lambda) = P_o(\lambda)\frac{C}{R^2}O(R)\beta(R,\lambda)e^{-2\int_0^R \alpha(x,\lambda)\,dx}$$

… MORE ON LIDAR EQUATION

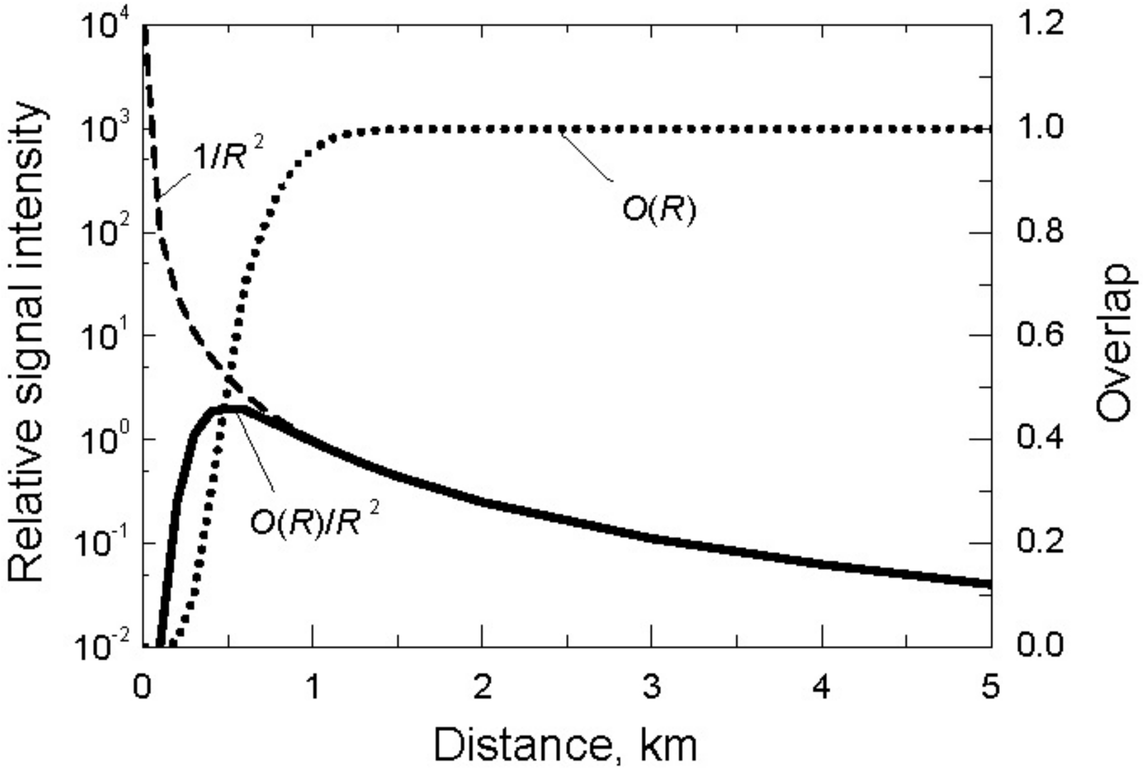

Elastic lidar equation including overlap:

$$P(R,\lambda) = P_o(\lambda)\frac{C}{R^2}O(R)\beta(R,\lambda)e^{-2\int_0^R \alpha(x,\lambda)\,dx}$$

LIDAR EQUATION

$$P(R,\lambda) = P_o(\lambda)\frac{C}{R^2}O(R)\,\beta(R,\lambda)\,e^{-2\int_0^R \alpha(x,\lambda)\,dx}$$

measured signal — $P(R,\lambda)$

instrumental features — $P_o(\lambda)\frac{C}{R^2}O(R)$

atmospheric properties — $\beta(R,\lambda)$, $\alpha(x,\lambda)$

$\beta(R, \lambda)$ = backscatter coeff. ($length^{-1}sr^{-1}$)

$\alpha(R, \lambda)$ = volume extinction coeff. ($length^{-1}$)

Depend on the particle properties as size, shape, composition, concentration, etc.

FIRST STEPS USING LIDAR EQUATION

Signal-to-noise ratio (SNR) is a critical issue when atmospheric properties are computed. To improve SNR, two methods are possible:

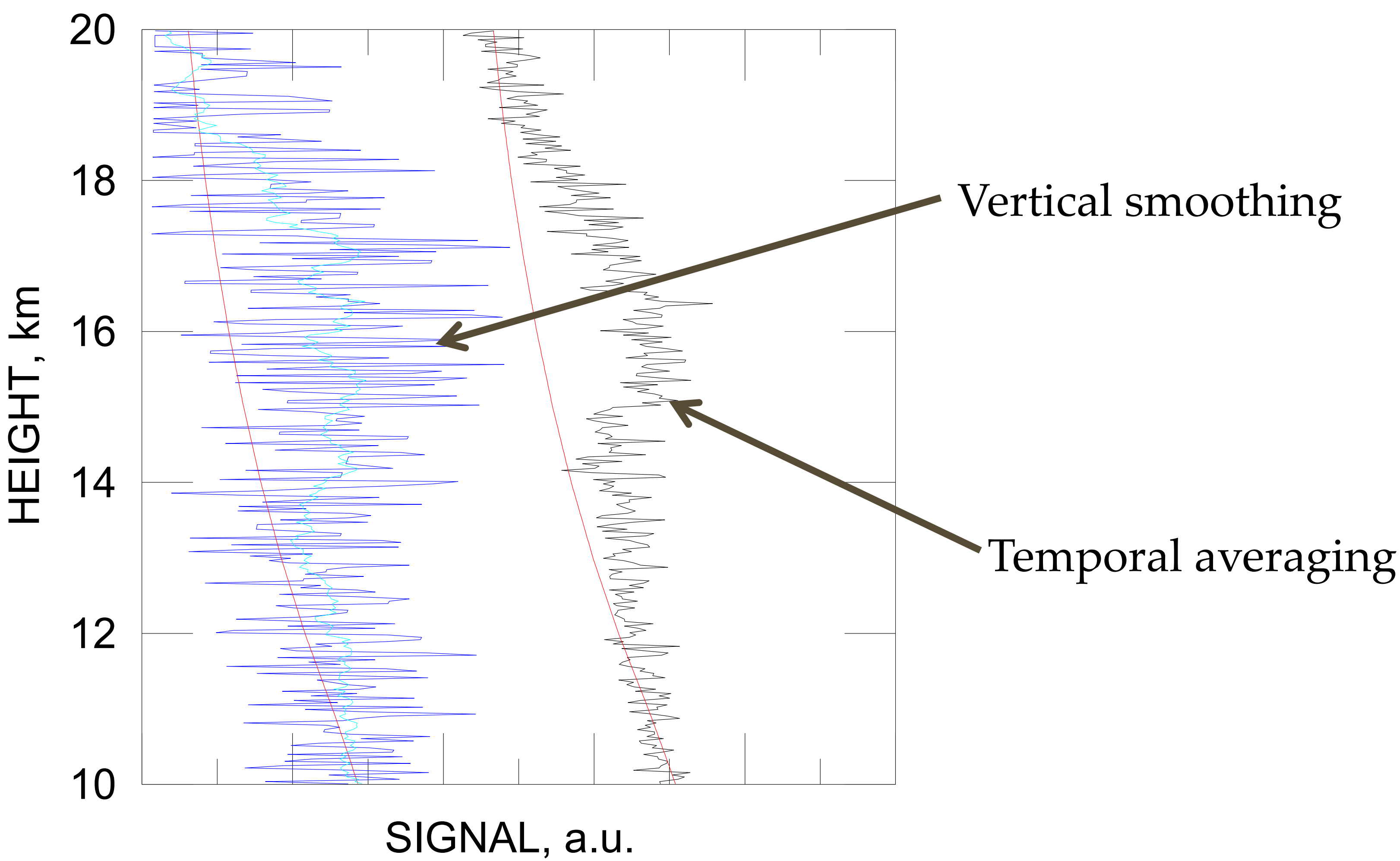

FIRST STEPS USING LIDAR EQUATION

…performing a basic calculation (range corrected signal) on the lidar equation, a first idea of the behavior of the atmosphere can be obtained…

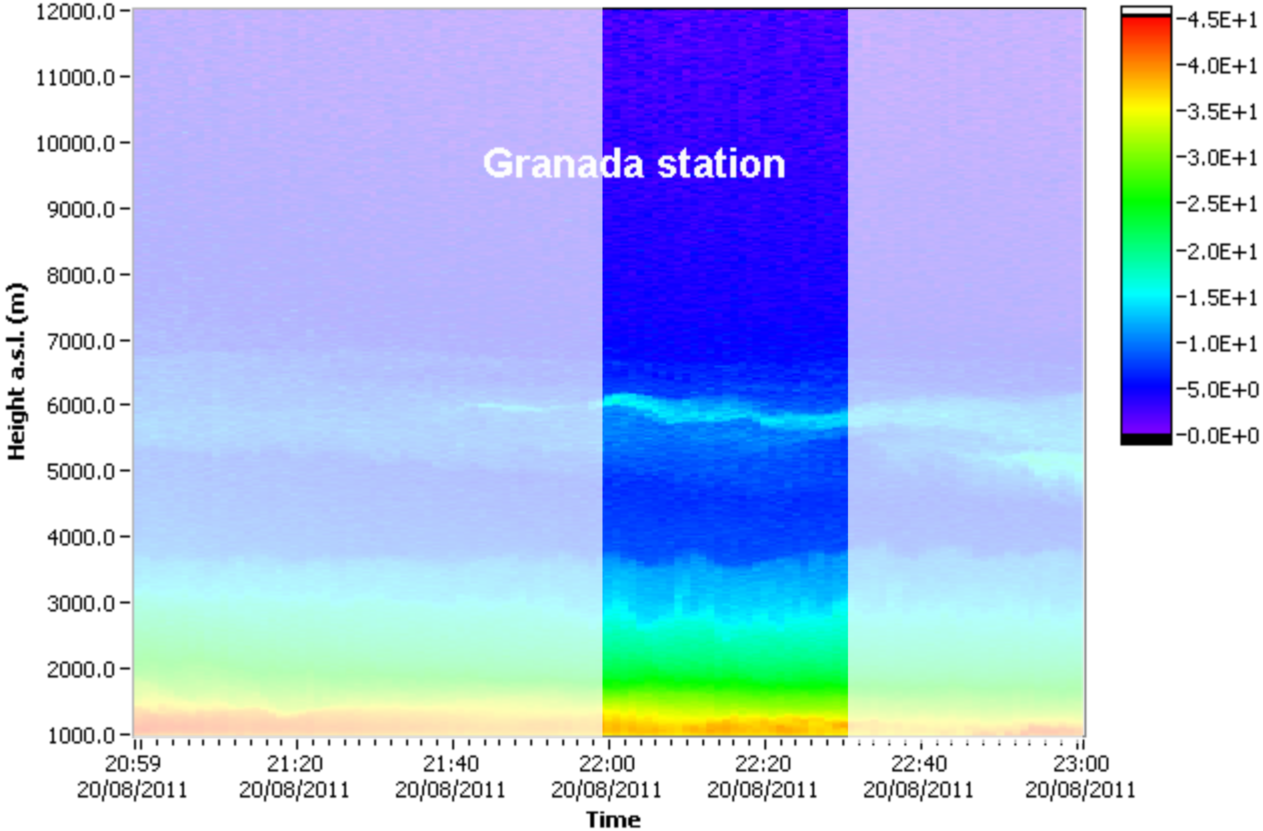

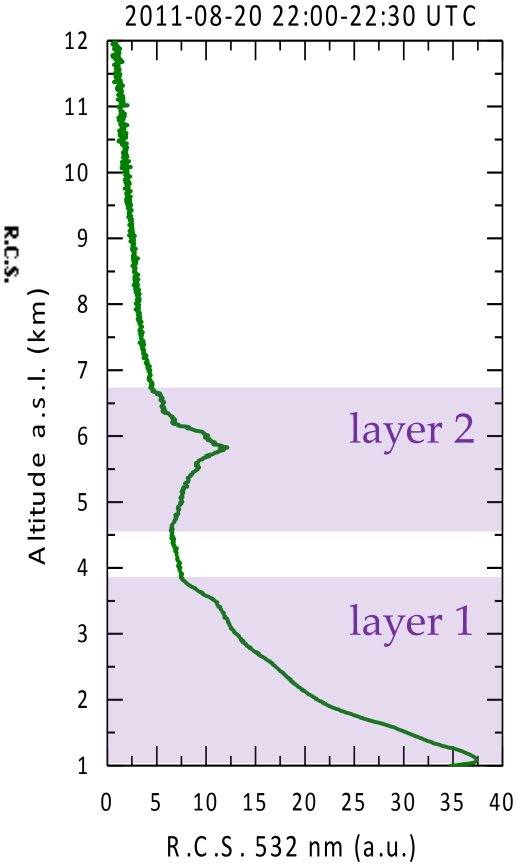

$$R.C.S.(R,\lambda) \equiv P(R,\lambda)\cdot R^2 = P_o(\lambda)\cdot C\cdot O(R)\cdot \beta(R,\lambda)\cdot e^{-2\int_0^R \alpha(x,\lambda)dx}$$

$$R.C.S.(R,\lambda) \propto \beta(R,\lambda)\cdot T(R,\lambda)^2$$

IISTA USP IFUSP

RECOMMENDED BIBLIOGRAPHY

KOVALEV, V.A, EICHINGER, W.E. Elastic Lidar. Wiley Interscience, New Jersey, 2004. **Chapters 3 and 4**.

WEITKAMP, C., Lidar. Range-resolved optical remote sensing of the Atmosphere, Springer, New York, 2005. **Chapter 1**.

IISTA Instituto Interuniversitario de Investigación del Sistema Tierra en Andalucía

USP

IFUSP Instituto de Física da USP

ASCENDING OUTLINE

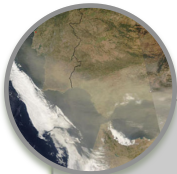
Introduction

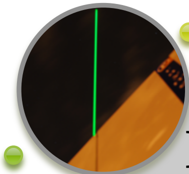
Fundamentals

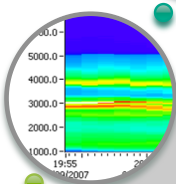
Geometrical properties

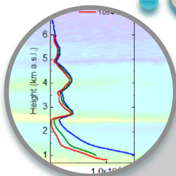
Optical properties

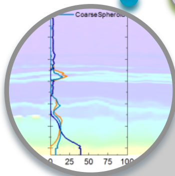
Microphysical properties


Instrumental tests

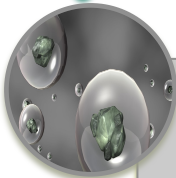
Aerosol-cloud interactions

GEOMETRICAL PROPERTIES

Geometrical properties:
- base height
- top height
- geometrical thickness
- center of mass

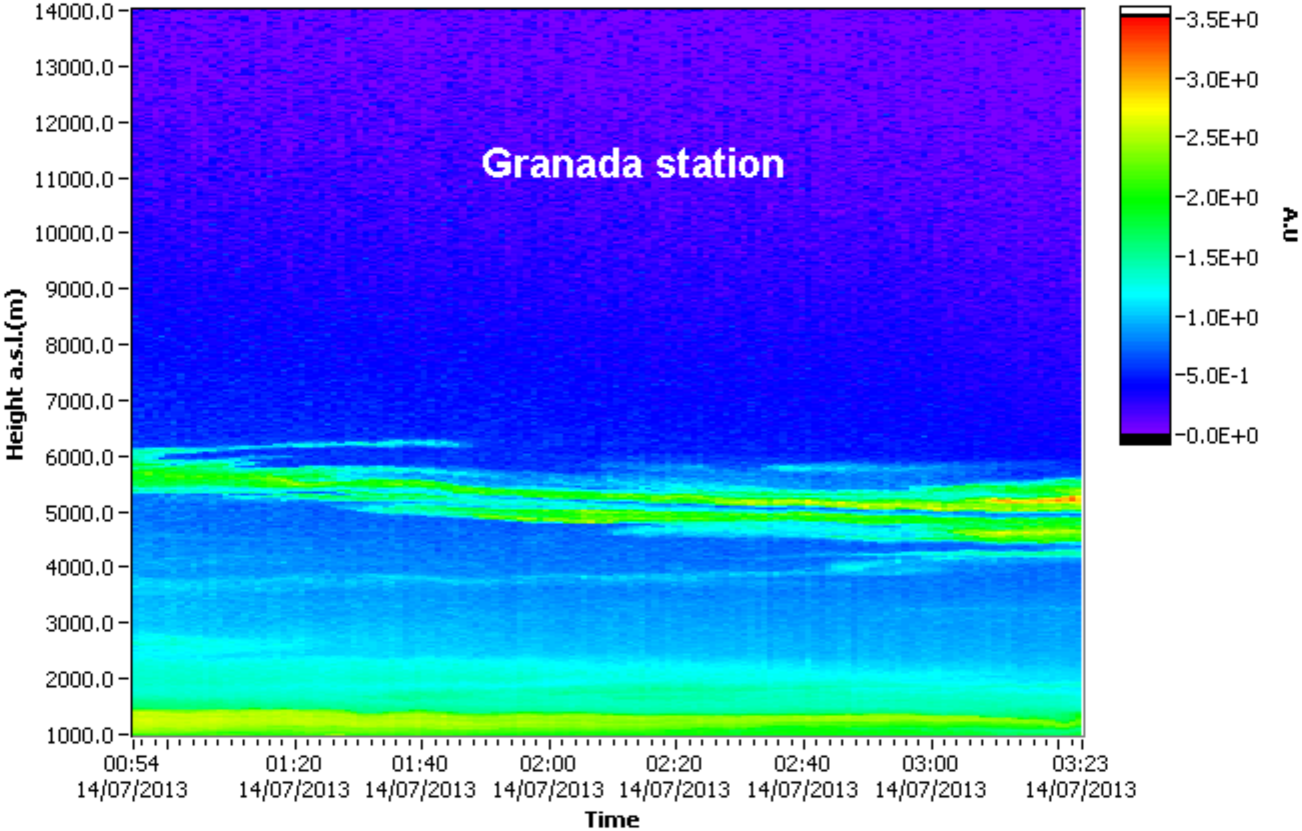

Quicklooks can provide a rough estimate of geometrical properties but quantitative information is needed

Forest fire smoke layers on 14/07/2013

GEOMETRICAL PROPERTIES

To quantify geometrical properties two groups of algorithms: threshold methods and derivative methods

Threshold methods: processed profiles are needed. Typically, this threshold is established in terms of the backscattering ratio:

$$R_{back}(R) = \frac{\beta_{part}(R) + \beta_{mol}(R)}{\beta_{mol}(R)} =$$

$$= 1 + \frac{\beta_{part}(R)}{\beta_{mol}(R)}$$

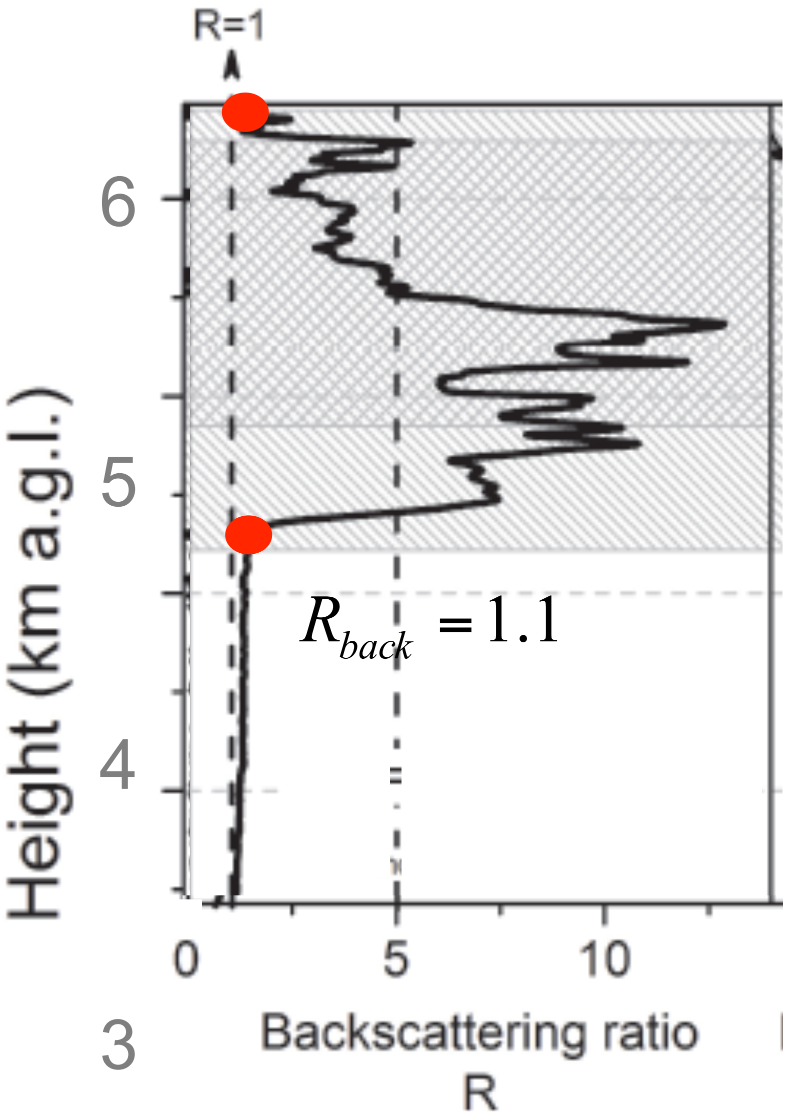

GEOMETRICAL PROPERTIES

Derivative methods:

- advantage of the derivative methods: applied directly to uncalibrated raw lidar data, i.e., no additional measurements, models or assumptions are required

- first derivate method, second derivate method, logarithm derivate method

- logarithmic derivate method because it mostly quantifies the relative change of the signal, instead of an absolute change as other derivative methods

GEOMETRICAL PROPERTIES

- the backscattered lidar signal of a clear atmosphere decreases monotonically with altitude (derivative is always negative)
- aerosol layer implies an abrupt increase in the signal values, such that around the layer base and layer top the sign of this derivative changes
- the change from negative to positive is identified as layer boundaries

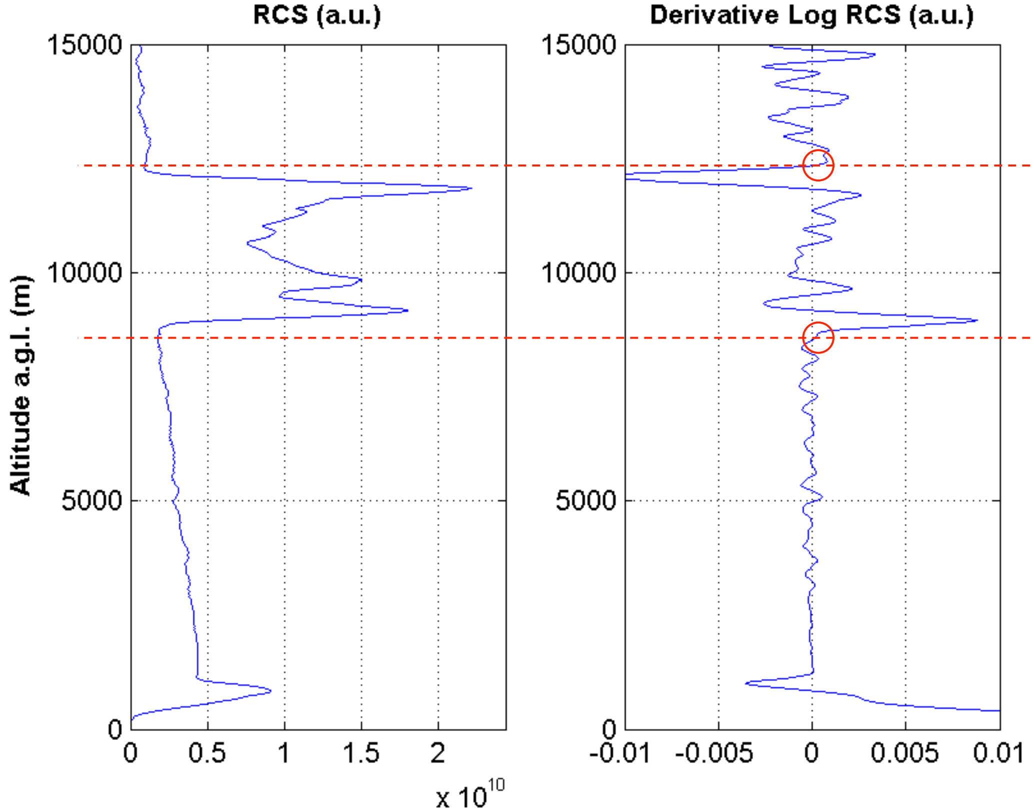

GEOMETRICAL PROPERTIES

Identification of layers

Center of mass

Geometrical thickness

Temporal serie of layer heights

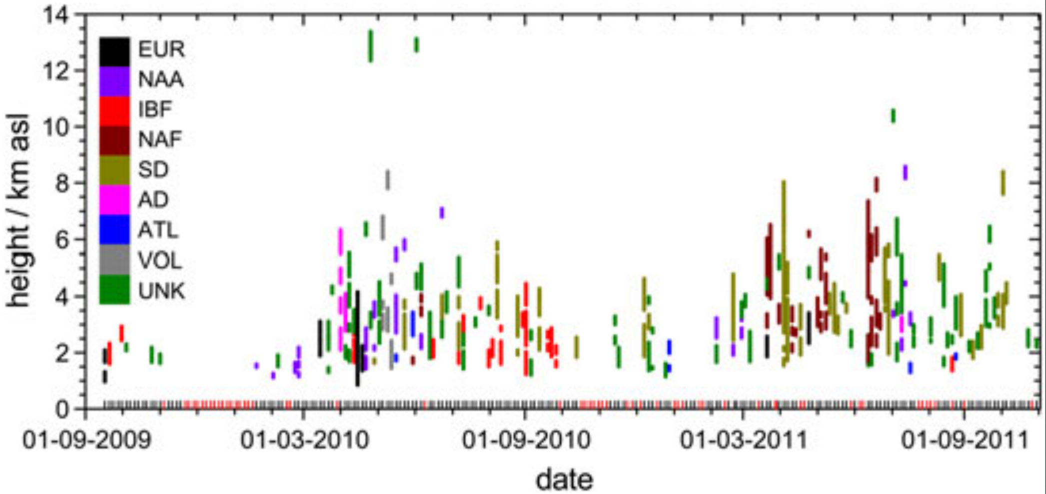

GEOMETRICAL PROPERTIES

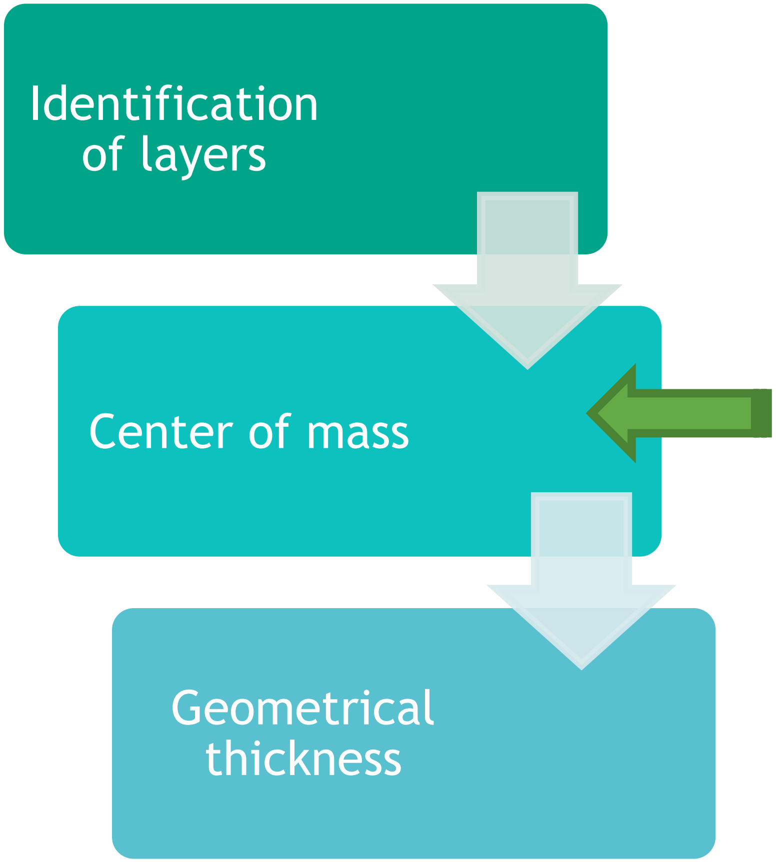

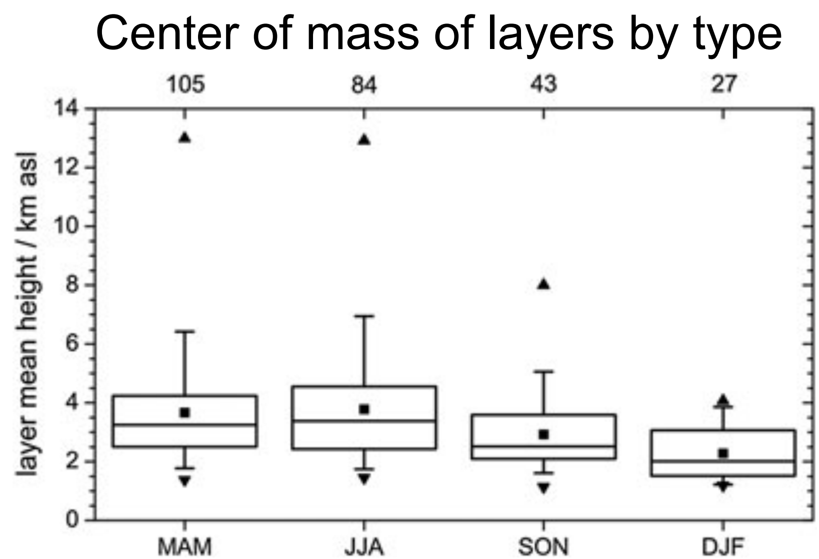

$$C_{mass} = \frac{\int_{z_{base}}^{z_{top}} z \cdot \beta(z)\ dz}{\int_{z_{base}}^{z_{top}} z\ dz}$$

GEOMETRICAL PROPERTIES

Identification of layers

Center of mass

Geometrical thickness

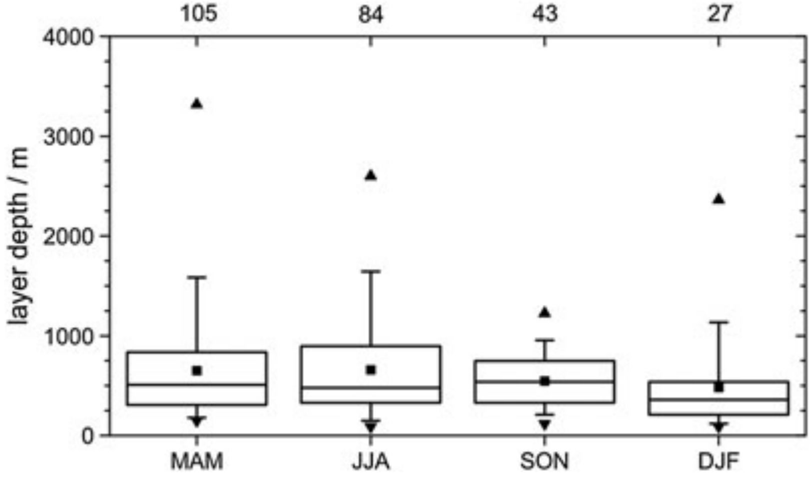

ASCENDING OUTLINE

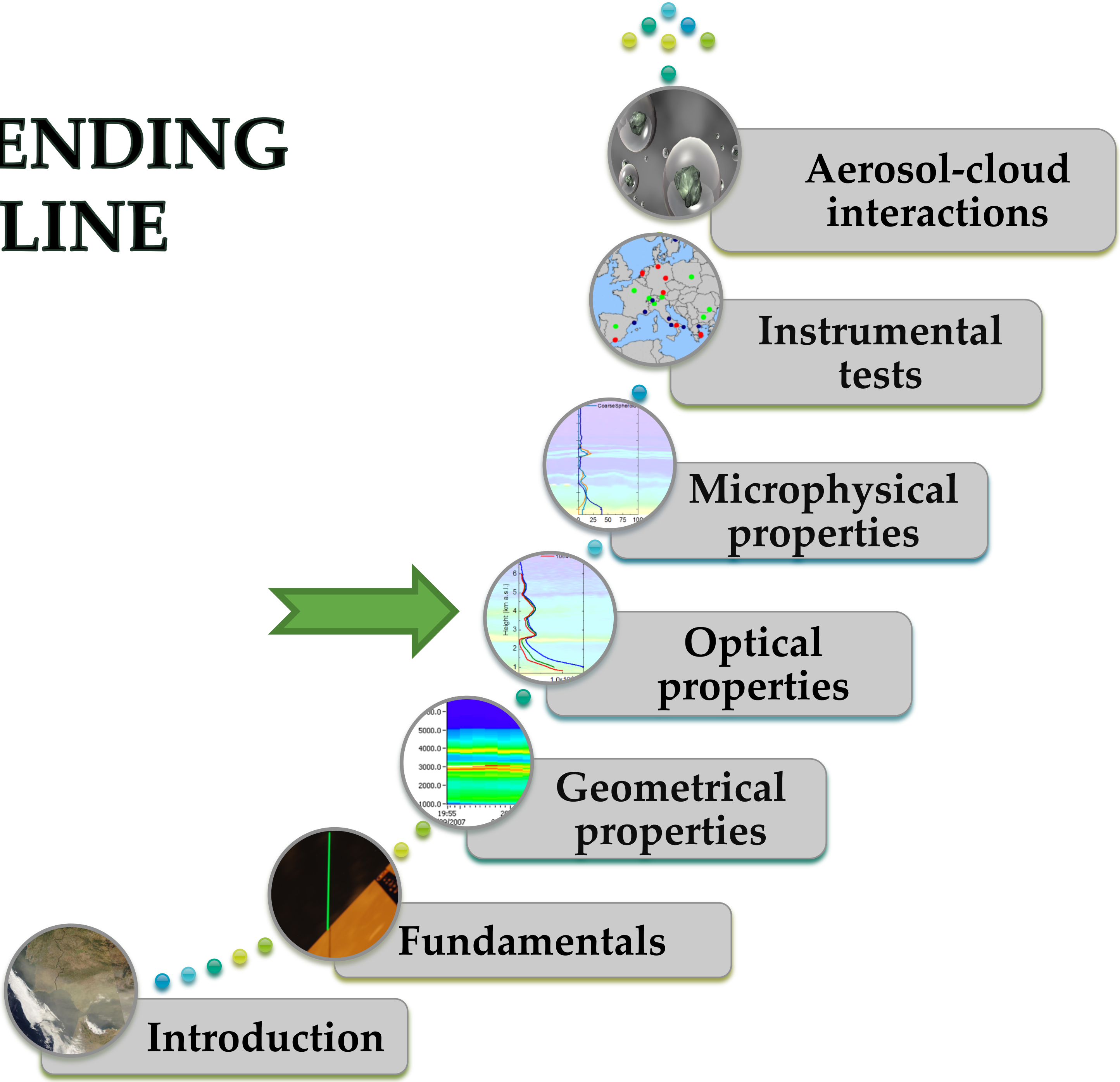

LIDAR OPTICAL ALGORITHMS

ELASTIC METHOD

First we will describe the technique used to compute the particle backscatter coefficient from return signals measured with the widely used elastic standard backscatter lidar

The main drawback of this method is that trustworthy profiles of the climate relevant volume extinction coefficient of the particles cannot be obtained. The extinction profile must be estimated from the determined backscatter coefficient profile

RAMAN METHOD

By applying the so-called Raman lidar technique, the profile of the particle extinction and backscatter coefficients can be independently determined

An aerosol Raman lidar measures two signal profiles, which permit the separation of particle and molecular backscatter contributions

KLETT-FERNALD METHOD

Starting point: lidar equation

$$P(R,\lambda) = P_o(\lambda)\frac{C}{R^2}O(R)\beta(R,\lambda)\,e^{-2\int_0^R \alpha(x,\lambda)\,dx} =$$

$$= P_o(\lambda)\frac{C}{R^2}O(R)\beta(R,\lambda)T(R,\lambda)^2$$

$\beta(R,\lambda)$ ($km^{-1}sr^{-1}$) and $\alpha(R, \lambda)$ (km^{-1}) are the backscatter and extinction coefficients in the atmosphere

Remembering the definition of lidar range corrected signal:

$$R.C.S.(R,\lambda) \equiv P(R,\lambda)\cdot R^2 = P_o(\lambda)\cdot C\cdot O(R)\cdot\beta(R,\lambda)\cdot e^{-2\int_0^R \alpha(x,\lambda)\,dx}$$

KLETT-FERNALD METHOD

$$R.C.S.(R,\lambda) \equiv P(R,\lambda)\cdot R^2 = P_o(\lambda)\cdot C\cdot O(R)\cdot \beta(R,\lambda)\cdot e^{-2\int_0^R \alpha(x,\lambda)\,dx}$$

The conversion of lidar signal into range corrected lidar signal causes a change in appearance:

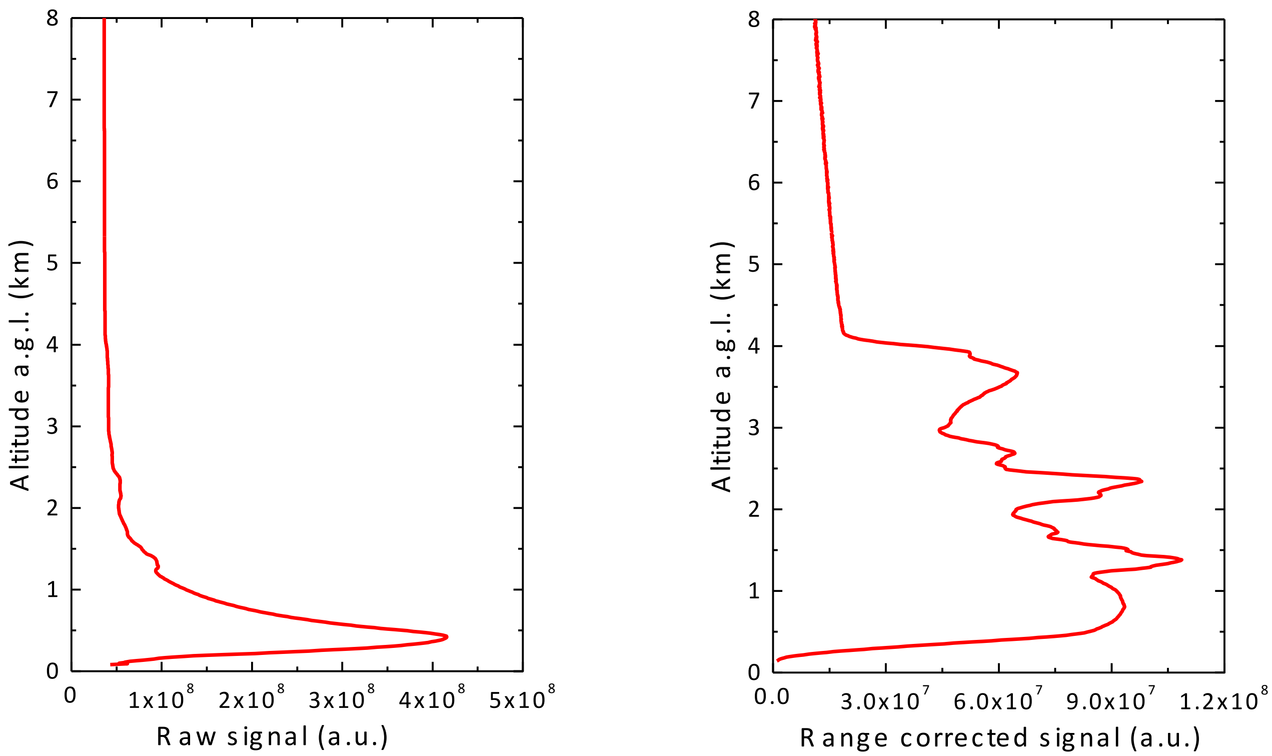

KLETT-FERNALD METHOD

$$R.C.S.(R,\lambda) \equiv P(R,\lambda)\cdot R^2 = P_o(\lambda)\cdot C\cdot O(R)\cdot \beta(R,\lambda)\cdot e^{-2\int_0^R \alpha(x,\lambda)dx}$$

… some considerations:

- the overlap is assumed to be complete , O(R) =1 ➔ $R \geq R_{min}$
- we dropp the wavelength dependence

$$R.C.S.(R) \equiv P(R)\cdot R^2 = P_o\cdot C\cdot \beta(R)\cdot e^{-2\int_0^R \alpha(x)dx}$$

- β(R) ($km^{-1}sr^{-1}$) and α(R) (km^{-1}) are caused by particles and molecules:

$$\beta(R) = \beta_{mol}(R) + \beta_{part}(R)$$

$$\alpha(R) = \sigma_{mol}^{scat}(R) + \sigma_{mol}^{abs}(R) + \sigma_{part}^{scat}(R) + \sigma_{part}^{abs}(R)$$

≈ 0 km^{-1}at lidar wavelengths

KLETT-FERNALD METHOD

Taking into account molecular absorption effects are ignored:

$$\alpha(R) = \sigma_{mol}^{scat}(R) + \sigma_{part}^{scat}(R) + \sigma_{part}^{abs}(R) = \alpha_{mol}(R) + \alpha_{part}(R)$$

Therefore, the range corrected signal is:

$$R.C.S.(R) = P_o \cdot C \cdot \left[\beta_{mol}(R) + \beta_{part}(R)\right] \cdot e^{-2\int_0^R \left[\alpha_{mol}(x) + \alpha_{part}(x)\right] dx}$$

unknowns

measurement

The molecular properties, $\beta_{mol}(R)$ and $\alpha_{mol}(R)$, can be determined from the Rayleigh theory using the best available meteorological data of temperature and pressure or approximated from appropriate standard atmospheres so that only the aerosol scattering and absorption properties, $\beta_{part}(R)$ and $\alpha_{part}(R)$, remain to be determined

IISTA

USP

IFUSP

KLETT-FERNALD METHOD

Shortcoming: 1 measurement versus 2 unknowns

$$R.C.S.(R) = P_o \cdot C \cdot \left[\beta_{mol}(R) + \beta_{part}(R)\right] \cdot e^{-2\int_0^R \left[\alpha_{mol}(x) + \alpha_{part}(x)\right] dx}$$

measurement **unknowns**

How to solve?: definition of the particle and molecular lidar ratio (extinction-to-backscatter ratio)

$$Lr_{part}(R,\lambda) = \frac{\alpha_{part}(R,\lambda)}{\beta_{part}(R,\lambda)}$$

dependent on range and wavelength because depends on:

- size distribution
- shape
- composition (refractive index)

$$Lr_{mol}(R,\lambda) = \frac{\alpha_{mol}(R,\lambda)}{\beta_{mol}(R,\lambda)} = \frac{8\pi}{3} sr$$

independent on range and wavelength

KLETT-FERNALD METHOD

In the next step:

- lidar ratio definitions are included
- the equation is reorganized
- the resulting Bernoulli equation is solved

Solution:

$$\beta_{part}(R) = -\beta_{mol}(R) + \frac{R.C.S(R)\cdot\exp\left\{-2\int_{R_0}^{R}\left[Lr_{part}(x)-Lr_{mol}\right]\beta_{mol}(x)dx\right\}}{\frac{R.C.S.(R_0)}{\beta_{part}(R_0)+\beta_{mol}(R_0)} - 2\int_{R_0}^{R} Lr_{part}(x')\cdot R.C.S.(x')\cdot\exp\left(-2\int_{R_0}^{x'}\left[Lr_{part}(x)-Lr_{mol}\right]\beta_{mol}(x)dx\right)dx'}$$

…many things … but they are known (almost)

KLETT-FERNALD METHOD

$$\beta_{part}(R) = -\beta_{mol}(R) + \frac{R.C.S(R)\cdot\exp\left\{-2\int_{R_0}^{R}\left[Lr_{part}(x) - Lr_{mol}\right]\beta_{mol}(x)dx\right\}}{\frac{R.C.S.(R_0)}{\beta_{part}(R_0)+\beta_{mol}(R_0)} - 2\int_{R_0}^{R} Lr_{part}(x')\, R.C.S.(x')\cdot\exp\left(-2\int_{R_0}^{x'}\left[Lr_{part}(x) - Lr_{mol}\right]\beta_{mol}(x)dx\right)dx'}$$

- lidar range corrected signal (R.C.S.) is known
- molecular properties are known from meteorological data of temperature and pressure or approximated from appropriate standard atmospheres
- particle lidar ratio is an input parameter
- boundary condition at R_0 … how to choose it?

KLETT-FERNALD METHOD

$$\beta_{part}(R) = -\beta_{mol}(R) + \frac{R.C.S(R)\cdot\exp\left\{-2\int_{R_0}^{R}\left[Lr_{part}(x) - Lr_{mol}\right]\beta_{mol}(x)dx\right\}}{\dfrac{R.C.S.(R_0)}{\beta_{part}(R_0)+\beta_{mol}(R_0)} - 2\int_{R_0}^{R} Lr_{part}(x')\cdot R.C.S.(x')\cdot\exp\left(-2\int_{R_0}^{x'}\left[Lr_{part}(x) - Lr_{mol}\right]\beta_{mol}(x)dx\right)dx'}$$

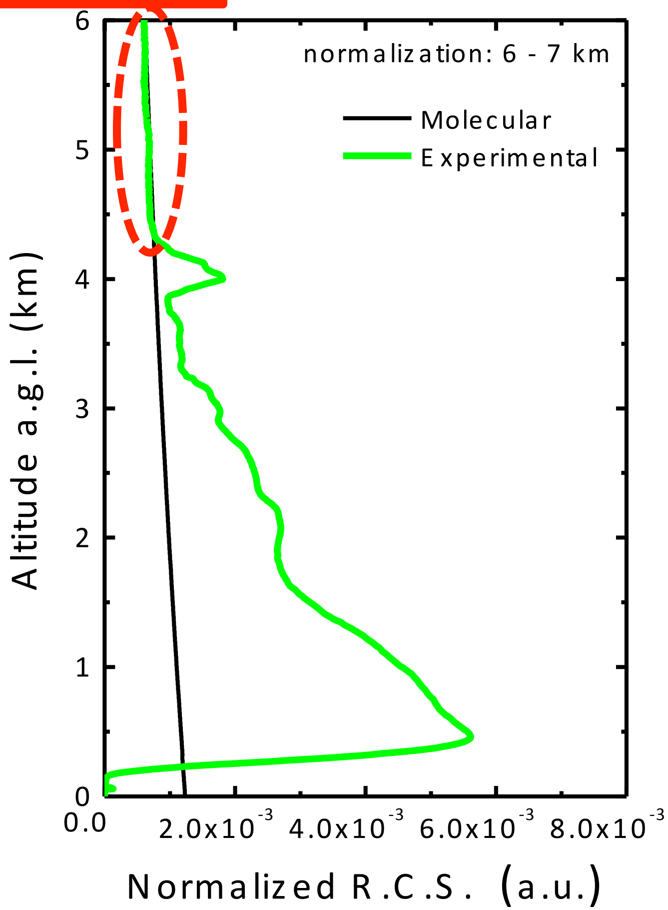

at R_0: $\beta_{part}(R_0) << \beta_{mol}(R_0)$

$$\beta_{part}(R_0) + \beta_{mol}(R_0) \approx \beta_{mol}(R_0)$$

(clean air conditions are normally given in the middle and upper troposhere)

Now, the boundary condition term is also known

KLETT-FERNALD METHOD

In principle, the solution for $\beta_{part}(R)$ can be integrated by starting from the reference range R_o, which may be either the near end ($R>R_o$, "forward integration") or the remote end ($R<R_o$, "backward integration") of the measuring range

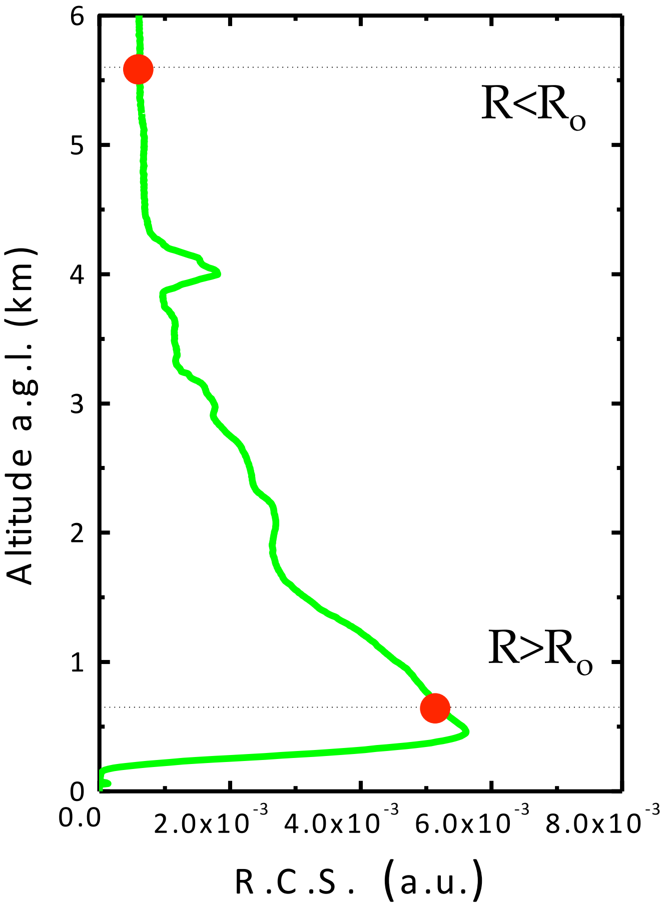

Forward integration	Backward integration
bad $\beta_{part}(R_0)$	good $\beta_{part}(R_0)$ (clean atmosphere)
numerically unstable	numerically stable
good SNR for R.C.S. at R_0	worse SNR for R.C.S. at R_0 (easily solved)

Backward integration method is preferred

KLETT-FERNALD METHOD

The most critical parameter in this method is the selection of a particle lidar ratio

$$Lr_{part}(R,\lambda) \equiv \frac{\alpha_{part}(R,\lambda)}{\beta_{part}(R,\lambda)}$$

Effect of Lr_{part} on β_{part} :

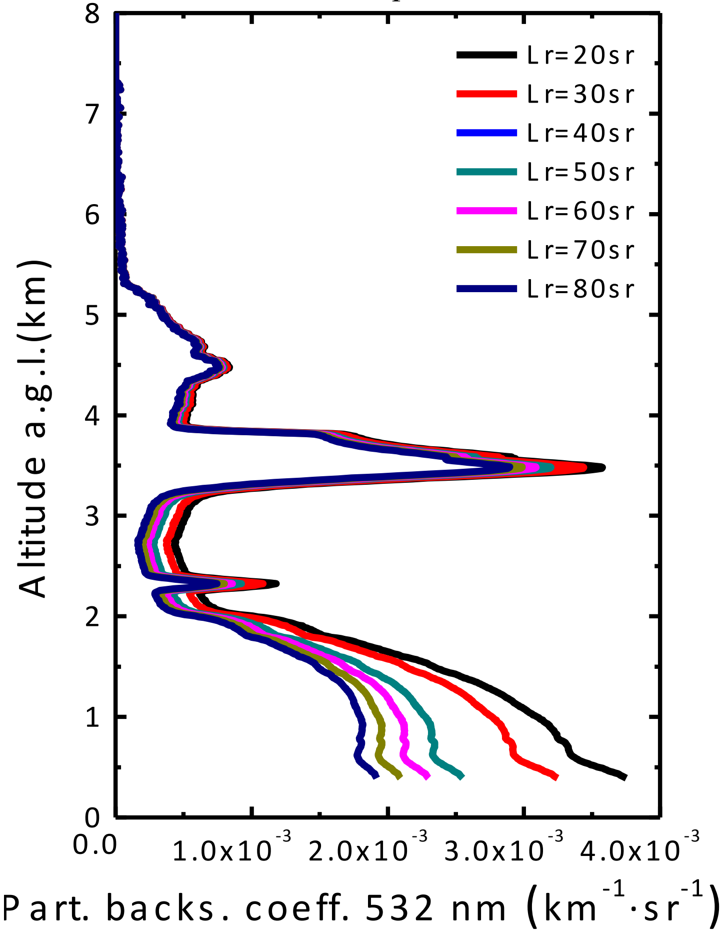

Lr_{part} values independent of altitude are typically used

Some values of particle lidar ratio:

Type	Lr (at 532 nm)
Marine particles	20-35 sr
Saharan dust	40-70 sr
Biomass burning	70-100 sr
Urban/continental	45-75 sr

KLETT-FERNALD METHOD

The spectral dependence of β_{part} is strongly dependent on particle size: commonly used for the qualitative description of particle size

$$\overset{o}{a}_{\beta}(R) = -\frac{\ln\left(\frac{\beta_{part}(R,\lambda_1)}{\beta_{part}(R,\lambda_2)}\right)}{\ln\left(\frac{\lambda_1}{\lambda_2}\right)}$$

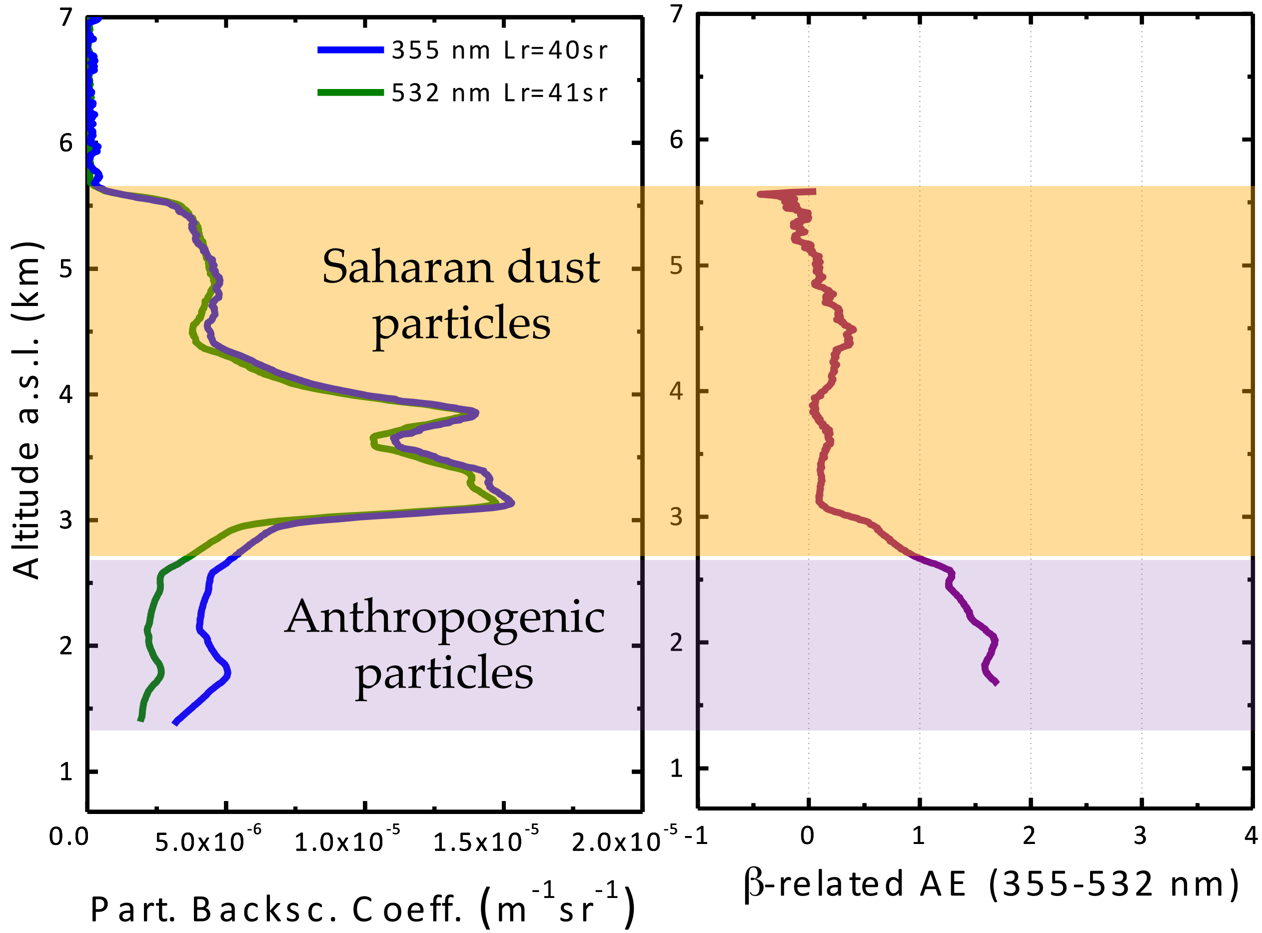

IISTA
USP
IFUSP

KLETT-FERNALD METHOD

In this way we obtain the profile of the particle backscatter coefficient and from this the profile of particle extinction coefficient can be estimated by:

$$\alpha_{part}(R) = Lr_{part}(R)\beta_{part}(R)$$

An example:

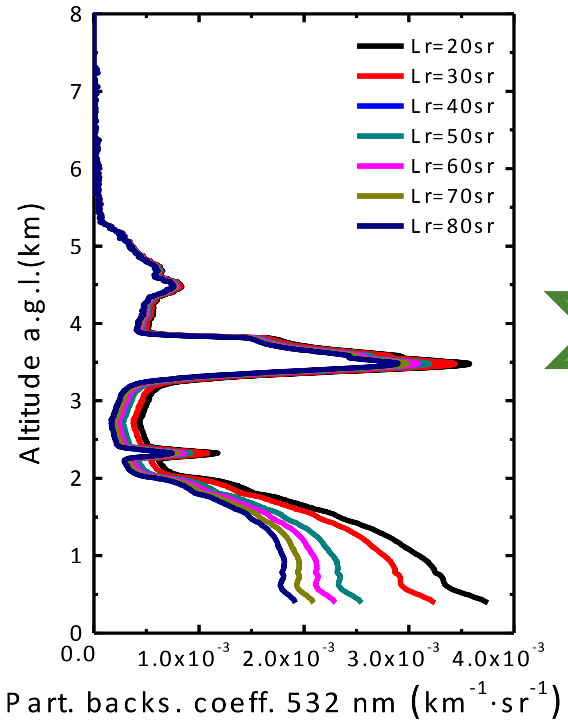

$$\cdot Lr_{part}$$

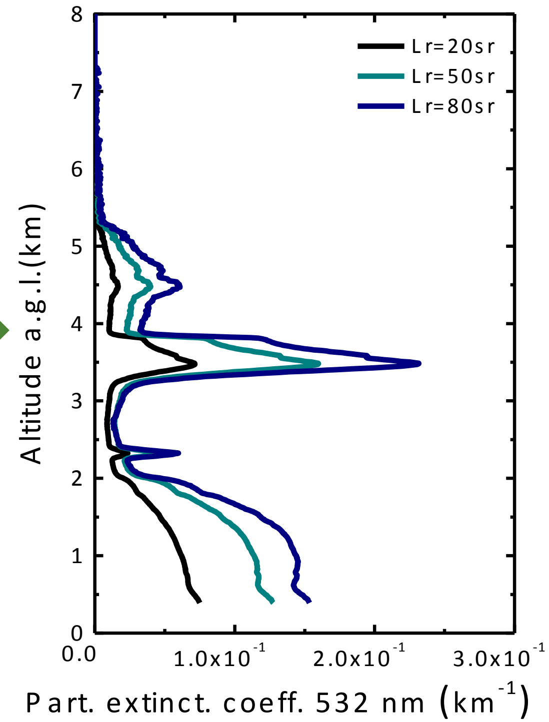

$$AOD = \int_0^{\infty} \alpha_{part}(R)dR$$

Lr	AOD
20 sr	0.17
50 sr	0.33
80 sr	0.44

KLETT-FERNALD METHOD

Improvement : K-F method constrained by $AOD_{photometer}$

1 – Aplication of K-F method with an initial value of Lr_{part}

2 – Computation of aerosol extinction profile and AOD from lidar:

$$\alpha_{part}(R) = Lr_{part}\beta_{part}(R) \Rightarrow AOD_{lidar} = \int_0^\infty \alpha_{part}(R)dR = Lr_{part}\int_0^\infty \beta_{part}(R)dR$$

3 – Comparison of AOD from lidar and photometer:

$$\left| AOD_{photometer} - AOD_{lidar} \right| \leq \varepsilon$$

4 – Modification of Lr_{part} if necessary (go to 1)

This column-related Lr_{part} must be considered as an effective Lr_{part} :
the true Lr_{part} profile remains unknown

SUMMARY ON K-F METHOD

- The K-F method allows for determining the β_{part} profile
- Numerical stability is given in the backward integration
- The reference range R_o is usually chosen such that β_{part} at R_o is negligible compared to the known β_{mol}
- The most critical input parameter is the $L_{part}(R)$. This quantity depends on the microphysical, chemical and morphological properties of the particles, and can vary strongly with height, specially when the atmospheric aerosols present a layered structure.
- The application of the K-F method constrained by $AOD_{photometer}$ allows for obtaining an an effective Lr_{part} , but the true Lr_{part} profile remains unknown
- Variations between 20 and 100 sr make it practically impossible to estimate trustworthy particle extinction profiles from backscatter ones

IISTA

USP

IFUSP

RECOMMENDED BIBLIOGRAPHY

KOVALEV, V.A, EICHINGER, W.E. Elastic Lidar. Wiley Interscience, New Jersey, 2004. **Chapters 5 (technique), 6 (uncertainties) and 7 (review on particle lidar ratio and impact)**.

WEITKAMP, C., Lidar. Range-resolved optical remote sensing of the Atmosphere, Springer, New York, 2005. **Chapter 7**.

MOLECULAR COMPONENT

As previously mentioned, the K-F method (and others that will be shown later) needs the molecular component

β_{mol} profile can be computed from the Rayleigh theory and ideal gas law:

$$\beta_{mol}(R) = \frac{9\pi^2(n_s^2-1)^2}{\lambda^4 N_s^2 (n_s^2+2)^2}\left(\frac{6+3\rho}{6-7\rho}\right) N_s \frac{T_0}{P_0}\frac{P(R)}{T(R)}$$

n_s refractive index

ρ depolarization factor (0.0301, 0.0284 and 0.0273 at 355, 532 and 1064 nm respectively)

$N_s = 2.547 \cdot 10^{19}\, cm^{-3}$ molecular number density for conditions of a standard atmosphere at sea level

$P_0 = 1013.25\, hPa$ $\qquad T_0 = 15^{\circ} C$

Only pressure and temperature profile are needed

LIDAR, AERONET AND AEROSOL-CLOUD INTERACTIONS

MOLECULAR COMPONENT

How to obtain T and P profiles?

Option 1: download radiosounding observations from…

University of Wyoming
College of Engineering
Department of Atmospheric Science

http://weather.uwyo.edu/upperair/sounding.html

Region	Type of plot	Year	Month	From	To	Station Number
South America	Text: List	2014	Jul	26/12Z	26/12Z	80222

Click on the image to request a sounding at that location or enter the station number above.

80222 Bogota/Eldorado (SKBO)

MOLECULAR COMPONENT

How to obtain T and P profiles?

Option 2: if no radiosoundings nearby, use model data from NOAA **online:** http://www.ready.noaa.gov/READYamet.php

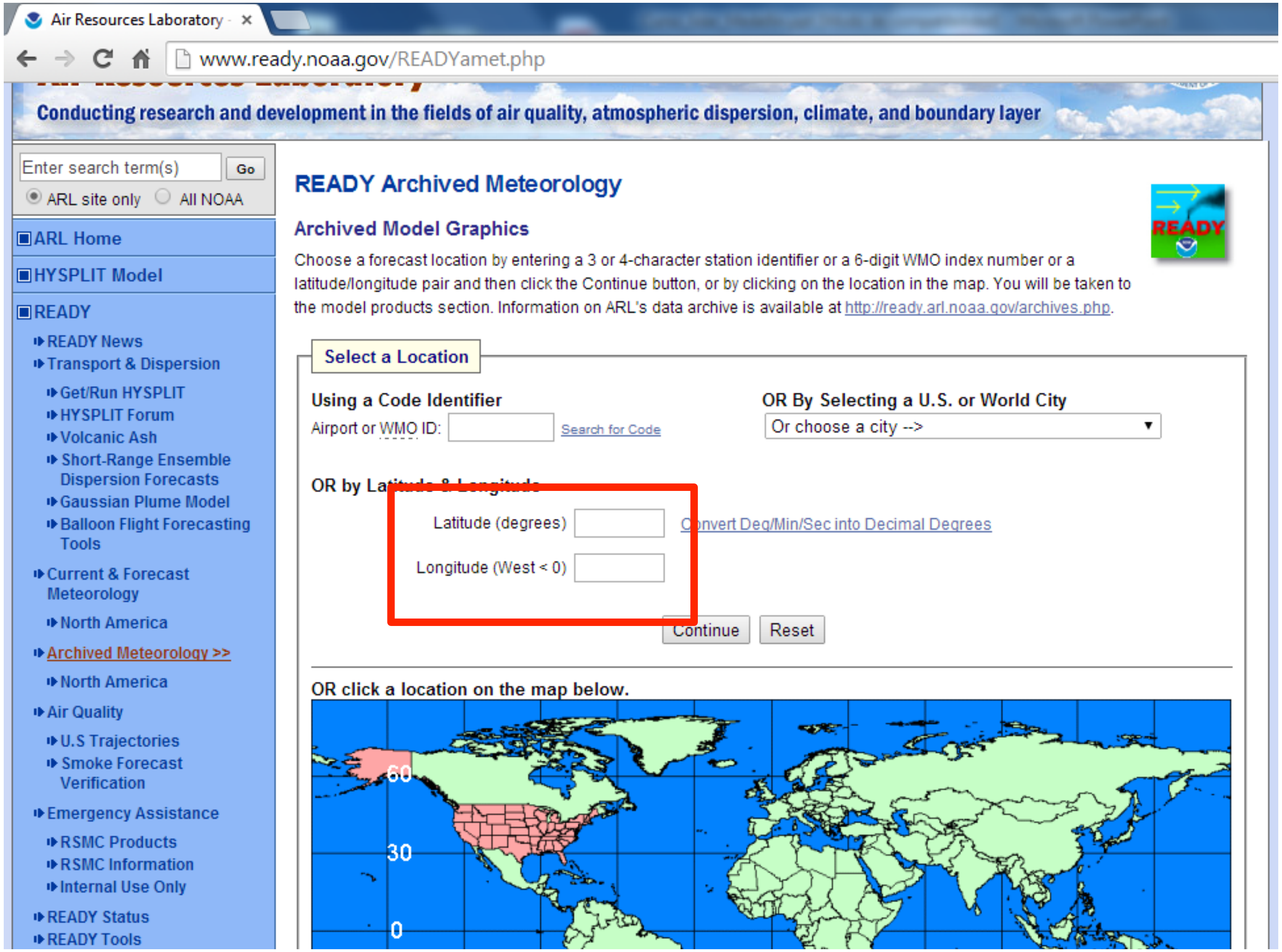

MOLECULAR COMPONENT

How to obtain T and P profiles?

Option 2: if no radiosoundings nearby, use model data from NOAA **online:** http://www.ready.noaa.gov/READYamet.php

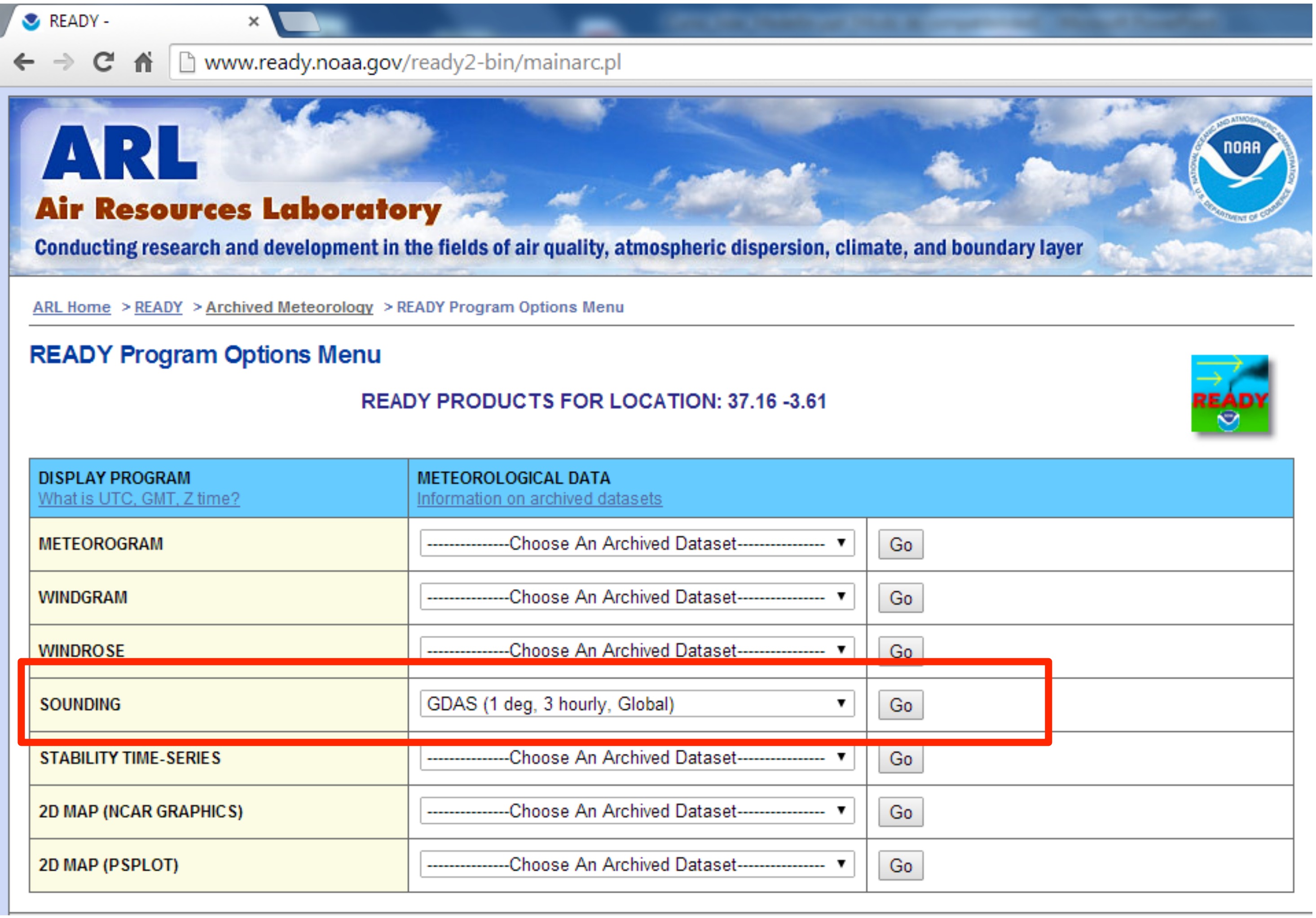
READY -

www.ready.noaa.gov/ready2-bin/mainarc.pl

ARL
Air Resources Laboratory
Conducting research and development in the fields of air quality, atmospheric dispersion, climate, and boundary layer

ARL Home > READY > Archived Meteorology > READY Program Options Menu

READY Program Options Menu

READY PRODUCTS FOR LOCATION: 37.16 -3.61

DISPLAY PROGRAM What is UTC, GMT, Z time?	METEOROLOGICAL DATA Information on archived datasets	
METEOROGRAM	---------------Choose An Archived Dataset---------------	Go
WINDGRAM	---------------Choose An Archived Dataset---------------	Go
WINDROSE	---------------Choose An Archived Dataset---------------	Go
SOUNDING	GDAS (1 deg, 3 hourly, Global)	Go
STABILITY TIME-SERIES	---------------Choose An Archived Dataset---------------	Go
2D MAP (NCAR GRAPHICS)	---------------Choose An Archived Dataset---------------	Go
2D MAP (PSPLOT)	---------------Choose An Archived Dataset---------------	Go

MOLECULAR COMPONENT

How to obtain T and P profiles?

Option 2: if no radiosoundings nearby, use model data from NOAA **online:** http://www.ready.noaa.gov/READYamet.php

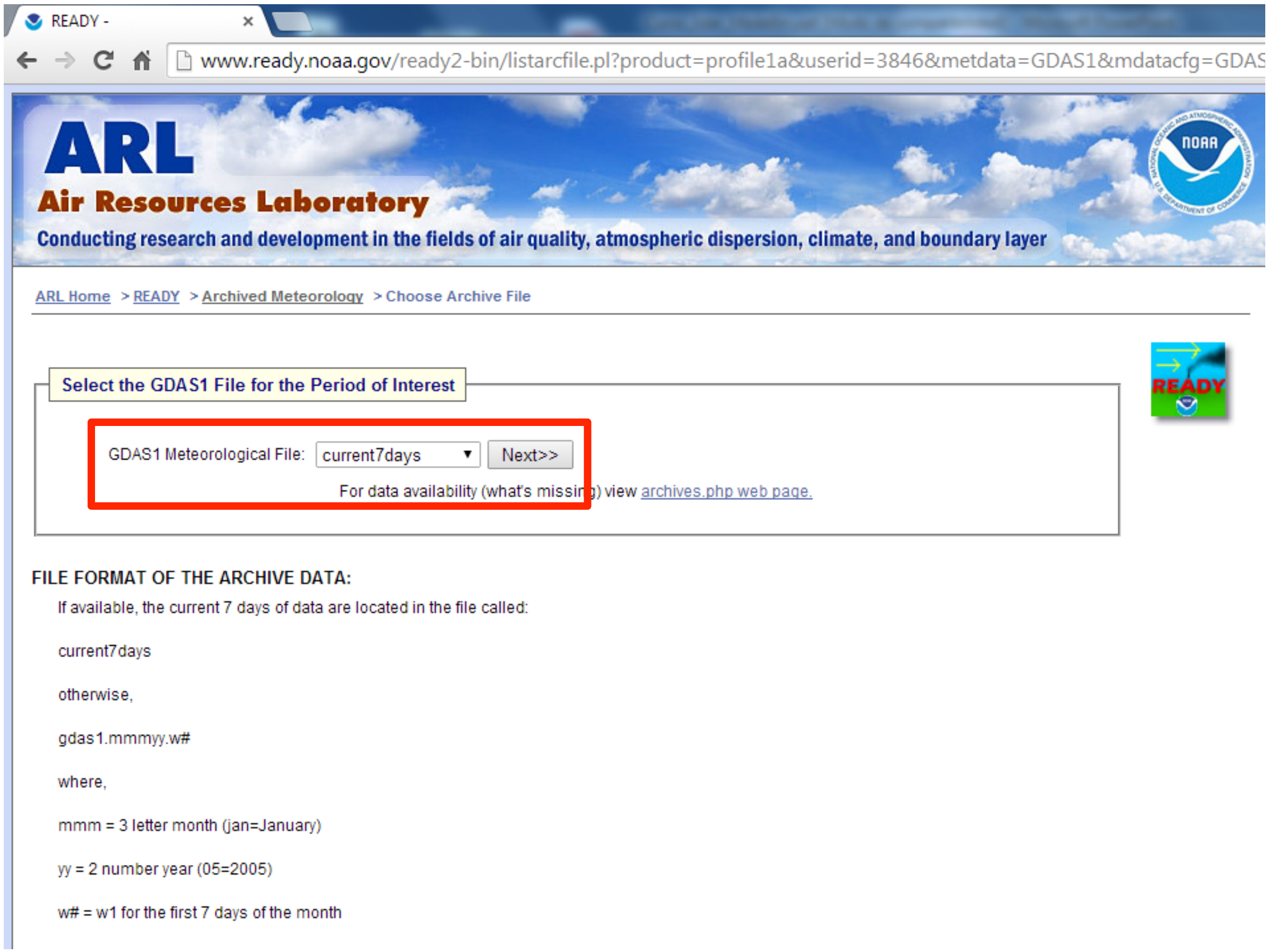

MOLECULAR COMPONENT

How to obtain T and P profiles?

Option 2: if no radiosoundings nearby, use model data from NOAA online: http://www.ready.noaa.gov/READYamet.php

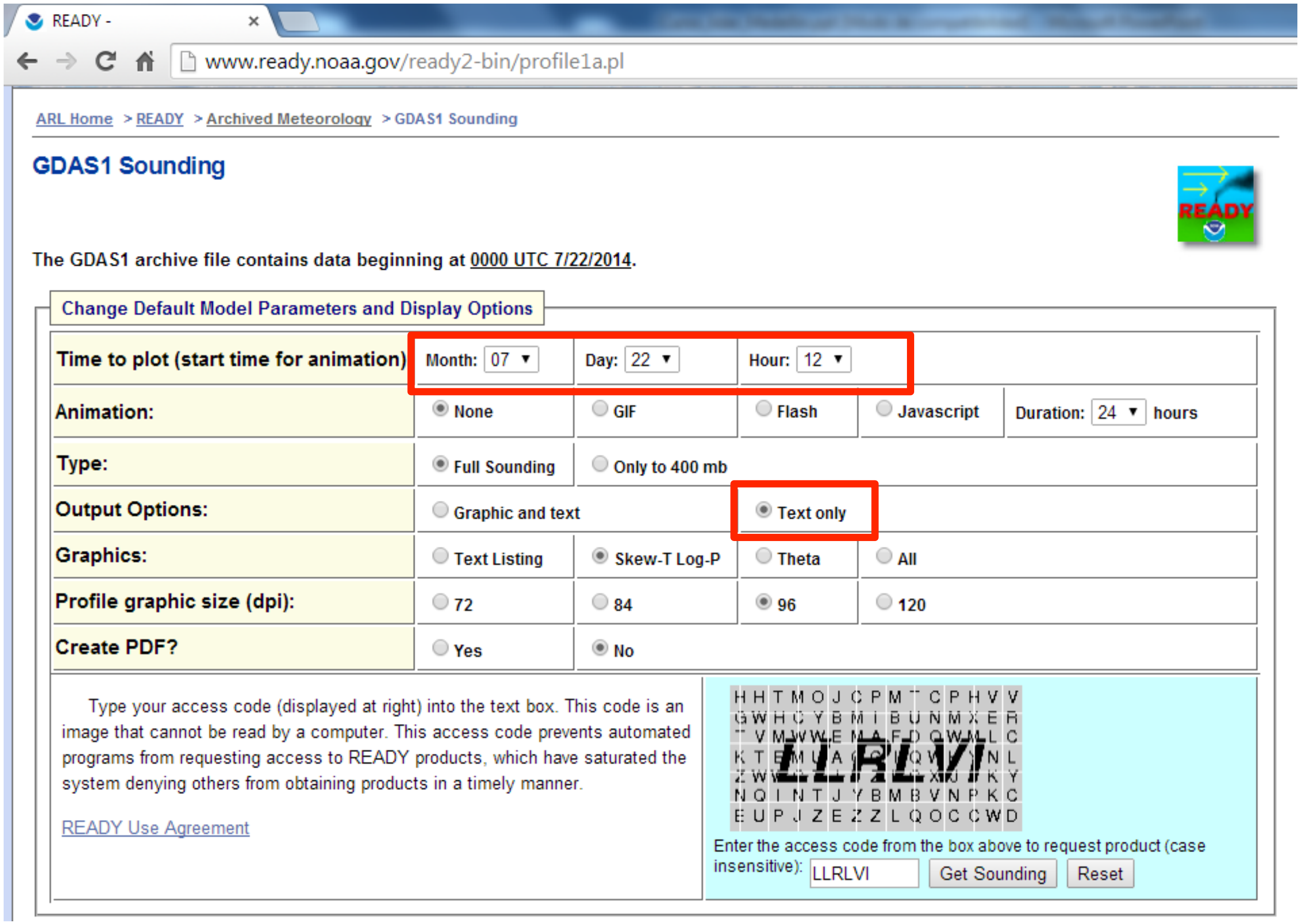

MOLECULAR COMPONENT

How to obtain T and P profiles?

Option 2: if no radiosoundings nearby, use model data from NOAA online: http://www.ready.noaa.gov/READYamet.php

READY -

www.ready.noaa.gov/ready2-bin/profile2a.pl

ARL Home > READY > Archived Meteorology > GDAS1 Sounding

GDAS1 Sounding

GDAS1 Sounding for location: 37.16 -3.61

READY

Another sounding	Another product	Another location	Start over

```
File start time : 14  7 22  0  0
File ending time: 14  7 28 21  0
Chosen date in meteorological file:         14          7          22          12

YR: 2014   MON: 07   DAY: 22   HOUR: 12    AT POSITION: 357.4 128.2  LAT.: 37.16  LON.:  -3.61
PRSS:     0.9169E+03
MSLP:     0.1016E+04
TPP6:     0.0000E+00
UMOF:     0.1810E-01
VMOF:    -0.8032E-01
SHTF:     0.2457E+03
DSWF:     0.6276E+03
RH2M:     0.2975E+02
U10M:    -0.1930E+00
V10M:     0.2643E+01
T02M:     0.3012E+03
TCLD:     0.0000E+00
SHGT:     0.8937E+03
CAPE:     0.0000E+00
CINH:     0.0000E+00
LISD:     0.2771E+03
LIB4:     0.4349E+01
PBLH:     0.7327E+03
TMPS:     0.3160E+03
CPP6:     0.0000E+00
SOLM:     0.1796E+00
CSNO:     0.0000E+00
CICE:     0.0000E+00
CFZR:     0.0000E+00
CRAI:     0.0000E+00
```

MOLECULAR COMPONENT

How to obtain T and P profiles?

Option 2: if no radiosoundings nearby, use model data from NOAA

off-line

Download HYSPLIT software from:

https://ready.arl.noaa.gov/HYSPLIT.php

Download GDAS meteorological data from:

ftp://arlftp.arlhq.noaa.gov/pub/archives/gdas1/

MOLECULAR COMPONENT

How to obtain T and P profiles?

Option 2: if no radiosoundings nearby, use model data from NOAA

off-line

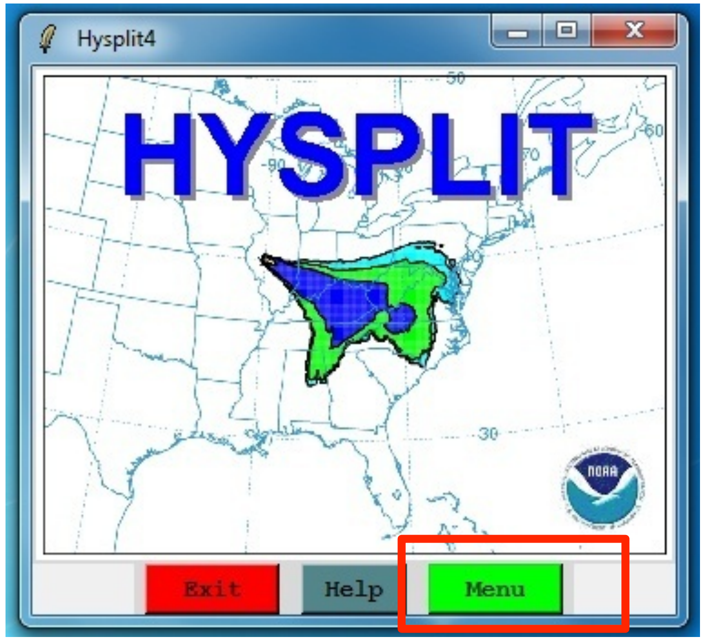

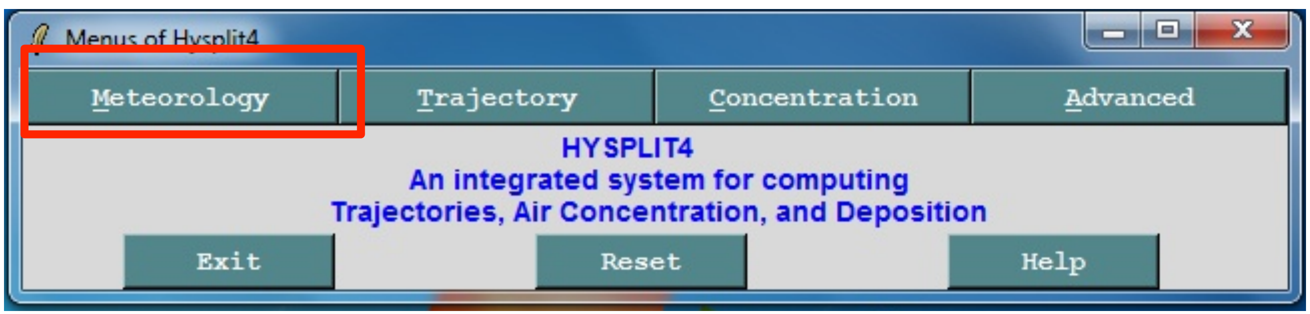

MOLECULAR COMPONENT

How to obtain T and P profiles?

Option 2: if no radiosoundings nearby, use model data from NOAA off-line

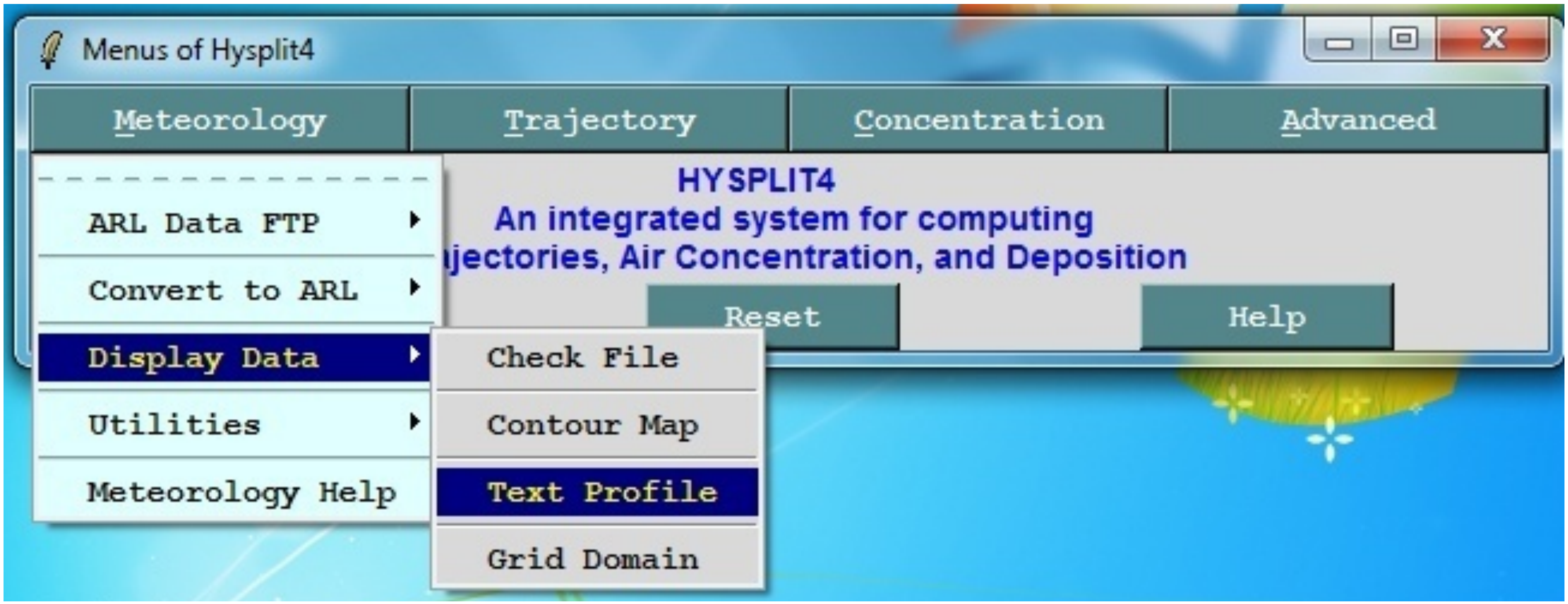

MOLECULAR COMPONENT

How to obtain T and P profiles?

Option 2: if no radiosoundings nearby, use model data from NOAA

off-line

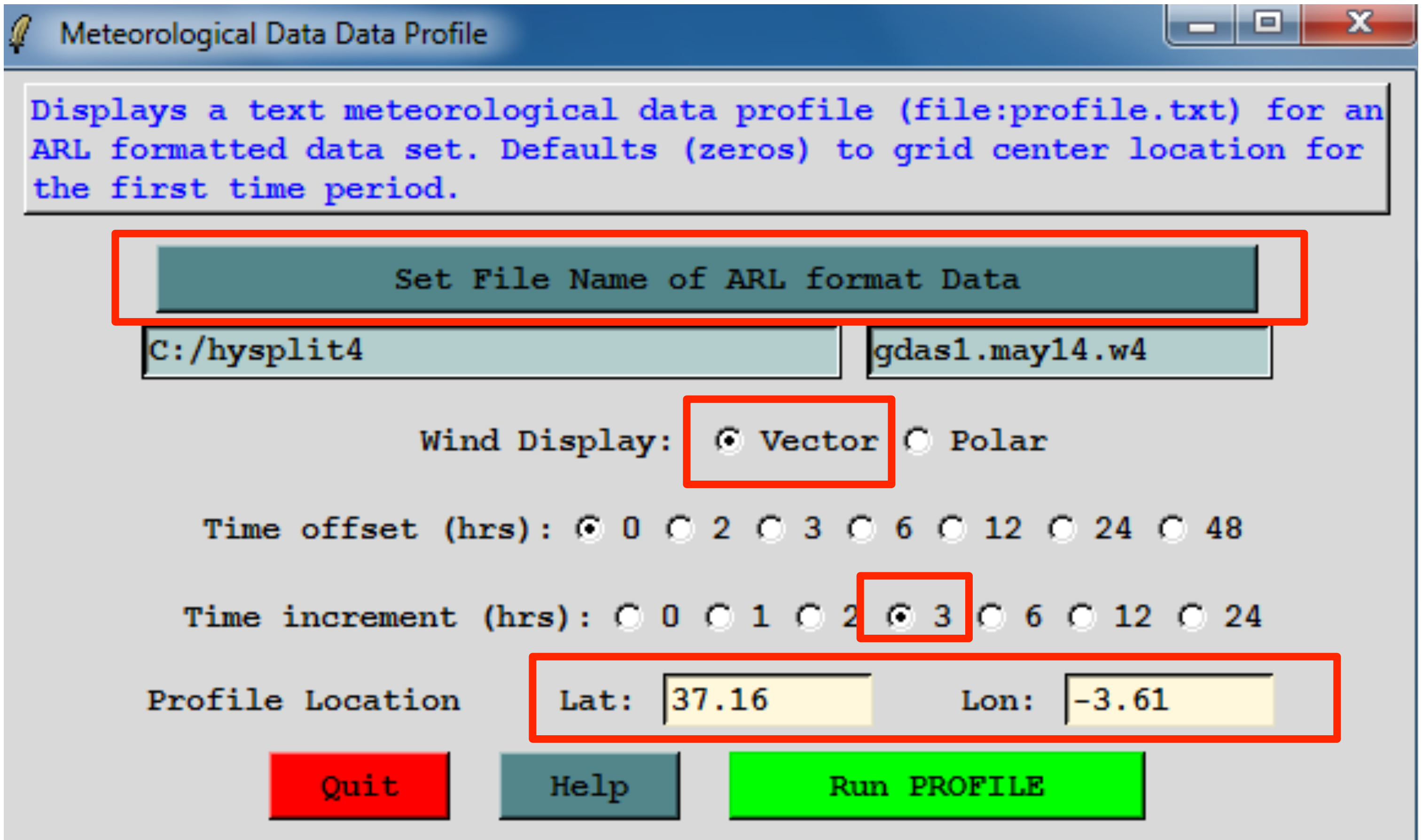

MOLECULAR COMPONENT

How to obtain T and P profiles?

Option 2: if no radiosoundings nearby, use model data from NOAA **off-line**

SIMULATION LOG

```
METEOROLOGICAL PROFILE LISTING ...
 Meteorological Profile: gdas1.may14.w4
 File start time : 14  5 22  0  0
 File ending time: 14  5 28 21  0


 Profile Time:   14  5 22  0  0
 Profile Location:    37.16   -3.61   (357,128)

        PRSS  MSLP  TPP6  UMOF  VMOF  SHTF  DSWF  RH2M  U10M
  SOLM  CSNO  CICE  CFZR  CRAI  LHTF  LCLD  MCLD  HCLD
         hPa          mm

   927   927  1015     0 -5E-2 -4E-2 -18.1  24.0  90.4   1.8
```

Exit

Radiosoundings for the whole week each 3 h are computed

Go to folder: …/hysplit4/working to find your file "profile.txt"

MOLECULAR COMPONENT

How to obtain T and P profiles?

Option 3: if no radiosoundings nearby, use standard atmosphere scaled to your surface temperature and pressure

Atmospheric layer(km)	dT/dz (K/km)
0-11	-6.5
11-20	0
20-32	1.0
32-47	2.8
47-51	0
51-71	-2.8
71-86	-2

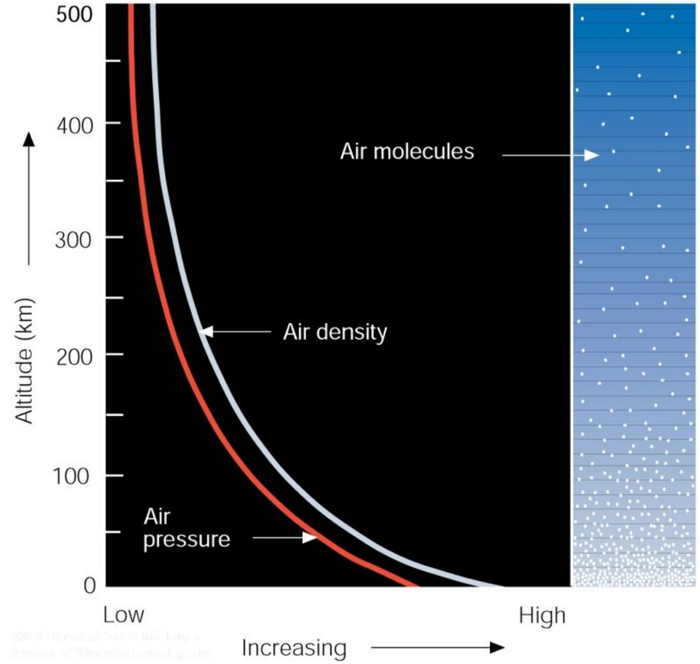

$$T = T_0 - \gamma \cdot z$$

$$p = p_0 \cdot e^{-\frac{z}{H}}$$

where T_0 and P_0 are measured surface temperature and pressure (co-located meteorological station) and H is the so-called "scaled height" with H=8.42 km

RAMAN METHOD

To solve the problems associated with the elastic backscatter lidar several solutions have been proposed

The Raman lidar measures lidar return signals elastically backscattered by air molecules and particles and inelastically (Raman) backscattered by nitrogen and/or oxygen molecules

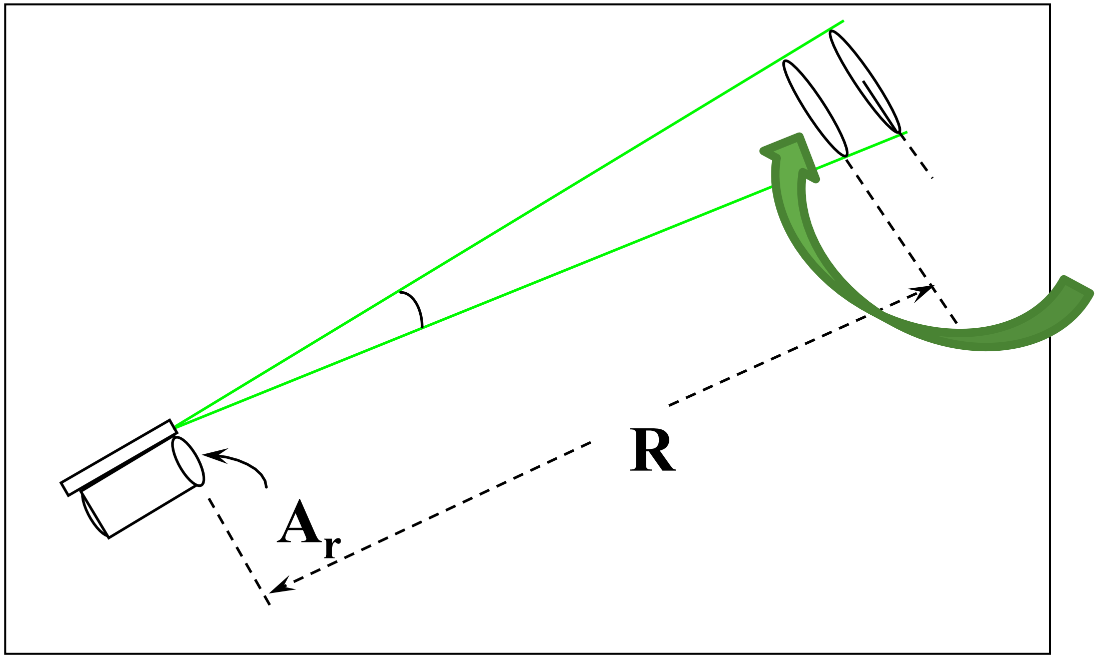

Raman lidar systems detect the wavelength-shifted molecular return produced by rotational and vibrational Raman scattering from the chosen molecule

RAMAN SCATTERING

Elastic scattering : scattered frequency <u>equal</u> to incident one

Raman scattering: scattered frequency <u>shifted</u> in a known amount depending on the scatterers

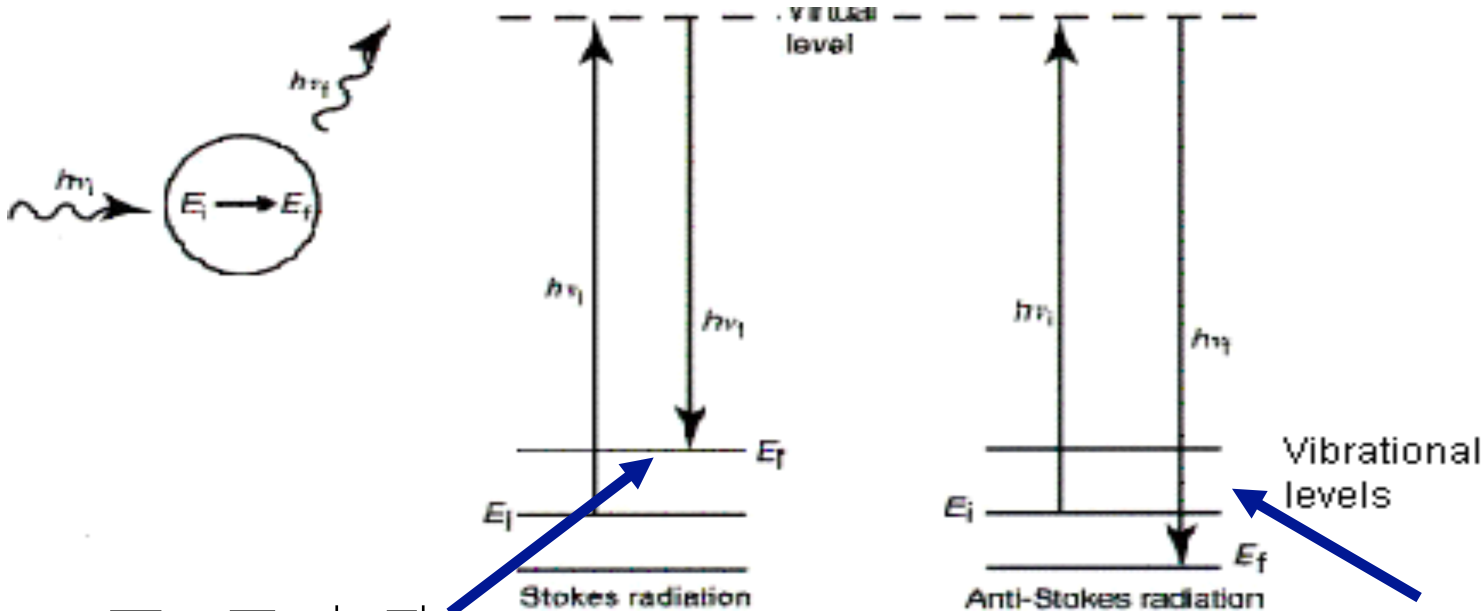

$$\overline{\nu}_s = \overline{\nu}_i - \left|\Delta\overline{\nu}\right|$$

(a)

(b)

$$\overline{\nu}_s = \overline{\nu}_i + \left|\Delta\overline{\nu}\right|$$

$$\Delta\overline{\nu} = \overline{\nu}_i - \overline{\nu}_s = \frac{\Delta E}{hc_0}$$

Key: this shift characterizes each molecule

RAMAN SCATTERING

Shifts for N_2 molecule:

Excitation wavelength (nm)	Shifted wavelength (nm)
355	387
488	551
532	607

The strength of Raman signals is a factor of 20 (rotational Raman lines) to 500 (vibration-rotational Raman lines) lower than the one of Rayleigh signals

The Raman lidar is mainly used during nighttime in absence of the strong daylight sky background

RAMAN LIDAR EQUATION

$$P(R,\lambda_{Raman}) = P_0(\lambda_L)\frac{C}{R^2}O(R)\beta_{Raman}(R,\lambda_{Raman})e^{-\int_0^R[\alpha(x,\lambda_L)+\alpha(x,\lambda_{Raman})]dx}$$

$P(R,\lambda_{Raman})$ = power received by the system after backscattering from range R

$P_o(\lambda_L)$= power transmitted

C = lidar calibration constant

$\beta_{Raman}(R,\lambda_{Raman})$ ($km^{-1}sr^{-1}$) is the Raman molecular backscatter coefficient

$\beta_{part}(R,\lambda_L)$ does not appear in the equation

The only particle scattering effect on the signal strength is the attenuation

$\alpha(R,\lambda_L)$ describes the extinction on the way up to the backscatter region and $\alpha(R,\lambda_{Raman})$ the extinction on the way back to the lidar

ELASTIC VS. RAMAN LIDAR EQUATION

$$P(R,\lambda_{Raman}) = P_0(\lambda_L)\frac{C_R}{R^2}O(R)\beta_{Raman}(R,\lambda_{Raman})e^{-\int_0^R[\alpha(x,\lambda_L)+\alpha(x,\lambda_{Raman})]dx}$$

$$P(R,\lambda_L) = P_0(\lambda_L)\frac{C}{R^2}O(R)\left[\beta_{part}(R,\lambda_L)+\beta_{mol}(R,\lambda_L)\right]e^{-2\int_0^R\alpha(x,\lambda_L)dx}$$

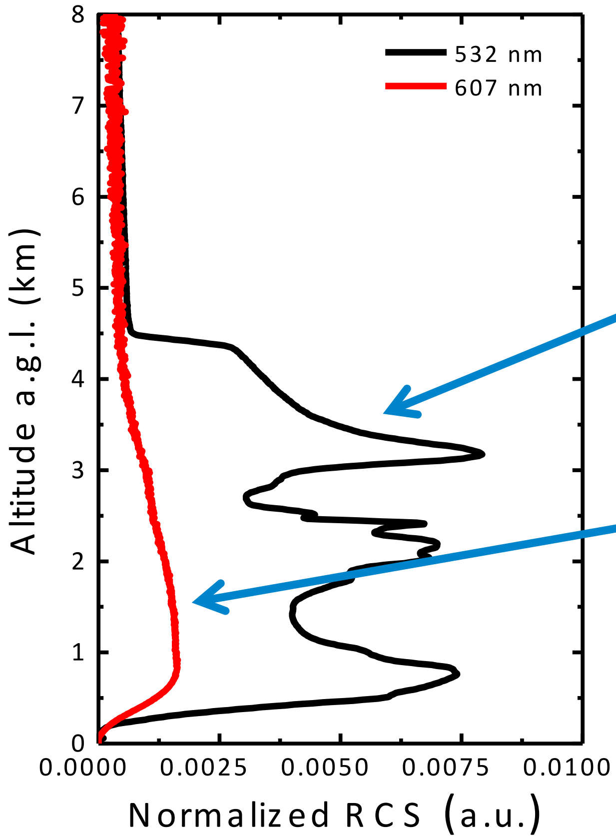

Elastic lidar signal (particles + molecules)

Raman lidar signal (molecule, N_2)

RAMAN METHOD: PARTICLE EXTINCTION

Starting point: Raman lidar equation

$$P(R,\lambda_{Raman}) = P_0(\lambda_L)\frac{C}{R^2}O(R)\beta_{Raman}(R,\lambda_{Raman})e^{-\int_0^R[\alpha(x,\lambda_L)+\alpha(x,\lambda_{Raman})]dx}$$

… some considerations:

- the overlap is assumed to be complete , O(R) =1 ➔ $R \geq R_{min}$
- $\beta_{Raman}(R,\lambda_{Raman})$ is calculated from the molecular number density N_{Raman} which is the N_2 or O_2 molecule number density and the Raman backscatter cross section:

$$\beta_{Raman}(R,\lambda_{Raman}) = N_{Raman}(R)\cdot\frac{d\sigma_{Raman}}{d\Omega}(\pi,\lambda_{Raman})$$

- N_{Raman} (R) is calculated from actual radio-sounding observations or standard atmosphere temperature and pressure profiles

RAMAN METHOD: PARTICLE EXTINCTION

After some operation on the Raman lidar equation that include the use of the Raman backscatter coefficient and the logarithm derivation of the equation, we obtain:

$$\alpha(R,\lambda_L) + \alpha(R,\lambda_{Raman}) = \frac{d}{dR}\ln\left[\frac{N_{Raman}(R)}{R.C.S.(R,\lambda_{Raman})}\right]$$

Total extinction coefficients are caused by particles and molecules. Therefore, the particle extinction coefficient is:

$$\alpha_{part}(R,\lambda_L) + \alpha_{part}(R,\lambda_{Raman}) =$$

$$= \frac{d}{dR}\ln\left[\frac{N_{Raman}(R)}{R.C.S.(R,\lambda_{Raman})}\right] - \alpha_{mol}(R,\lambda_L) - \alpha_{mol}(R,\lambda_{Raman})$$

RAMAN METHOD: PARTICLE EXTINCTION

To obtain the particle extinction coefficient at the transmitted wavelength we have to introduce the k-exponent which describes the wavelength dependence of the particle extinction coefficient for this spectral range:

$$\alpha_{part}(\lambda) \propto \lambda^{-k} \quad \Rightarrow \quad \alpha_{part}(\lambda_L) = \alpha_{part}(\lambda_{Raman})\left(\lambda_L / \lambda_{Raman}\right)^{-k}$$

$k \approx 1$ for particles at these "small" spectral ranges $[\lambda_L, \lambda_{Raman}]$

[355, 387] nm

[532, 607] nm

Solution:

$$\alpha_{part}(R,\lambda_L) = \frac{\dfrac{d}{dR}\ln\left[\dfrac{N_{Raman}(R)}{R.C.S.(R,\lambda_{Raman})}\right] - \alpha_{mol}(R,\lambda_L) - \alpha_{mol}(R,\lambda_{Raman})}{1+\left(\dfrac{\lambda_L}{\lambda_{Raman}}\right)^k}$$

(without any assumption on Lr_{part})

RAMAN METHOD: PARTICLE BACKSCATTER

Because now α_{part} (R) is known, β_{part}(R) can also be calculated using the elastic lidar equation

Elastic lidar equation:

$$P(R,\lambda_L) = P_0(\lambda_L)\frac{C}{R^2}O(R)\left[\beta_{part}(R,\lambda_L)+\beta_{mol}(R,\lambda_L)\right]e^{-2\int_0^R \alpha(x,\lambda_L)dx}$$

Raman lidar equation:

$$P(R,\lambda_{Raman}) = P_0(\lambda_L)\frac{C_R}{R^2}O(R)\beta_{Raman}(R,\lambda_{Raman})e^{-\int_0^R\left[\alpha(x,\lambda_L)+\alpha(x,\lambda_{Raman})\right]dx}$$

where $$\beta_{Raman}(R,\lambda_{Raman}) = N_{Raman}(R)\cdot\frac{d\sigma_{Raman}}{d\Omega}(\pi,\lambda_{Raman})$$

By forming the ratio: $$\frac{P(R,\lambda_L)P(R_0,\lambda_{Raman})}{P(R_0,\lambda_L)P(R,\lambda_{Raman})}$$

RAMAN METHOD: PARTICLE BACKSCATTER

Inserting the respective lidar equations and rearranging the resulting equation, the solution is:

$$\beta_{part}(R,\lambda_L) = -\beta_{mol}(R,\lambda_L) + \left[\beta_{part}(R_0,\lambda_L) + \beta_{mol}(R_0,\lambda_L)\right] \frac{P(R,\lambda_L)P(R_0,\lambda_{Raman})N_{Raman}(R)}{P(R_0,\lambda_L)P(R,\lambda_{Raman})N_{Raman}(R_0)} \cdot \frac{\exp\left\{-\int_{R_0}^{R}\left[\alpha_{part}(x,\lambda_{Raman}) + \alpha_{mol}(x,\lambda_{Raman})\right]dx\right\}}{\exp\left\{-\int_{R_0}^{R}\left[\alpha_{part}(x,\lambda_L) + \alpha_{mol}(x,\lambda_L)\right]dx\right\}}$$

- overlap effects cancel out because β_{part} is determined from the ratio of two lidar equations: β_{part} is determined even at R very close to the lidar
- the air density, β_{mol} and α_{mol} must be estimated from measured or standard atmosphere profiles of pressure and temperature
- lidar signals are measured by the instrument
- as in the Klett method, a reference value for β_{part} at R_o must be estimated. It is recommended to choose R_o in the upper troposphere where particle scattering is negligible compared to Rayleigh scattering

RAMAN METHOD: LIDAR RATIO

Finally, the height profile of the particle lidar ratio can be derived through the independent determination of α_{part} and β_{part}:

$$L_{part}(R,\lambda_L) = \frac{\alpha_{part}(R,\lambda_L)}{\beta_{part}(R,\lambda_L)}$$

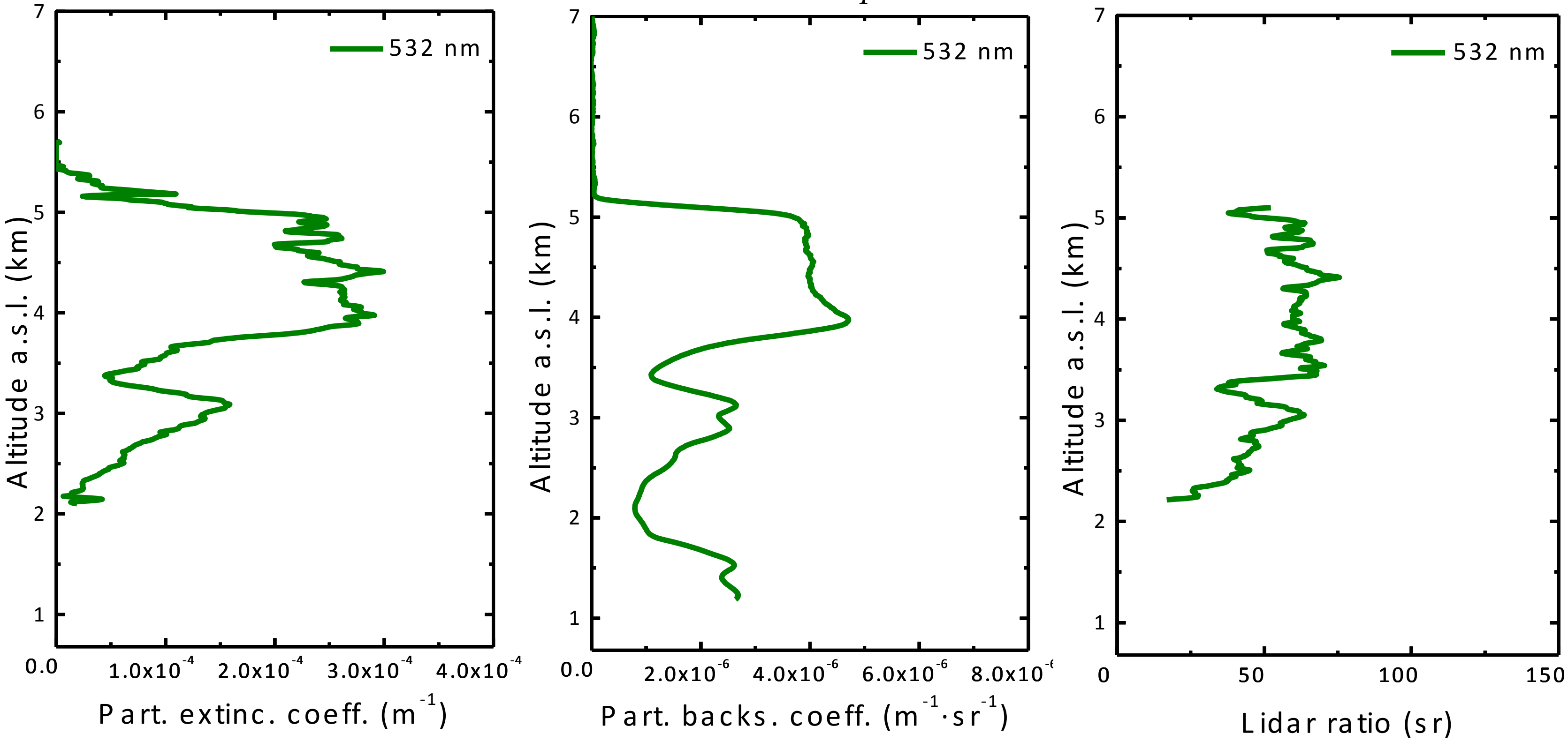

IISTA

USP

IFUSP

SUMMARY ON RAMAN METHOD

- The Raman method allows for independently determining the $\alpha_{part}(R)$ and $\beta_{part}(R)$, and therefore also $L_{part}(R)$
- Lidar ratio assumptions or other critical assumptions are not needed
- The reference range R_o is usually chosen such that β_{part} at R_o is negligible compared to the known β_{mol}
- β_{part} can be obtained even at altitudes very close to the lidar, due to overlap effects are canceled out because β_{part} is determined from the ratio of two lidar equations
- Multiwavelength Raman lidar provides this information at several wavelengths. The “multiwavelength“ information allows obtaining particle microphysical properties

RECOMMENDED BIBLIOGRAPHY

WEITKAMP, C., Lidar. Range-resolved optical remote sensing of the Atmosphere, Springer, New York, 2005. **Chapter 9**.

Ansmann, A., U. Wandinger, M. Riebesell, C. Weitkamp, and W. Michaelis, Independent measurement of extinction and backscatter profiles in cirrus clouds by using a combined Raman elastic-backscatter lidar, Appl. Opt., 31, 7113-7131 (1992)

LIDAR DEPOLARIZATION

- A fundamental principle of light is that the electric field **E**-vector of the electromagnetic wave at any instant of time displays some orientation in space
- This orientation can be fixed (linearly polarized light), rotating with time (circularly or elliptically polarized light) and randomly changing with time (natural light). Importantly, any state of polarization can be converted to any other state with the help of a set of optical devices
- Pulsed lasers generally used in lidars produce linearly polarized light
- The lidar depolarization technique involves the transmission of a linearly polarized laser pulse and the detection via a beam splitter of the perpendicular and parallel planes of polarization of the backscattered light

LIDAR DEPOLARIZATION

- According to Mie theory, spherical particles always backscatter linearly polarized electromagnetic radiation in the same (incident) plane of polarization. A variety of approximate scattering theories predict that non-spherical particles introduce a depolarized component into the backscattered radiation

- Application of depolarization measurements is discrimination of spherical versus non-spherical aerosol particles and liquid and solid phase clouds

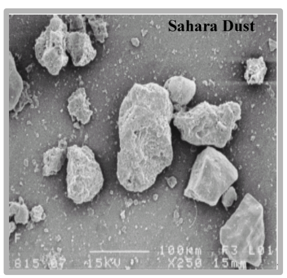

LIDAR DEPOLARIZATION

Types of depolarization lidar systems

Detection perpendicular and parallel

Detection perpendicular and total

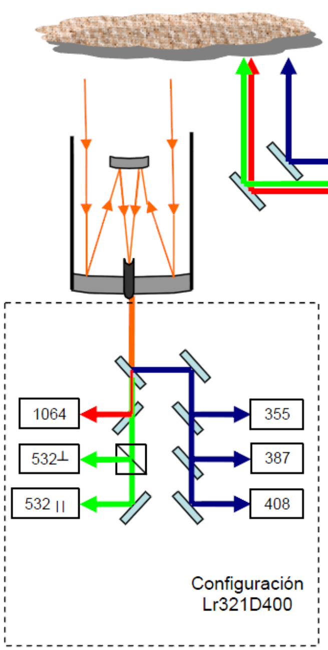

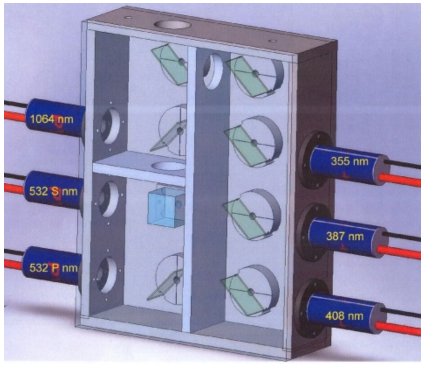

Granada lidar (MULHACÉN)

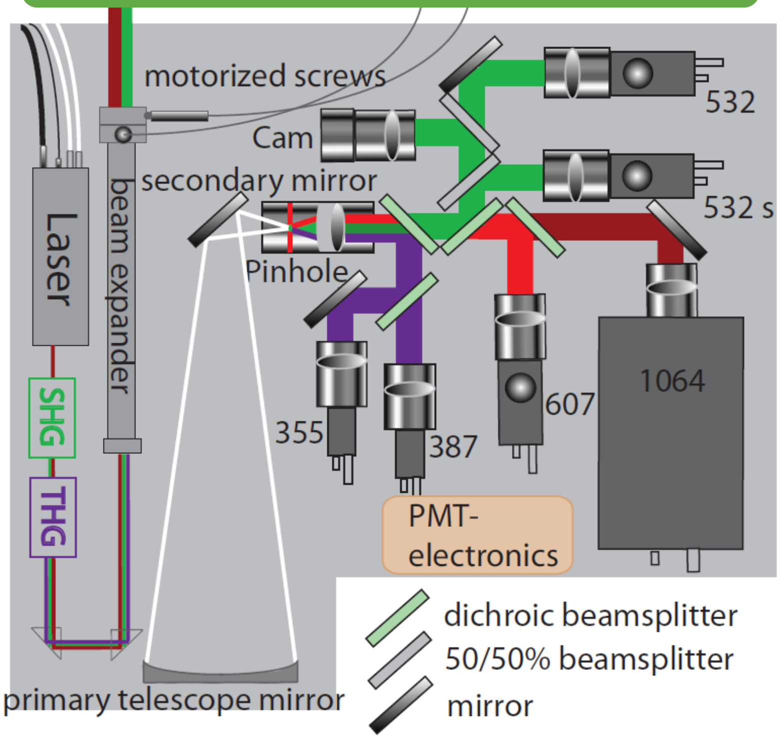

Évora lidar (PAOLI)

LIDAR DEPOLARIZATION

Starting point: elastic lidar equation

$$P(R,\lambda) = P_o(\lambda)\frac{C}{R^2}O(R)\beta(R,\lambda)\,e^{-2\int_0^R \alpha(x,\lambda)\,dx}$$

Lidars use polarized light, and many of them are able to discriminate between components. The elastic lidar equations for both components are (dropping the wavelength dependence):

$$P^{\parallel}(R) = P_o\frac{C^{\parallel}}{R^2}O(R)\beta^{\parallel}(R)\,e^{-2\int_0^R \alpha^{\parallel}(x)\,dx}$$

$$P^{\perp}(R) = P_o\frac{C^{\perp}}{R^2}O(R)\beta^{\perp}(R)\,e^{-\int_0^R \left[\alpha^{\parallel}(x)+\alpha^{\perp}(x)\right]dx}$$

Initial definition of “depolarization ratio”:

$$"\delta(R)" = \frac{C^{\perp}\beta^{\perp}(R)\,e^{-\int_0^R \left[\alpha^{\parallel}(x)+\alpha^{\perp}(x)\right]dx}}{C^{\parallel}\beta^{\parallel}(R)\,e^{-2\int_0^R \alpha^{\parallel}(x)\,dx}} = \frac{\beta^{\perp}(R)}{\beta^{\parallel}(R)}\,e^{\int_0^R \left[\alpha^{\parallel}(x)-\alpha^{\perp}(x)\right]dx} \approx \frac{\beta^{\perp}(R)}{\beta^{\parallel}(R)}$$

LIDAR DEPOLARIZATION

Several definitions:

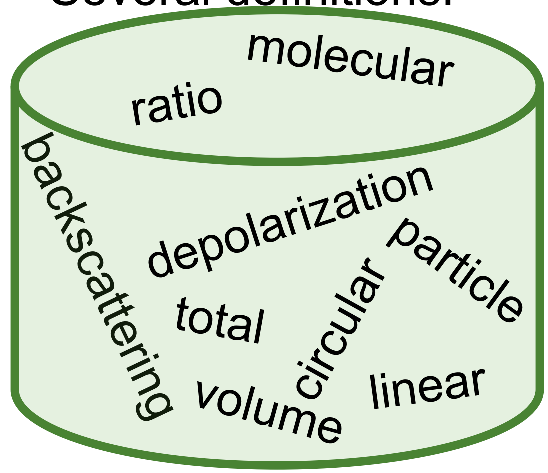

Mess came from the beginning:
- different instrumental setups
- different research interests

1-. Volume linear depolarization ratio:

$$\delta_v(R) = \frac{\beta^{\perp}(R)}{\beta^{\parallel}(R)} = \frac{\beta^{\perp}_{part}(R) + \beta^{\perp}_{mol}(R)}{\beta^{\parallel}_{part}(R) + \beta^{\parallel}_{mol}(R)} = \frac{C^{\parallel}}{C^{\perp}} \frac{P^{\perp}(R)}{P^{\parallel}(R)} = K_{cal} \frac{P^{\perp}(R)}{P^{\parallel}(R)}$$

Features:
-components: particles and molecules
- signals: cross and parallel
-no processing on raw data
-no overlap effects

LIDAR DEPOLARIZATION

Table of depolarization's parameters

Parameter	Symbol	Features	Formula
volume linear depolarization ratio	δ_v	Part.+mol ; cross and parallel; raw data	-
volume linear depolarization ratio (total)			
particle linear depolarization ratio			
particle linear depolarization ratio (total)			

2-. Volume linear depolarization ratio (total):

$$\delta_v^{total}(R) = \frac{\beta^{\perp}(R)}{\beta^{total}(R)} = \frac{\beta^{\perp}(R)}{\beta^{\perp}(R)+\beta^{\parallel}(R)} = \frac{\beta^{\perp}_{part}(R)+\beta^{\perp}_{mol}(R)}{\beta^{\perp}_{part}(R)+\beta^{\perp}_{mol}(R)+\beta^{\parallel}_{part}(R)+\beta^{\parallel}_{mol}(R)} =$$

$$= \frac{C^{total}}{C^{\perp}}\frac{P^{\perp}(R)}{P^{total}(R)} = K_{cal}\frac{P^{\perp}(R)}{P^{total}(R)}$$

… definitions of δ_v and δ_v^{total}:

$$\delta_v(R) = \frac{\beta^{\perp}(R)}{\beta^{\parallel}(R)}$$

$$\delta_v^{total}(R) = \frac{\beta^{\perp}(R)}{\beta^{\perp}(R)+\beta^{\parallel}(R)}$$

$$\delta_v^{total}(R) = \frac{\delta_v(R)}{\delta_v(R)+1}$$

Features:
- components: part. and mol.
- signals: cross and total
- no processing on raw data
- no overlap effects

LIDAR DEPOLARIZATION

Table of depolarization's parameters

Parameter	Symbol	Features	Formula
volume linear depolarization ratio	δ_v	Part.+mol; cross and parallel; raw data	-
volume linear depolarization ratio (total)	δ_v^{total}	Part.+mol ; cross and total; raw data	$\delta_v^{total}(R) = \dfrac{\delta_v(R)}{\delta_v(R)+1}$
particle linear depolarization ratio			
particle linear depolarization ratio (total)			

3-. Particle linear depolarization ratio:

$$\delta_{part}(R) = \frac{\beta^{\perp}_{part}(R)}{\beta^{\parallel}_{part}(R)} = \frac{R_{backs}\delta_v(\delta_{mol}+1) - \delta_{mol}(\delta_v+1)}{R_{backs}(\delta_{mol}+1) - (\delta_v+1)}$$

$$R_{backs} = \frac{\beta_{part}+\beta_{mol}}{\beta_{mol}}$$ backscattering ratio (range dependent)

$$\delta_{mol} = \frac{\beta^{\perp}_{mol}}{\beta^{\parallel}_{mol}}$$ molecular depolarization (range independent)

Features:
- -components: particles
- -signals: cross and parallel
- -retrieved backscatter coeff.
- -overlap effects if K-F is used

LIDAR DEPOLARIZATION

Table of depolarization's parameters

Parameter	Symbol	Features	Formula
volume linear depolarization ratio	δ_v	Part.+mol; cross and parallel; raw data	-
volume linear depolarization ratio (total)	δ_v^{total}	Part.+mol ; cross and total; raw data	$\delta_v^{total} = \frac{\delta_v}{\delta_v + 1}$
particle linear depolarization ratio	δ_{part}	Part. ; cross and parallel; retrieved data	$\delta_{part} = \frac{R_{backs}\delta_v(\delta_{mol}+1) - \delta_{mol}(\delta_v+1)}{R_{backs}(\delta_{mol}+1) - (\delta_v+1)}$
particle linear depolarization ratio (total)			

4-. Particle linear depolarization ratio (total):

$$\delta_{part}^{total}(R) = \frac{\beta_{part}^{\perp}(R)}{\beta_{part}^{total}(R)} = \frac{R_{backs}\delta_v(\delta_{mol}+1) - \delta_{mol}(\delta_v+1)}{(\delta_{mol}+1)(\delta_v+1)(R_{backs}-1)}$$

Features:

- -components: particles
- -signals: cross and total
- -retrieved backscatter coeff.
- -overlap effects if K-F is used

… definitions of δ_{part} and δ_{part}^{total}:

$$\delta_{part}(R) = \frac{\beta_{part}^{\perp}(R)}{\beta_{part}^{\parallel}(R)}$$

$$\delta_{part}^{total}(R) = \frac{\beta_{part}^{\perp}(R)}{\beta_{part}^{total}(R)}$$

$$\delta_{part}^{total}(R) = \frac{\delta_{part}(R)}{\delta_{part}(R) + 1}$$

LIDAR DEPOLARIZATION

Summary of depolarization's parameters

Parameter	Symbol	Features	Formula
volume linear depolarization ratio	δ_v	Part.+mol; cross and parallel; raw data	-
volume linear depolarization ratio (total)	δ_v^{total}	Part.+mol ; cross and total; raw data	$\delta_v^{total} = \frac{\delta_v}{\delta_v + 1}$
particle linear depolarization ratio	δ_{part}	Part. ; cross and parallel; retrieved data ´	$\delta_{part} = \frac{R_{backs}\delta_v(\delta_{mol}+1) - \delta_{mol}(\delta_v+1)}{R_{backs}(\delta_{mol}+1) - (\delta_v+1)}$
particle linear depolarization ratio (total)	δ_{part}^{total}	Part. ; cross and total; retrieved data	$\delta_{part}^{total} = \frac{R_{backs}\delta_v(\delta_{mol}+1) - \delta_{mol}(\delta_v+1)}{(\delta_{mol}+1)(\delta_v+1)(R_{backs}-1)}$

IISTA Instituto Interuniversitario de Investigación del Sistema Tierra en Andalucía

USP

IFUSP Instituto de Física da USP

LIDAR DEPOLARIZATION

- great range of aerosol shapes

- many aerosols consist of spherical particles: very small aerosols (small size parameter), anthropogenic aerosols, volcanic acid sulfuric droplets, sea drops released by the action of wind on water waves… All shows low volume linear depolarization ratio

- irregularly shaped aerosols (particularly volcanic and desert dusts and partially crystallized acid droplets) show larger volume linear depolarization ratio

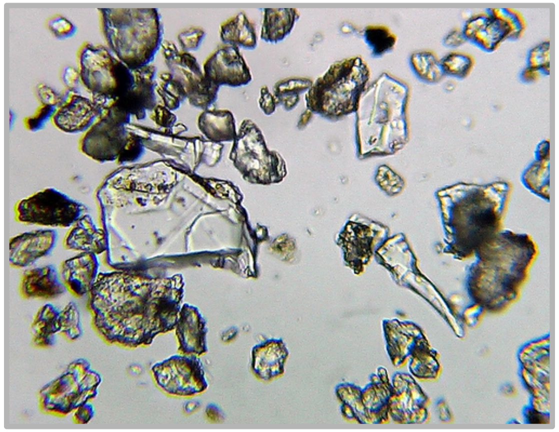

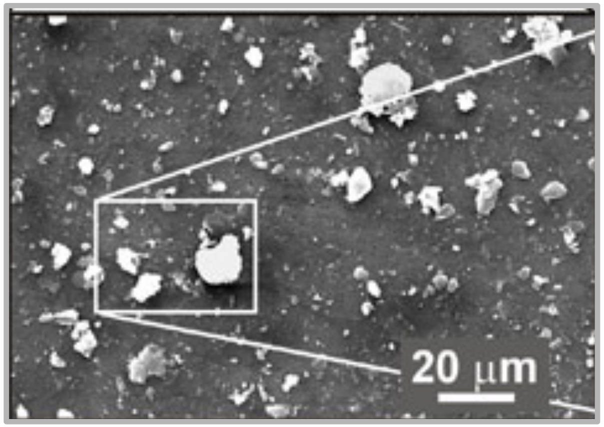

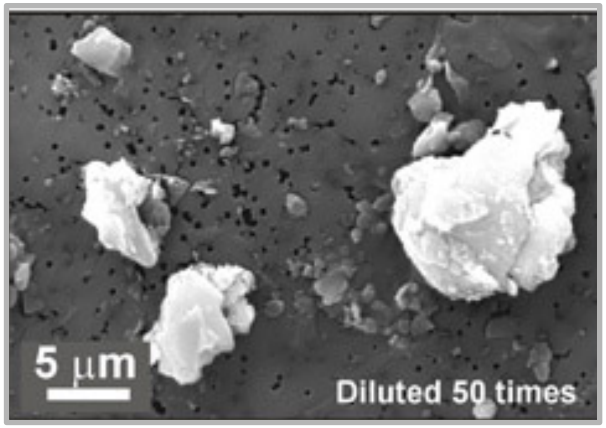

IISTA

USP

IFUSP

LIDAR DEPOLARIZATION

Aerosol type	Volume linear depol. ratio
arctic haze	~ 0.013
PBL (anthropogenic)	0.02-0.10
ammonium sulfate droplets	0.02
ammonium sulfate after crystallization	0.10-0.12
NaCl droplets partially crystallized	0.06-0.12
desert dust (Sahara)	~ 0.15-0.30
desert dust (Gobbi)	~ 0.18
desert dust (Taklamakan)	0.11-0.19

LIDAR DEPOLARIZATION

R.C.S. 532 nm

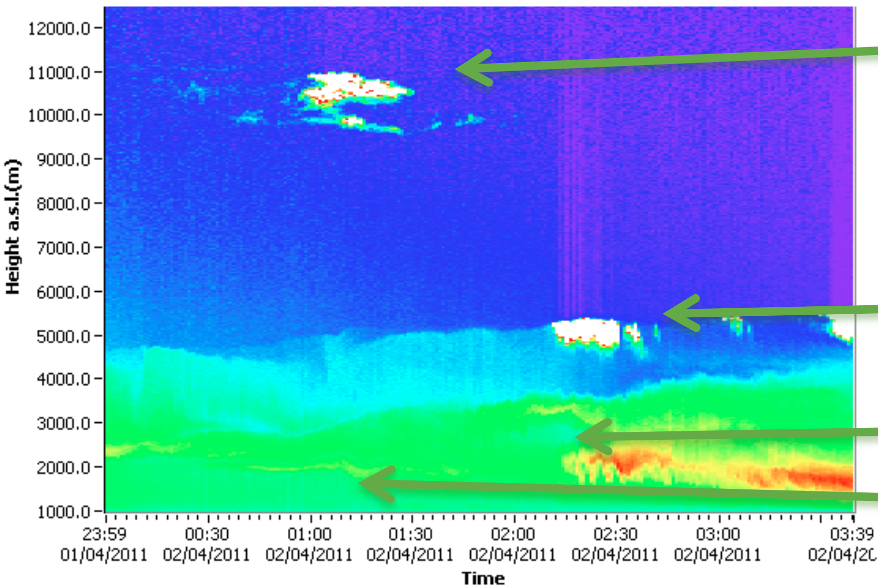

Volume linear depolarization ratio

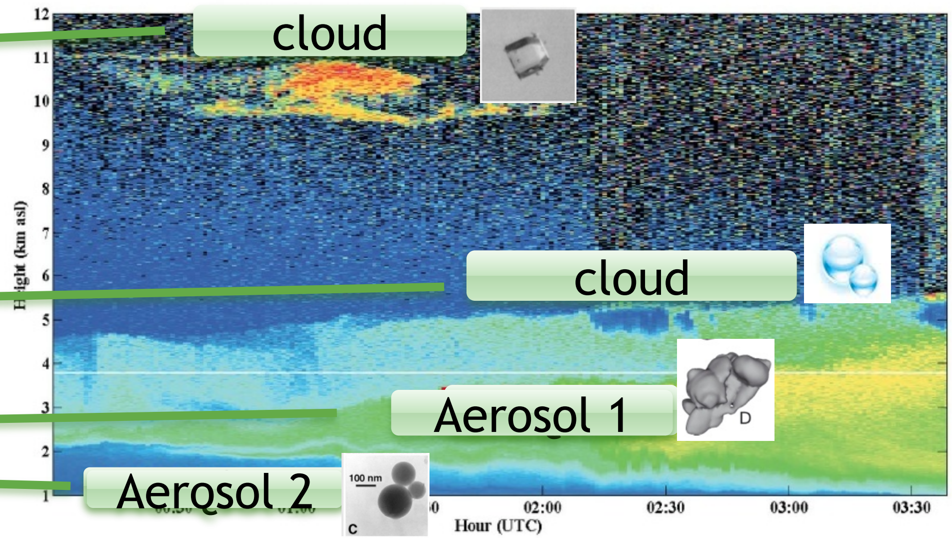

SUMMARY ON LIDAR DEPOLARIZATION

- The lidar depolarization technique is based on the fact that spherical particles always backscatter linearly polarized electromagnetic radiation in the same plane of polarization, whereas non-spherical particles introduce a depolarized component into the backscattered radiation

- Due to the different definitions for depolarization parameters, it's necessary to clarify what is used (parallel vs. total; particles vs. particles+molecules)

- Mainly, spherical particles show $\delta_v < 0.10$ and non-spherical particles show δ_v ~0.15-0.30

RECOMMENDED BIBLIOGRAPHY

WEITKAMP, C., Lidar. Range-resolved optical remote sensing of the Atmosphere, Springer, New York, 2005. **Chapter 2 (introduction and some cloud applications)**.

ASCENDING OUTLINE

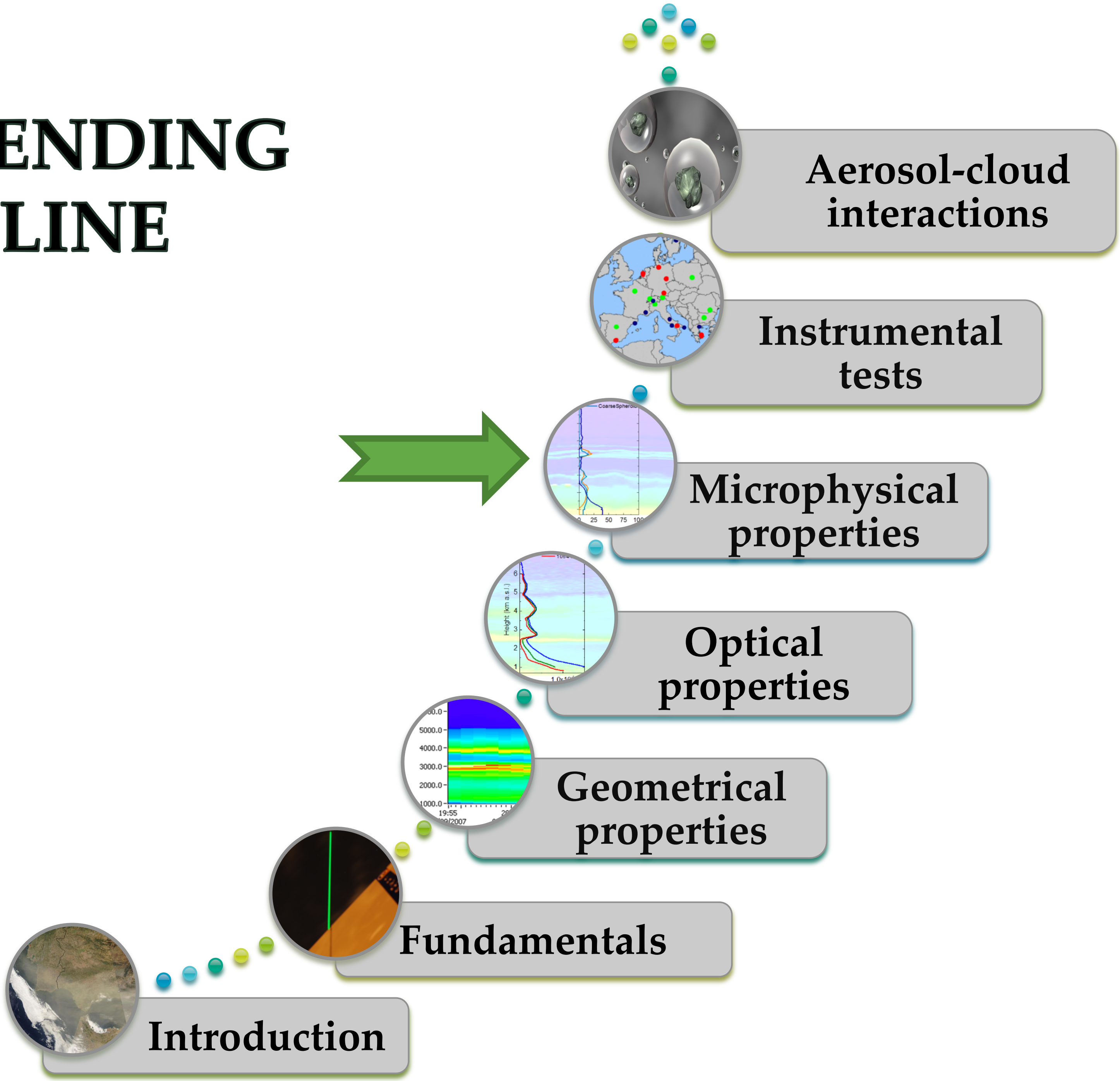

MICROPHYSICAL PROPERTIES

In nature, particle size distributions can be described rather well by analytic expressions such as logarithmic-normal distributions:

$$\mathrm{d}n(r) = \frac{n_\mathrm{t}}{\sqrt{2\pi}\,\ln\sigma}\exp\left[-\frac{\left(\ln r - \ln r_{\mathrm{mod,N}}\right)^2}{2\,(\ln\sigma)^2}\right]\mathrm{d}\ln r$$

$dn(r)$	number concentration of particles in the radius interval $[\ln r, \ln r + d\ln r]$
n_t	total number concentration
$n_{\mathrm{mod},N}$	mode radius with respect to the number concentration
σ	mode width (geometric standard deviation)

This is a monomodal distribution, however multimodal distributions (i.e. sum of ≥2 monomodal distributions) can be found

MICROPHYSICAL PROPERTIES

From the number concentration, other distributions can be obtained:

Number concentration distribution:

$$dn(r) = \frac{n_t}{\sqrt{2\pi}\ln\sigma}\exp\left[-\frac{\left(\ln r - \ln r_{\mathrm{mod,N}}\right)^2}{2\left(\ln\sigma\right)^2}\right] d\ln r$$

Surface-area concentration distribution:

$$da(r) = 4\pi r^2 dn(r)$$

Volume concentration distribution:

$$dv(r) = \frac{4}{3}\pi r^3 dn(r)$$

Integrated properties of the particle ensemble determined from the inverted distributions are:

Effective radius:

$$r_{\mathrm{eff}} = \frac{\int n(r)\, r^3\, dr}{\int n(r)\, r^2\, dr}$$

Total surface-area concentration:

$$a_t = 4\pi \int n(r)\, r^2\, dr$$

Total volume concentration:

$$v_t = \frac{4\pi}{3}\int n(r)\, r^3\, dr$$

MICROPHYSICAL PROPERTIES

A variety of methods have been proposed since the early 1970s. Examples:

Combined use of elastic lidar with other instruments

IF SUNPHOTOMETER IS USED:

- the drawback is that two colocated instruments are needed simultaneously to provide reliable data on the same particles
- different observational geometry of the instrumentation
- thus represents an additional source
- only daytime data

Inversion with regularization from Raman lidar

- uses the spectral information contained in the backscatter and extinction profiles at several wavelengths and its change with the particle size
- limitation in number of wavel.
- in most cases only night time data
- high data quality

IISTA

USP

IFUSP

METHOD OF INVERSION WITH REGULATIZATION

It is the standard method for the retrieval of particle microphysical properties from multiwavelength Raman lidar observations

Input: spectrally resolved particle backscatter and extinction coefficients

The optical data are related to the physical quantities by the Fredholm integral equations of the first kind:

$$g_i(\lambda_k) = \int_{r_{\min}}^{r_{\max}} K_i(r, m, \lambda_k, s) v(r) dr + \varepsilon_i^{\exp}(\lambda_k)$$

$$i = \beta_{aer}\,,\ \alpha_{aer}\,, \quad k = 1, \ldots, n$$

METHOD OF INVERSION WITH REGULATIZATION

$$g_i(\lambda_k) = \int_{r_{\min}}^{r_{\max}} K_i(r, m, \lambda_k, s) v(r) dr + \varepsilon_i^{\exp}(\lambda_k)$$

$$i = \beta_{aer}, \alpha_{aer}, \quad k = 1, \ldots, n$$

$g_i(\lambda_k)$ — optical data at wavelengths λ_k at a specific height R

i — kind of information, i.e., whether it is the particle backscatter or extinction coefficient

k — wavelength: 355, 532 and 1064 nm

$\varepsilon_i^{\exp}(\lambda_k)$ — experimental error of backscatter or extinction coefficients

METHOD OF INVERSION WITH REGULATIZATION

$$g_i(\lambda_k) = \int_{r_{\min}}^{r_{\max}} K_i(r,m,\lambda_k,s)v(r)dr + \varepsilon_i^{\exp}(\lambda_k)$$

$$i = \beta_{aer}\,,\ \alpha_{aer}\,,\quad k=1,\ \ldots,\ n$$

$K_i(r,m,\lambda_k,s)$ kernel functions of backscatter and extinction, depending on radius, complex refractive index, wavelength and shape of particles

For spherical particles, are calculated from the respective extinction and backscatter efficiencies for individual particles weighted with their geometrical cross section πr^2

$$K_i(r,m,\lambda,s) = \frac{3}{4r} Q_i(r,m,\lambda)$$

$v(r)$ volume concentration distribution of particles

METHOD OF INVERSION WITH REGULATIZATION

$$g_i(\lambda_k) = \int_{r_{\min}}^{r_{\max}} K_i(r, m, \lambda_k, s) v(r) dr + \varepsilon_i^{\exp}(\lambda_k)$$

$$i = \beta_{aer}, \alpha_{aer}, \quad k = 1, \ldots, n$$

$r_{\min}$ radius down to which particles are optically efficient. For measurements ≥ 355 nm (typical in lidars), the minimum particle size is 50 nm (in radius)

$r_{\max}$ radius at which concentrations are so low that particles no longer contribute significantly to the signal (typically ≤ 10 microns in troposphere)

METHOD OF INVERSION WITH REGULATIZATION

To simplify, the subscript p will be used summarizing the kind and wavelength of optical data:

$$g_p = \int_{r_{\min}}^{r_{\max}} K_p(r,m)v(r)dr + \varepsilon_p^{\exp} \qquad \text{where} \quad p = (i,\ \lambda_k)$$

- it can not be solved analytically
- the microphysical retrieval from lidars is an ill-posed inverse problem
- incompleteness of the available information: small number of wavelengths and only backscatter and extinction information is available
- non-uniqueness of the solutions: highly complex structure of tropospheric aerosols (maybe multimodal , of variable shape, particle refractive index can be wavelength-dependent)

METHOD OF INVERSION WITH REGULATIZATION

- even uncertainties as small as round-off errors in the input data lead to disproportionately large changes in the final solution

- measurement errors are much larger than round-off errors

- different combinations of microphysical parameters may lead to similar optical properties within the measurement uncertainty

- many improvements have been done during the last decade. The most important: the reduction of measurement wavelengths to a realistic number

- the **minimum number of wavelengths is three** (355, 532 and 1064 nm) assuming simplifications for complex refractive index: the so-called 3+2 lidar systems (3 backscatters, 2 extinctions)

- the accuracy increases if backscatter up to six wavelengths are used

METHOD OF INVERSION WITH REGULATIZATION

To solve the equation: $$g_p = \int_{r_{\min}}^{r_{\max}} K_p(r,m)v(r)dr + \varepsilon_p^{\exp}$$ where $p = (i,\ \lambda_k)$

… v(r) is discretized by a linear combination of triangular base functions $B_j(r)$ and weight factors w_j as …

$$v(r) = \sum_i w_j B_j(r) + \varepsilon^{math}(r)$$

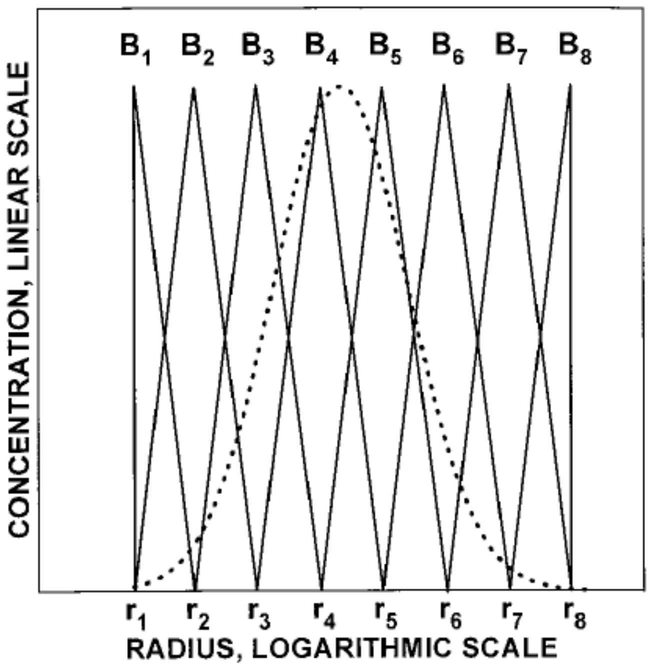

- $\varepsilon^{math}(r)$ is the mathematical residual error caused by the approximation with base functions
- $B_j(r)$ are distributed equidistantly on a logarithmic scale (to reproduce the high dinamic range of particle size distributions)
- minimum number of $B_j(r)$ is the number of input parameters
- typical number of $B_j(r)$ is 8

METHOD OF INVERSION WITH REGULATIZATION

In general the exact position of the investigated particle size distribution over the size range used is not known

To solve this: used of a inversion window of variable width and variable position over the investigated size range

No sensible solutions are obtained if the inversion window does not cover the position of the investigated particle size distribution

Currently 50 different inversion windows within the particle size range from 0.01 to 10 μm are used to obtain an estimate of the position of the particle size distribution

METHOD OF INVERSION WITH REGULATIZATION

Rewriting the equations into a vector-matrix equation:

$$\mathbf{g} = \mathbf{A}\mathbf{w} + \boldsymbol{\varepsilon}$$

$\mathbf{g} = [g_p]$	$\mathbf{A} = [A_{pj}]$	$\mathbf{w} = [w_j]$	$\boldsymbol{\varepsilon} = [\varepsilon_p]$
optical data	weight matrix	weight factors	errors

$$A_{pj}(m) = \int_{r_{min}}^{r_{max}} K_p(r,m) B_j(r)\, dr$$

$$\varepsilon_p = \varepsilon_p^{exp} + \varepsilon_p^{math}$$

The simple solution of this equation for the weight factors is:

$$\mathbf{w} = \mathbf{A}^{-1}\mathbf{g} + \boldsymbol{\varepsilon}'$$

IISTA USP IFUSP

METHOD OF INVERSION WITH REGULATIZATION

$$\mathbf{w} = \mathbf{A}^{-1}\,\mathbf{g} + \boldsymbol{\varepsilon}'$$

It fails to provide reasonable results although the optical data can be reproduced within the error limits **ε**. Why?

High dynamic range of several orders of magnitude of the elements of **A** and $\mathbf{A}^{-1}$

The term **ε' = -**$\mathbf{A}^{-1}$ **ε,** which describes the respective errors, and $\mathbf{A}^{-1}$, which denotes the inverse of the matrix **A**, lead to error amplification of the solutions

How to solve it? Application of a procedure called regularization

METHOD OF INVERSION WITH REGULATIZATION

Procedure of regularization: it is used to reduce the number of solutions by restricting the highest acceptable difference between the vector **Aw** and **g**:

$$e^2 \geq \|\varepsilon\|^2 = \|Aw - g\|^2$$

Only solutions that minimize **ε** are accepted

However, due to smoothed size distributions are expected, the penalty function Γ(*v*) is introduced and the minimization problem is rewritten as:

$$e^2 \geq \|\varepsilon\|^2 = \|Aw - g\|^2 + \gamma\Gamma(v)$$

where $\Gamma(v) = \mathbf{w}^T \mathbf{H} \mathbf{w}$

transposed vector **w**

$$\mathbf{H} = \begin{bmatrix} 1 & -2 & 1 & 0 & 0 & 0 & 0 & 0 \\ -2 & 5 & -4 & 1 & 0 & 0 & 0 & 0 \\ 1 & -4 & 6 & -4 & 1 & 0 & 0 & 0 \\ 0 & 1 & -4 & 6 & -4 & 1 & 0 & 0 \\ 0 & 0 & 1 & -4 & 6 & -4 & 1 & 0 \\ 0 & 0 & 0 & 1 & -4 & 6 & -4 & 1 \\ 0 & 0 & 0 & 0 & 1 & -4 & 5 & -2 \\ 0 & 0 & 0 & 0 & 0 & 1 & -2 & 1 \end{bmatrix}$$

METHOD OF INVERSION WITH REGULATIZATION

Therefore…

$$\mathbf{w} = (\mathbf{A}^{T}\mathbf{A} + \gamma\,\mathbf{H})^{-1}\mathbf{A}^{T}\mathbf{g}$$

The final solution is:

$$v(r) = \sum_{j} w_j B_j(r)$$

Errors:
effective radius: ~20%
volume and surface-area concentrations: <±50%
real part of the complex refractive index: ±0.05,
imaginary part: ±50%
number concentrations >±50%

METHOD OF INVERSION WITH REGULATIZATION

An example of forest fire smoke (17/10/2011):

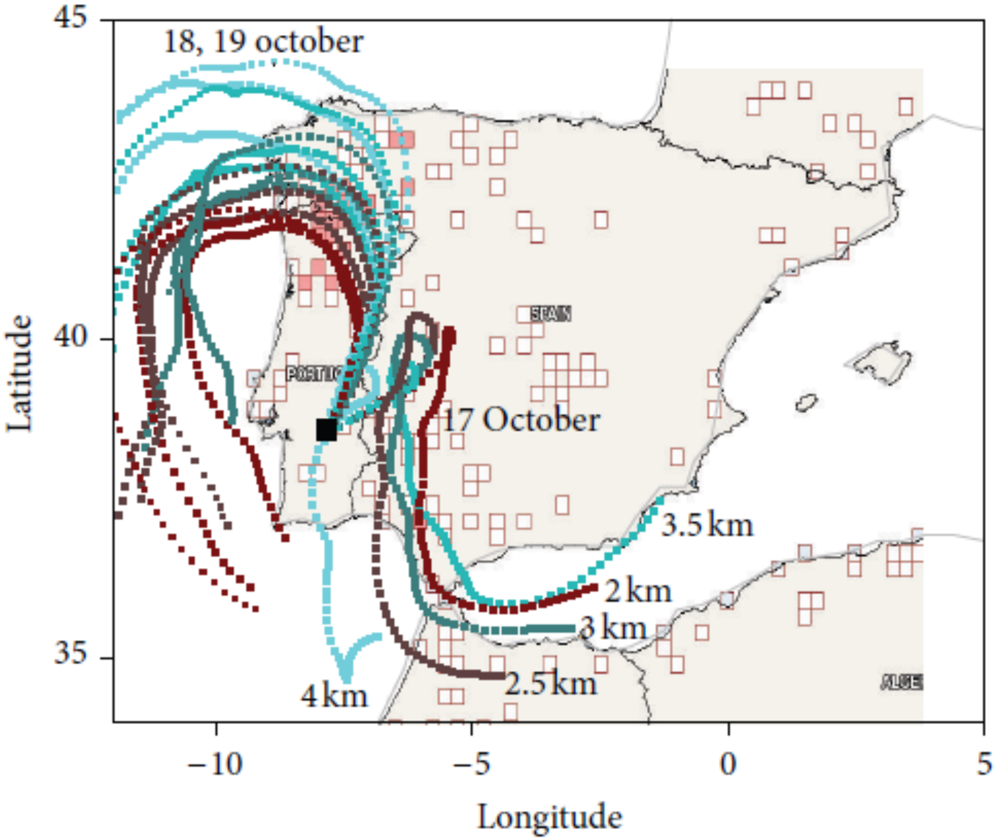

Reff (μm)	0.15 ± 0.03	(20%)
S ($\mu m^2\ cm^{-3}$)	376 ± 130	(35%)
V ($\mu m^3\ cm^{-3}$)	18 ± 8	(44%)
CRI_{real}	1.61 ± 0.13	(8%)
CRI_{imag}	0.018 ± 0.012	(67%)

Pereira et al. (2014)

METHOD OF COMBINATION OF LIDAR AND SUNPHOTOMETER

- Sun-photometers: widespread tool to retrieve column integrated values of aerosol optical, microphysical and radiative properties

- r the vertical profiling of aerosols in the atmosphere. roperties profiles are not easy to derive

- ne of European project ACTRI Research InfraStructure Netwo ,

- tion of AERONET sun-photon s T multiwavelength lidar data l profiles of aerosol microphysical properties, l algorithm developed in the National Acad f Belarus

ACTRiS

LIRIC

LIDAR
- 3 elastic backscattered signals (355, 532 and1064 nm)
- parallel and cross-polarized backscattered signal (532 nm)

SUN-PHOTOMETER
AERONET Retrieved properties:
- columnar particle size distribution
- volume concentrations
- refractive index
- radiative properties

LIRIC
(Lidar-Radiometer Inversion Code)

- **fine mode concentration profile**
- **coarse mode concentration profile**: spherical/non-spherical if depolarization is available

- AOD
- column mode concentrations
- integrated backscatter

LIRIC

LIDAR

- 3 elastic backscattered signals (355, 532 and1064 nm)
- parallel and cross-polarized backscattered signal (532 nm)

SUN-PHOTOMETER

AERONET Retrieved properties:

- columnar particle size distribution
- volume concentrations
- refractive index
- radiative properties

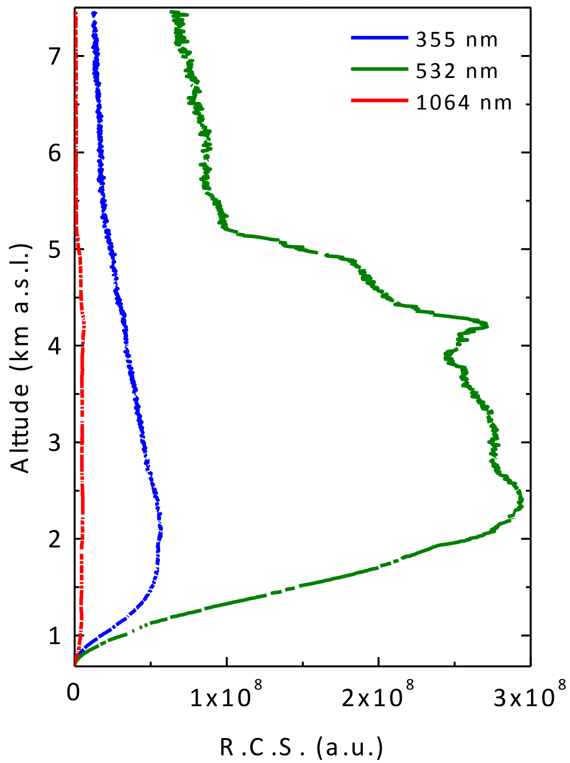

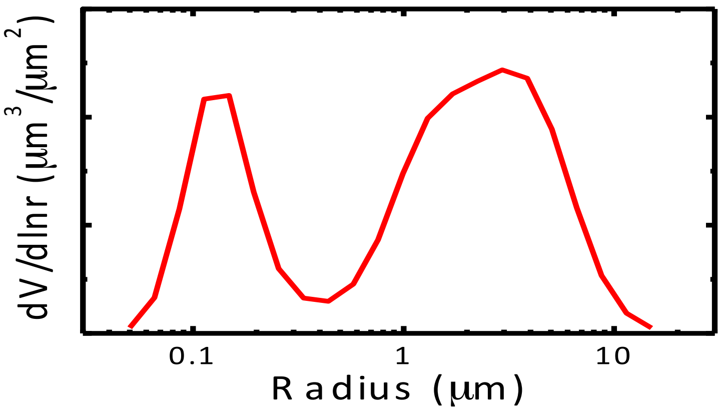

LIRIC

LIDAR
- 3 elastic backscattered signals (355, 532 and1064 nm)
- parallel and cross-polarized backscattered signal (532 nm)

SUN-PHOTOMETER
AERONET retrieved properties:
- columnar particle size distribution
- volume concentrations
- refractive index
- radiative properties

LIRIC
(Lidar-Radiometer Inversion Code)

- ➢ the results of sun-photometric measurements represent the "truth" particle properties over the atmosphere
- ➢ the objective is to construct the particle vertical distribution matching both the integrated aerosol properties observed by ground-based radiometer and the vertically variable signal of multi-wavelength lidar

LIRIC

LIDAR

- 3 elastic backscattered signals (355, 532 and1064 nm)
- parallel and cross-polarized backscattered signal (532 nm)

SUN-PHOTOMETER

AERONET Retrieved properties:

- columnar particle size distribution
- volume concentrations
- refractive index
- radiative properties

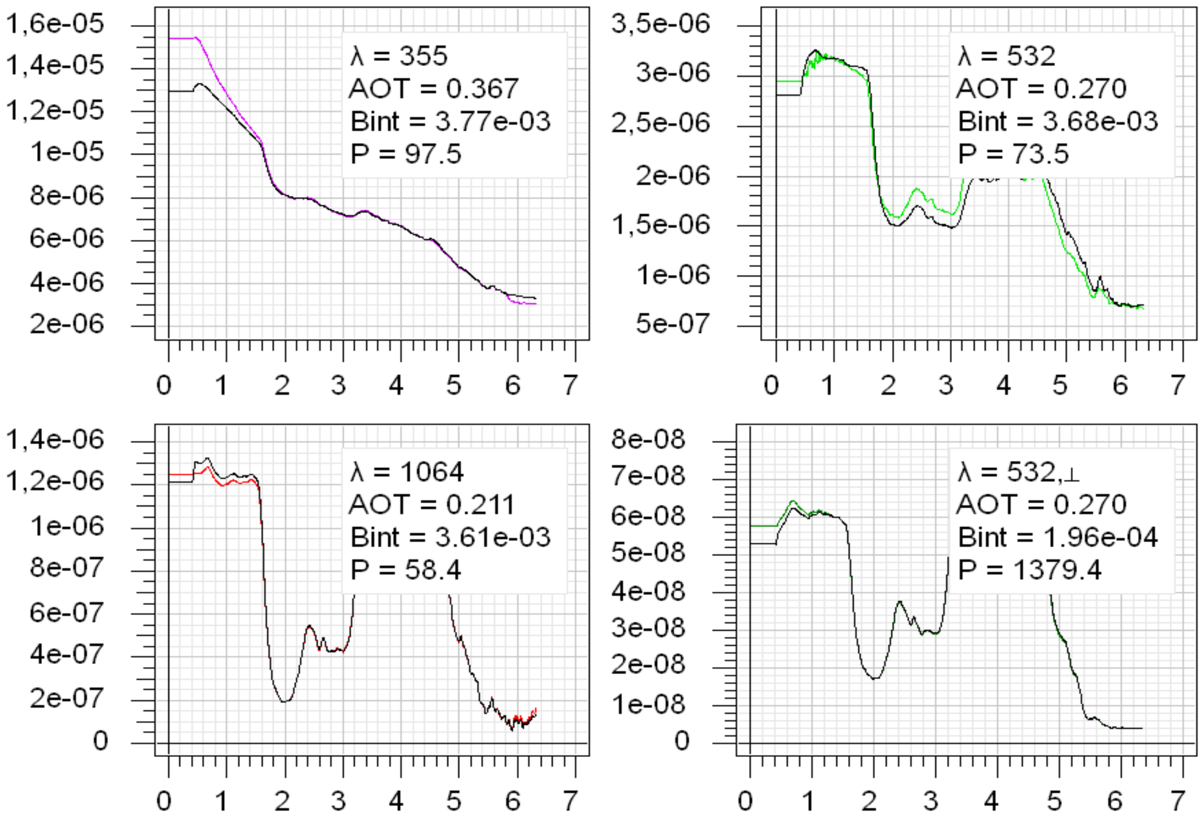

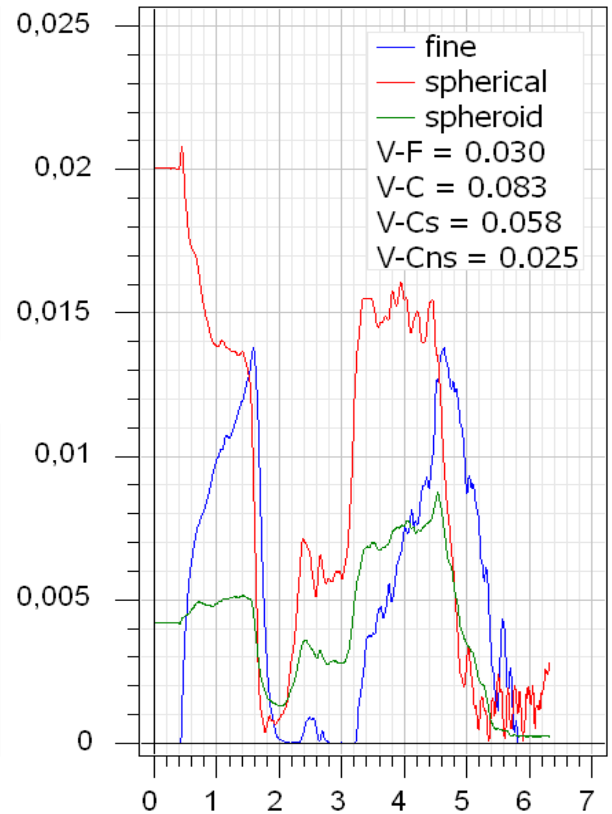

LIRIC

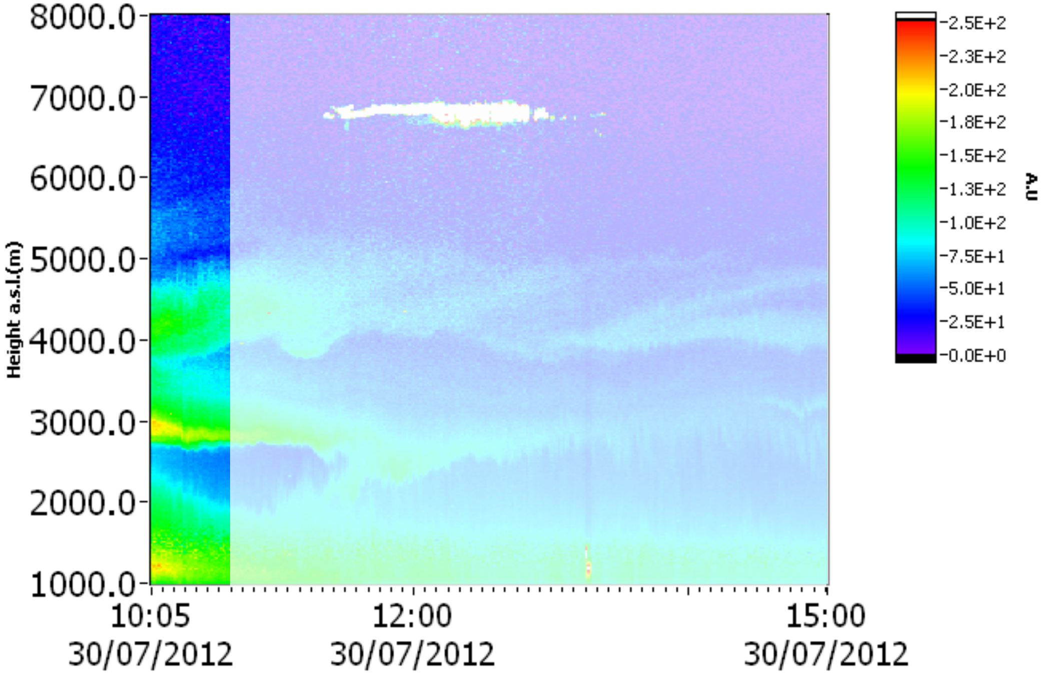

30/07/2012 10:00-10:30

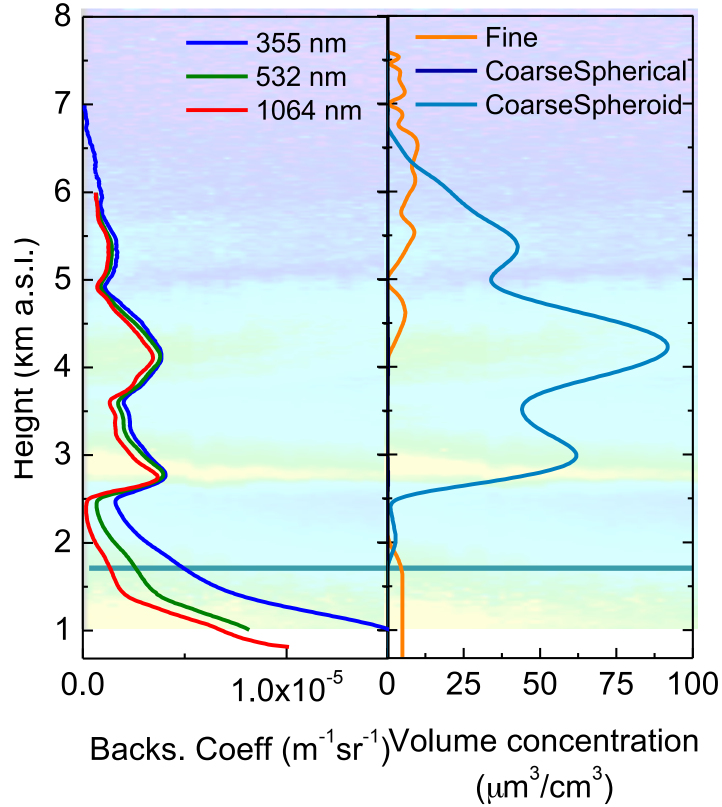

NOAA HYSPLIT MODEL
Backward trajectories ending at 1000 UTC 30 Jul 12
GDAS Meteorological Data

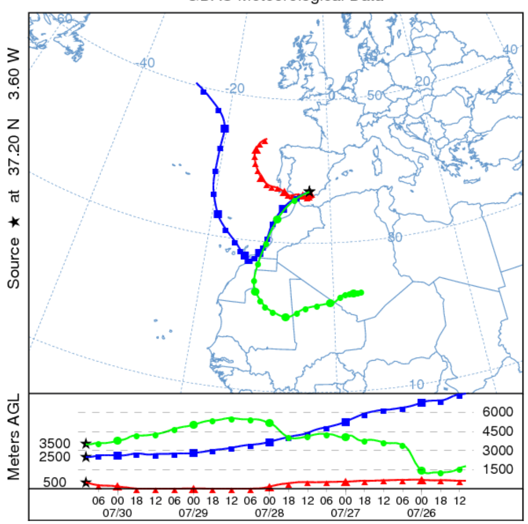

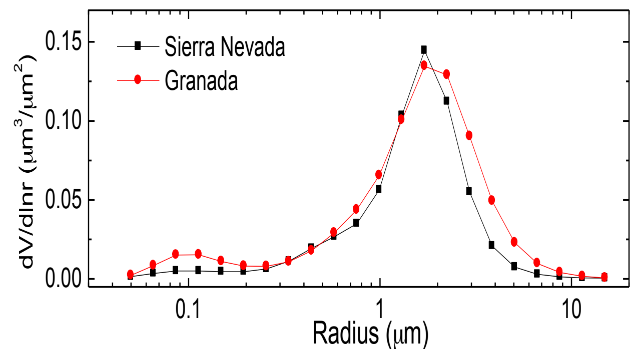

LIDAR, AERONET AND AEROSOL-CLOUD INTERACTIONS

ASCENDING OUTLINE

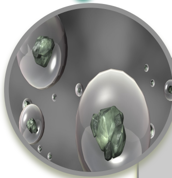

Aerosol-cloud interactions

Instrumental tests

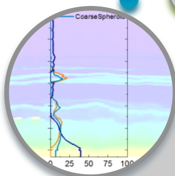

Microphysical properties

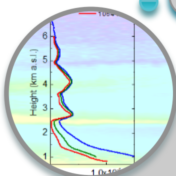

Optical properties

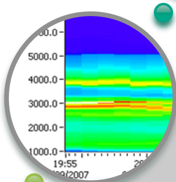

Geometrical properties

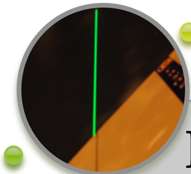

Fundamentals

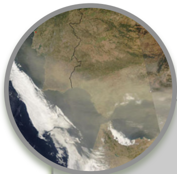

Introduction

TEST #1: ZERO-BIN AND BIN-SHIFT

Lidar (*light detection and ranging*) … but ranging based on <u>timing</u>

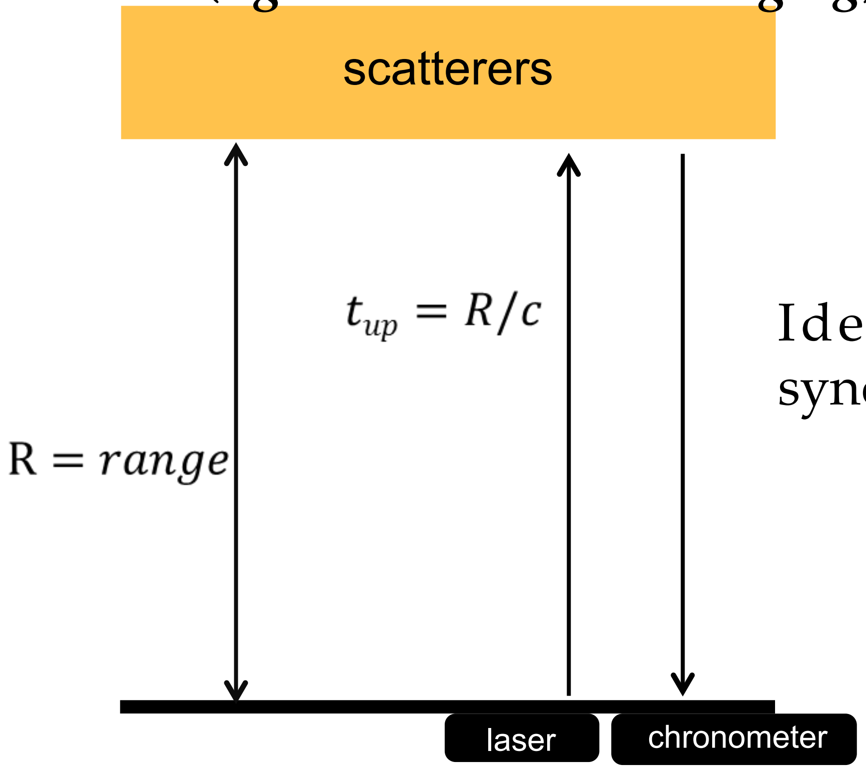

$$t_{total} = t_{up} + t_{down} = 2\,R/c$$

Ideally laser and chronometer are synchronized

In practise… not

wrong range determination!!!

TEST #1: ZERO-BIN AND BIN-SHIFT

Zero-bin test: a target is placed at the output of the laser window in order to produce strong backscattered radiation. Thus, the first intense peak observed by the detector system should correspond to the zero position of our measurements

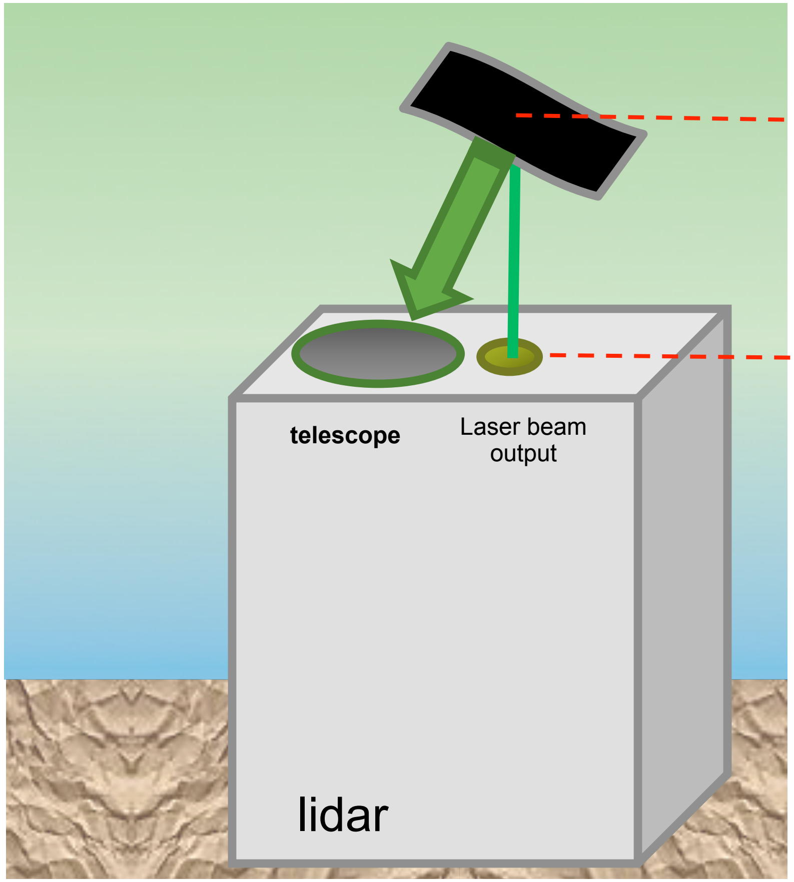

$$R < \Delta z$$

Our target is placed at zero-bin, however…

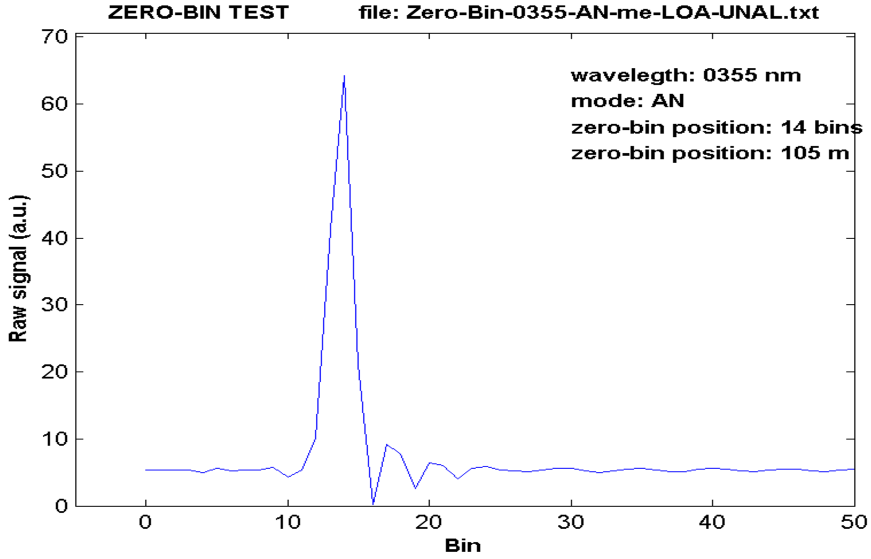

TEST #1: ZERO-BIN AND BIN-SHIFT

This test was only carried out for AN signals, since the saturation suffered in PC mode at close height range could lead to wrong results

For measuring a possible delay between AN and PC signals (bin-shift), target as clouds or aerosol layers are used

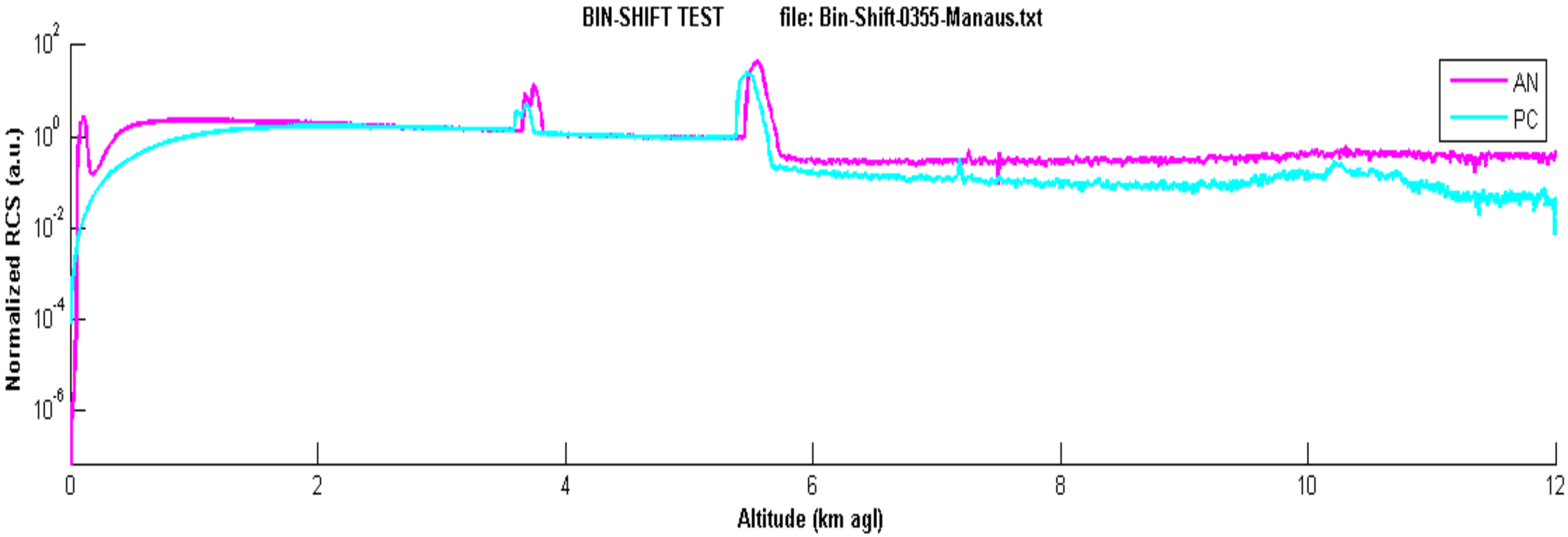

TEST #1: ZERO-BIN AND BIN-SHIFT

Bin-shift is determined by the best linear fit between AN and PC signals fixing the AN signal and displacing the PC signal from -20 to +20 bins

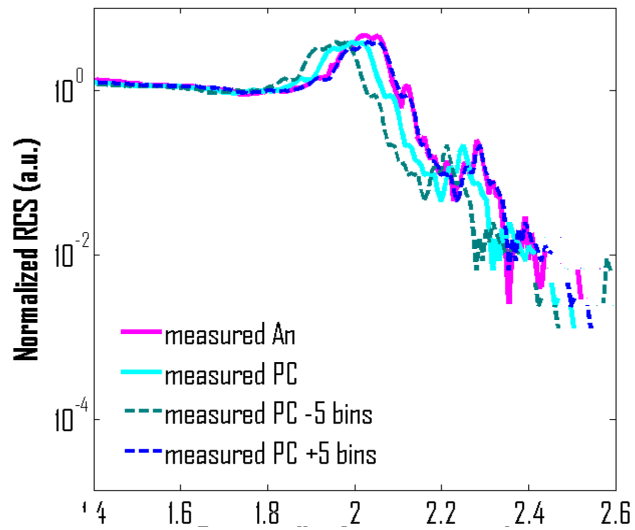

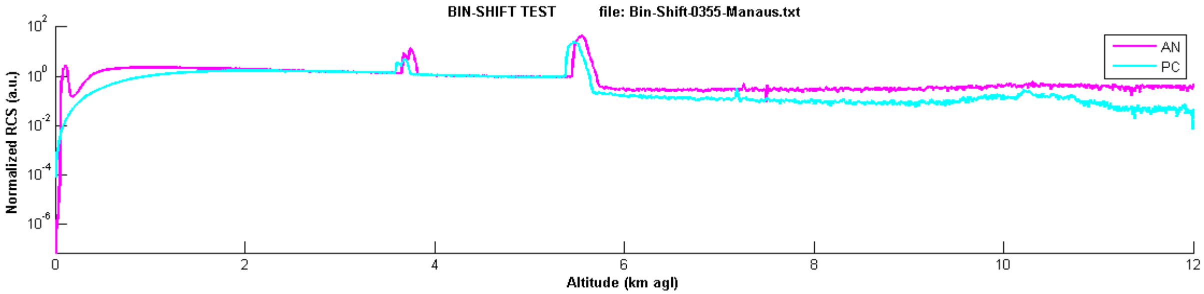

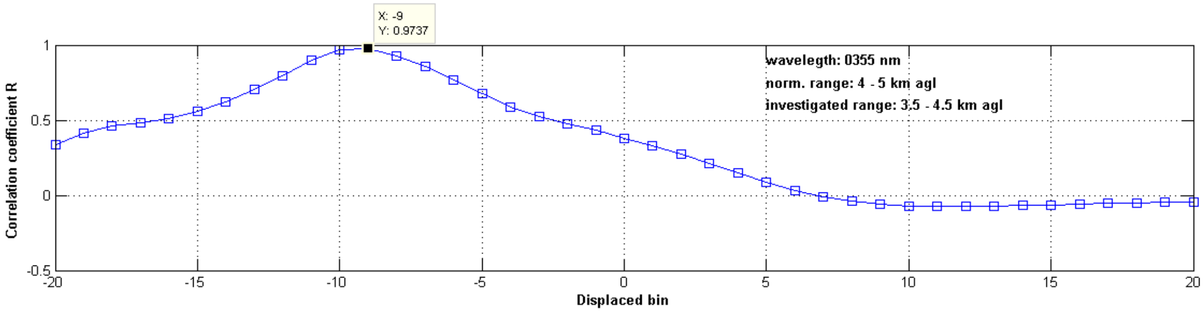

In this case,
Bin-shift = - 9bins

$$bin_0^{PC} = bin_0^{AN} + \Delta bin_{AN-PC}$$

TEST #1: ZERO-BIN AND BIN-SHIFT

Example of results for system sp-CLA-IPEN-MSP-LIDAR-I (São Paulo)

$$bin_0^{PC} = bin_0^{AN} + \Delta bin_{AN-PC}$$

Channel (nm)	Zero-bin AN (bins)	Bin-shift (bins)	Zero-bin PC (bins)
355	8	-10	-2
387	8	-10	-2
408	8	-10	-2
532	1	-2	-1
607	6	-9	-3
660	7	-9	-2

To properly use the lidar signals, the some bins of the AN signals must be removed and several blank bins must be introduced in the PC signals following this table

TEST #2: DARK CURRENT

Dark current (DC) is the response exhibited by a receptor of radiation even during periods when it is not actively illuminated

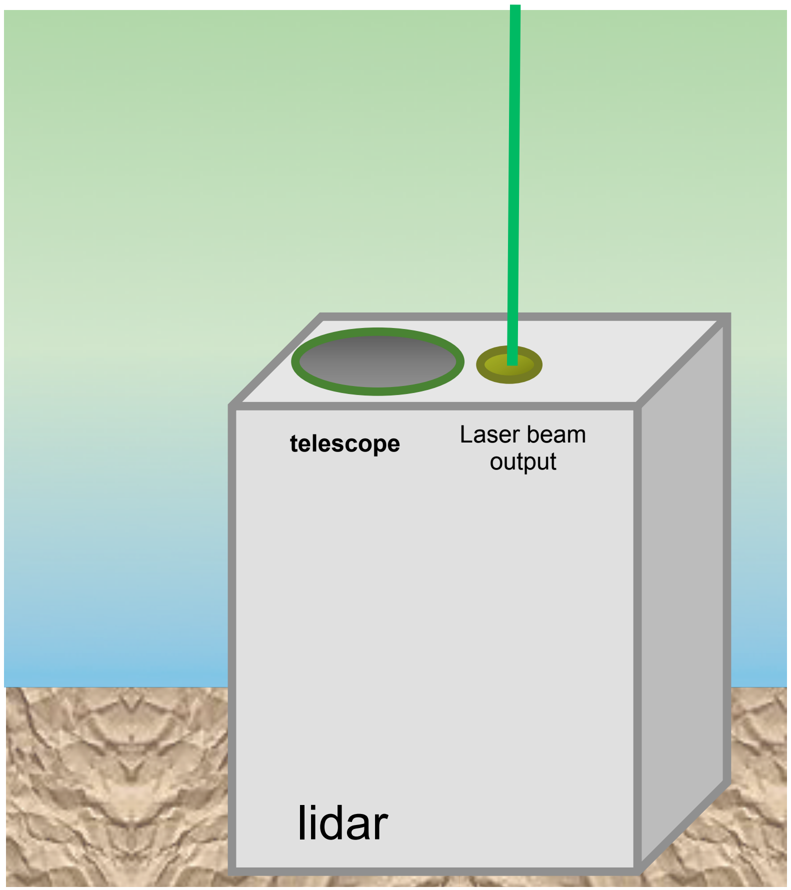

-measurement taken by covering totally the telescope or detectors performed with enough averaging time (~10 min)

-all parameters (voltages, pulse repetition frequency ...) are configured as a usual measurement

TEST #2: DARK CURRENT

Example of results for systems co_CEFOP-UDEC (Medellín) and ma-MA (Manaus)

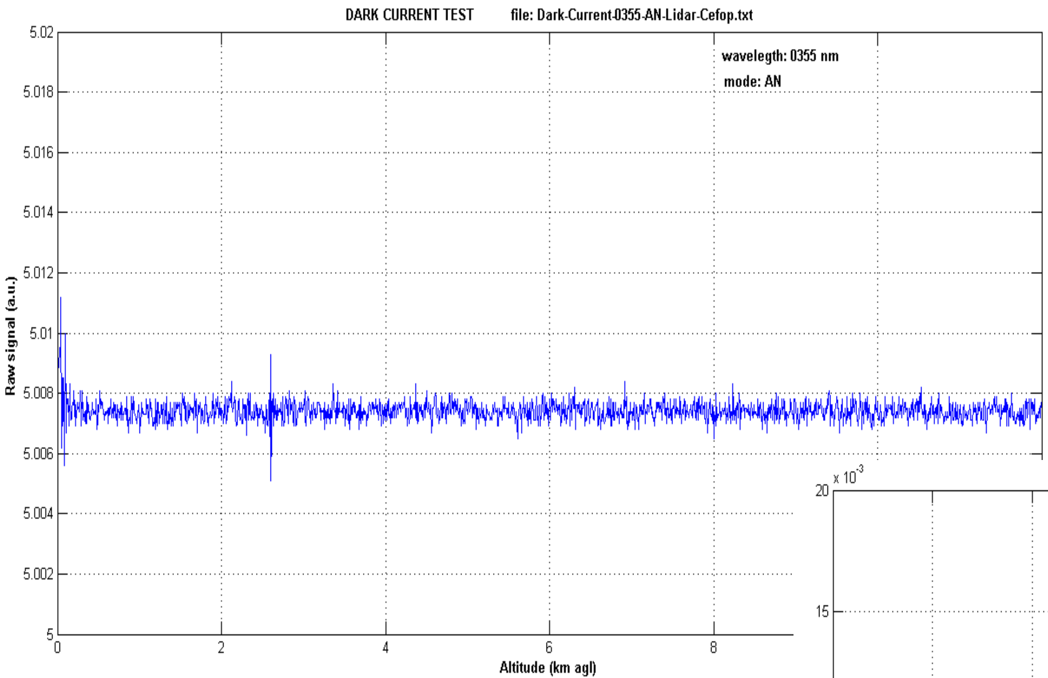

Important to know during preprocessing step

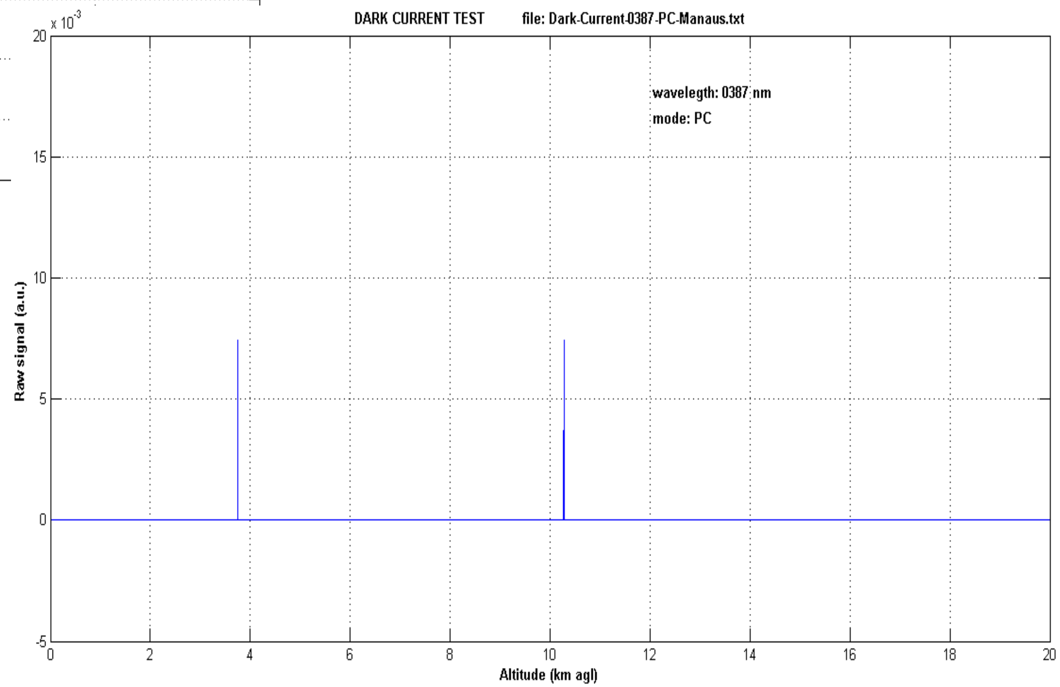

TEST #3: TELECOVER TEST

Overlap function O(R): geometrical overlap between laser beam and telescope field of view

O(R) accounts for the partial overlap in the near height-range and tends to estabilize (ideally to 1) in the far height-range

O(R) depends, among other factors, on the alignment

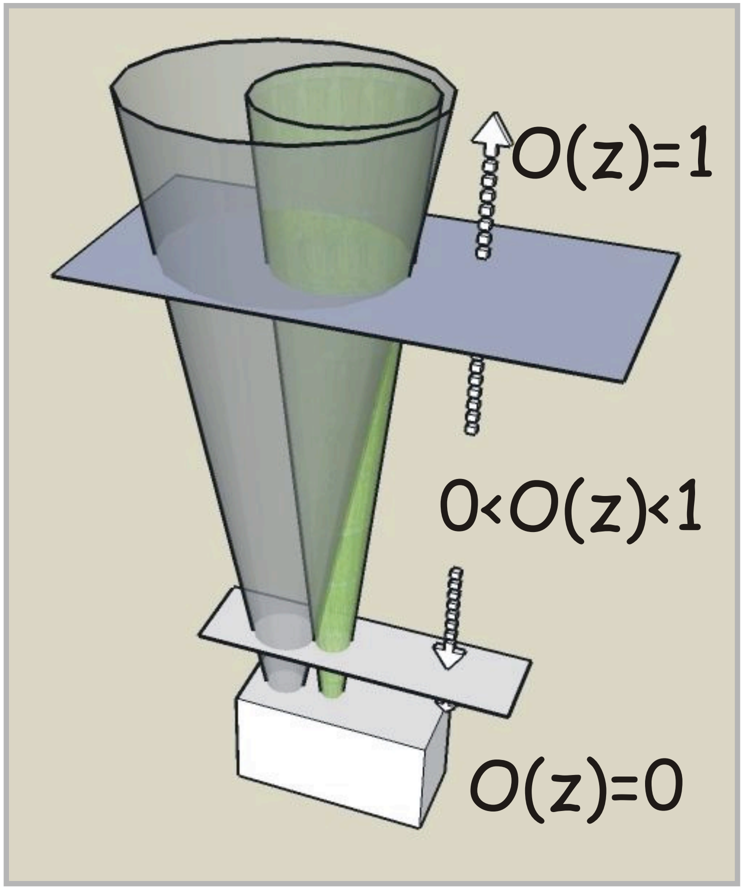

Guerrero-Rascado et al., Óptica Pura y Aplicada, 2011

TEST #3: TELECOVER TEST (QUADRANTS)

<u>Telecover test (quadrants)</u>:

-based on the comparison of signals measured using different quadrants of the telescope

-named as N, E, S and W, where N is the quadrant nearest to the laser beam axis and the others named following the clockwise sense

-N measurement is performed at the end of the telecover test (N2) to check the atmospheric stability
-Measurements ~2 min

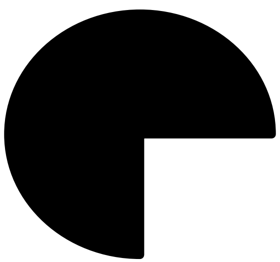

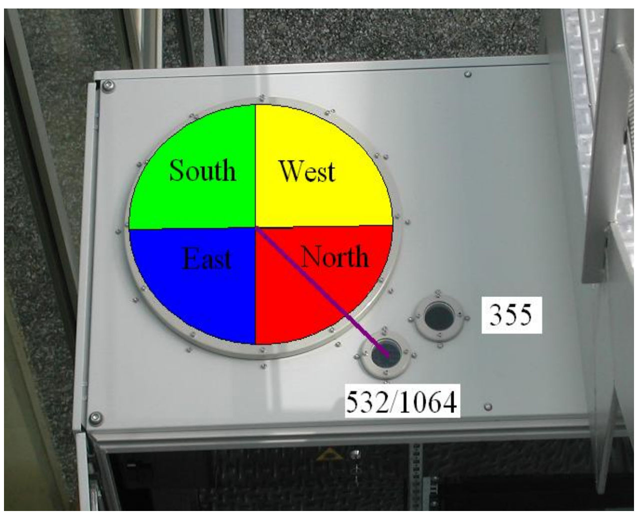

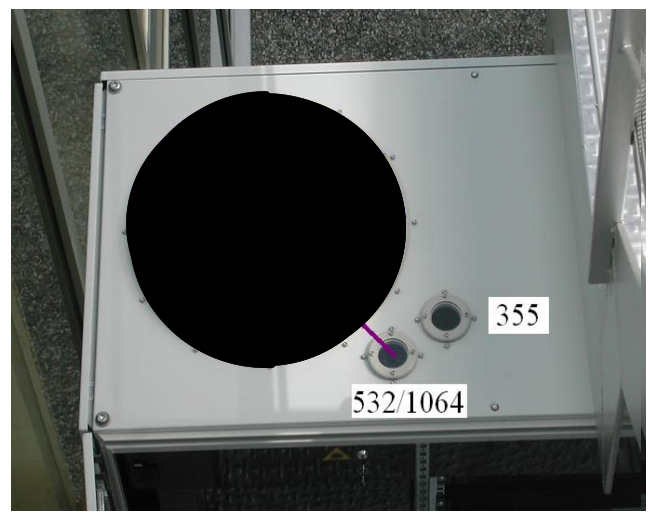

TEST #3: TELECOVER TEST (QUADRANTS)

Atmospheric variability: Bad telecover!!!

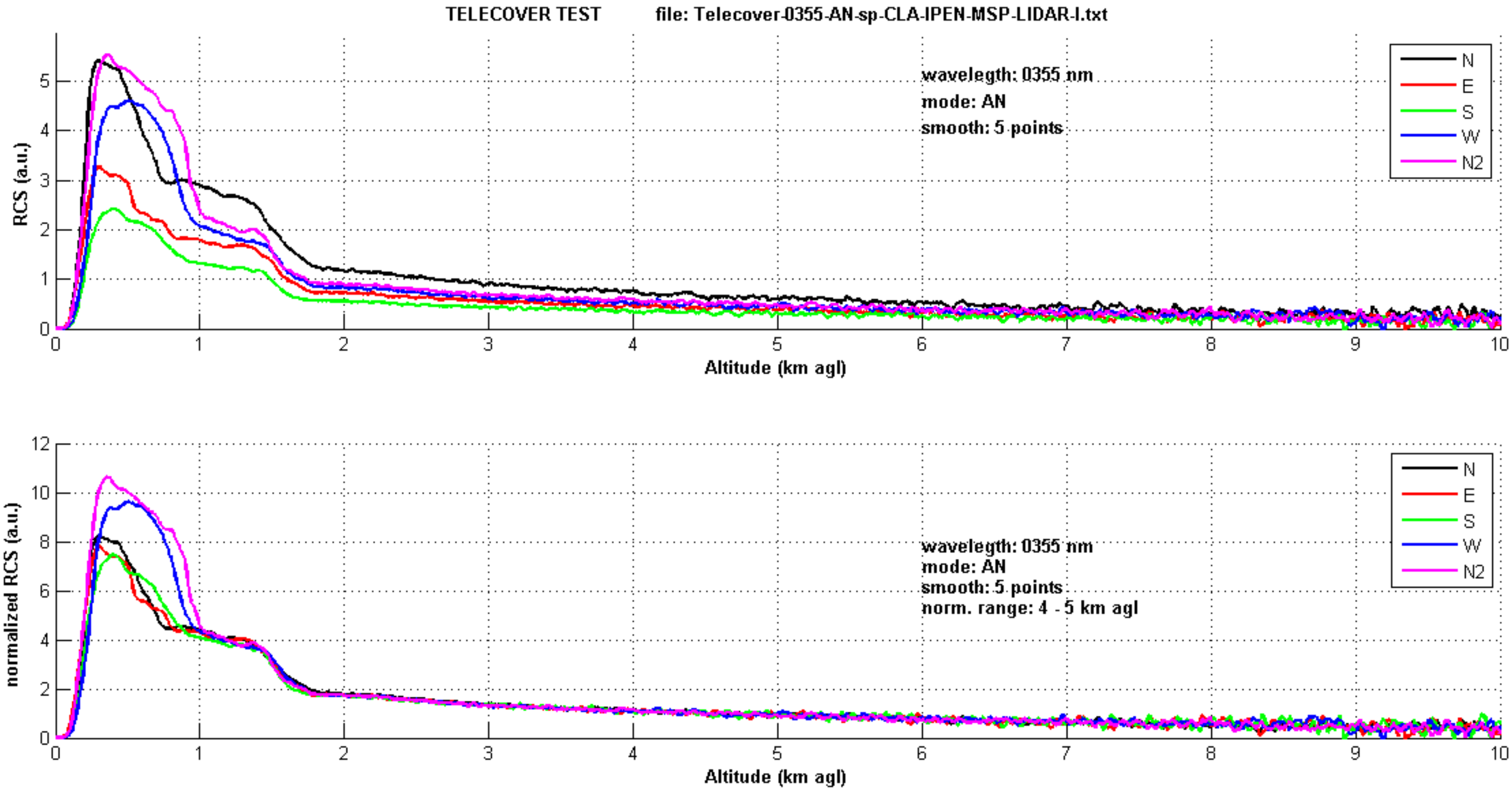

IISTA

USP

IFUSP

TEST #3: TELECOVER TEST (QUADRANTS)

Biaxial systems: N=N2 < E = W < S

Coaxial systems: N=N2 = E = W = S

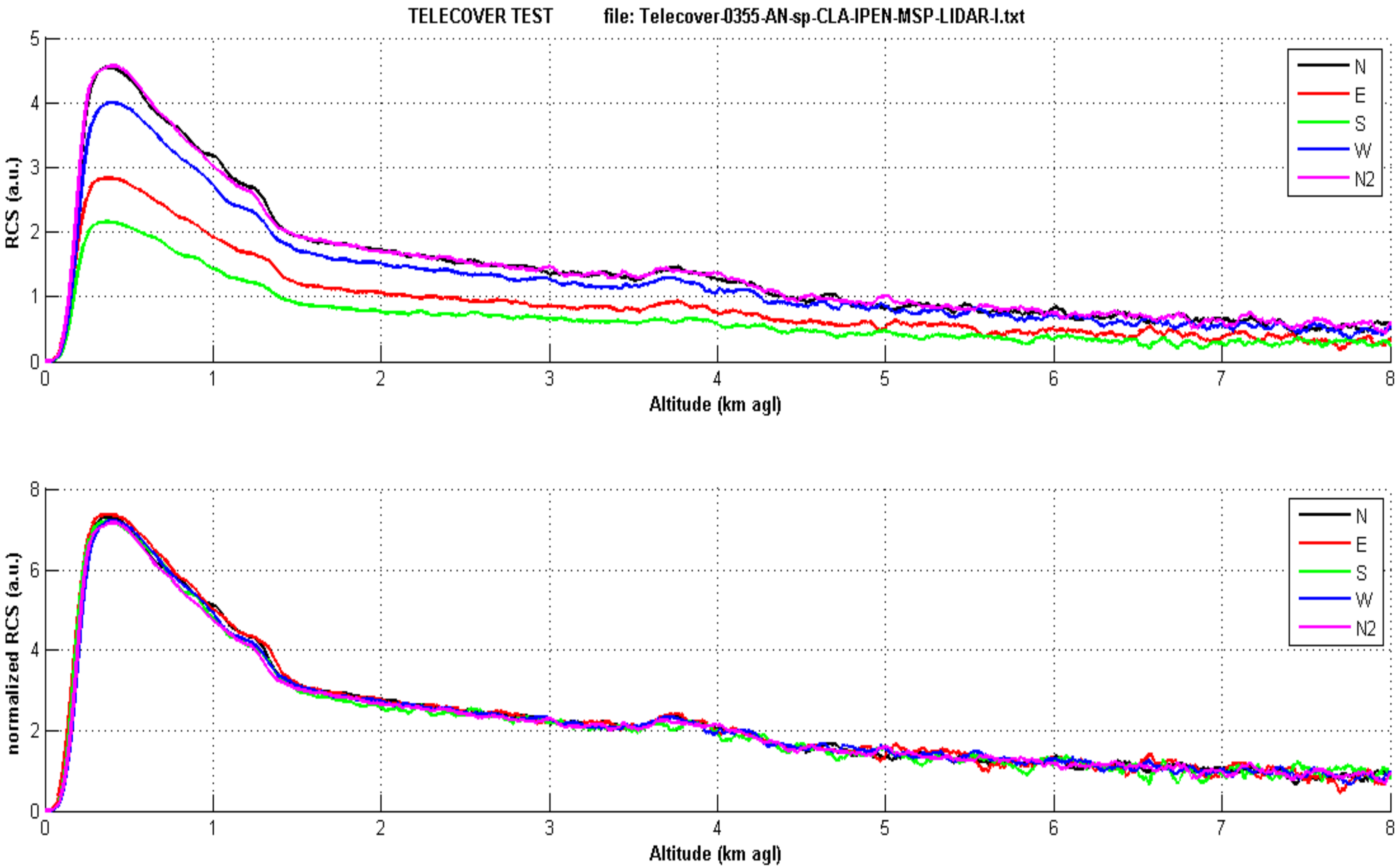

TEST #3: TELECOVER TEST (IN-OUT)

<u>Telecover test (in-out)</u>:

-based on the comparison of signals measured using different rings of the telescope, named as IN and OUT

-IN measurement is performed at the end of the telecover test (IN2) to check the atmospheric stability

-Measurements ~2 min

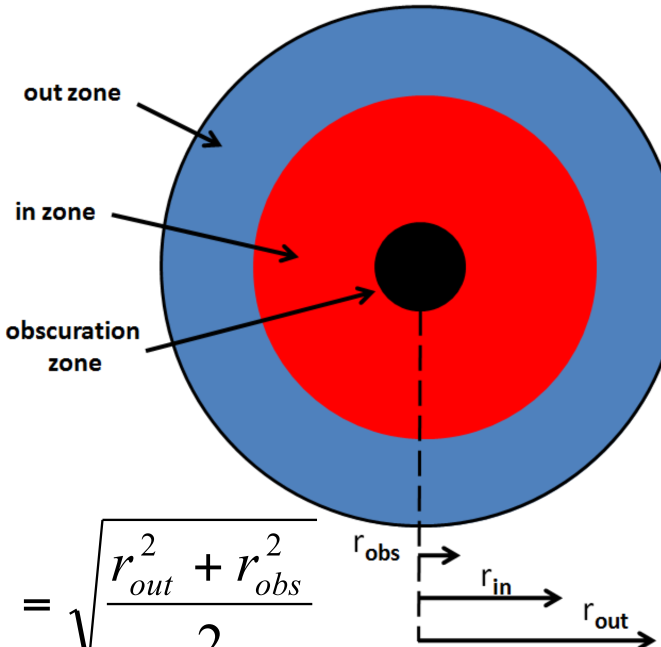

$$r_{in} = \sqrt{\frac{r_{out}^2 + r_{obs}^2}{2}}$$

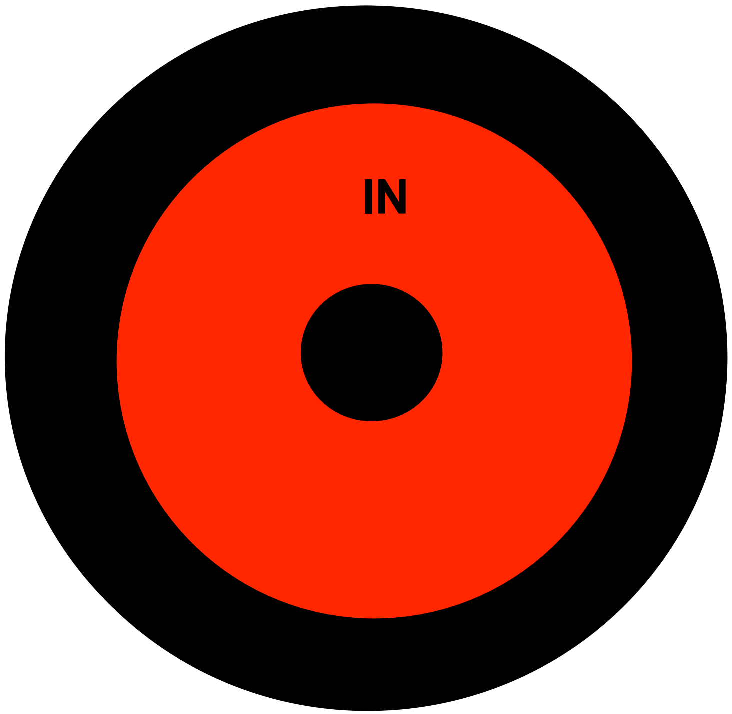

TEST #3: TELECOVER TEST (IN-OUT)

Coaxial systems: IN=IN2 < OUT

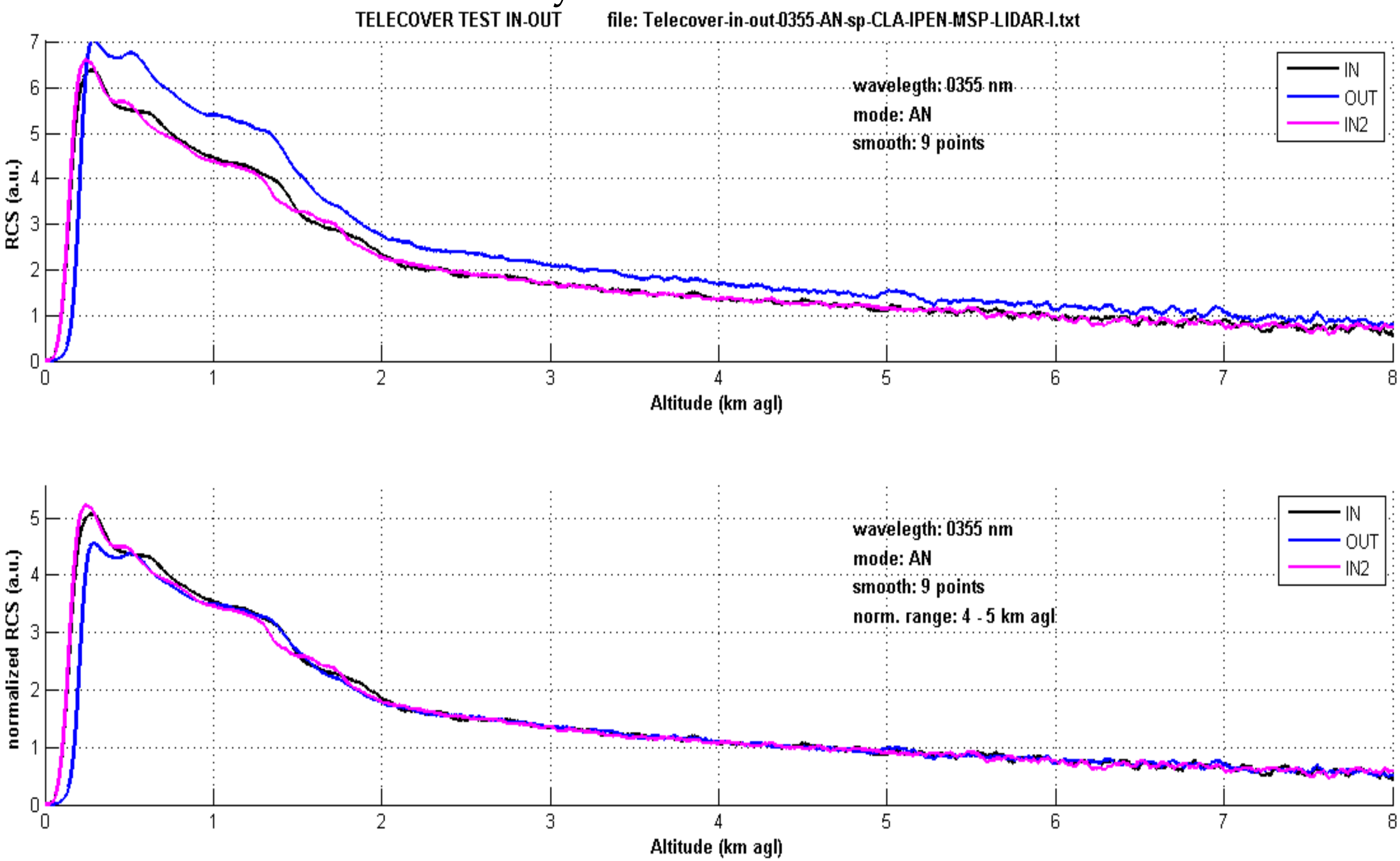

TEST #4: RAYLEIGH FIT

The Rayleigh (or molecular) fit is a tool to analyze the quality of far range lidar signal:

-the range corrected signal measured by the lidar system is compared to the expected molecular range corrected signal

$$R.C.S._{mol}(z) = \beta_{mol}(z)\cdot\exp\left\{-2\int_0^z \alpha_{mol}(\xi)d\xi\right\} \equiv \beta_{mol}^{att}(z)$$

$$R.C.S.(z) = K\cdot\beta(z)\cdot\exp\left\{-2\int_0^z \alpha(\xi)d\xi\right\} \propto \beta^{att}(z)$$

-measurement ~30 min

TEST #4: RAYLEIGH FIT

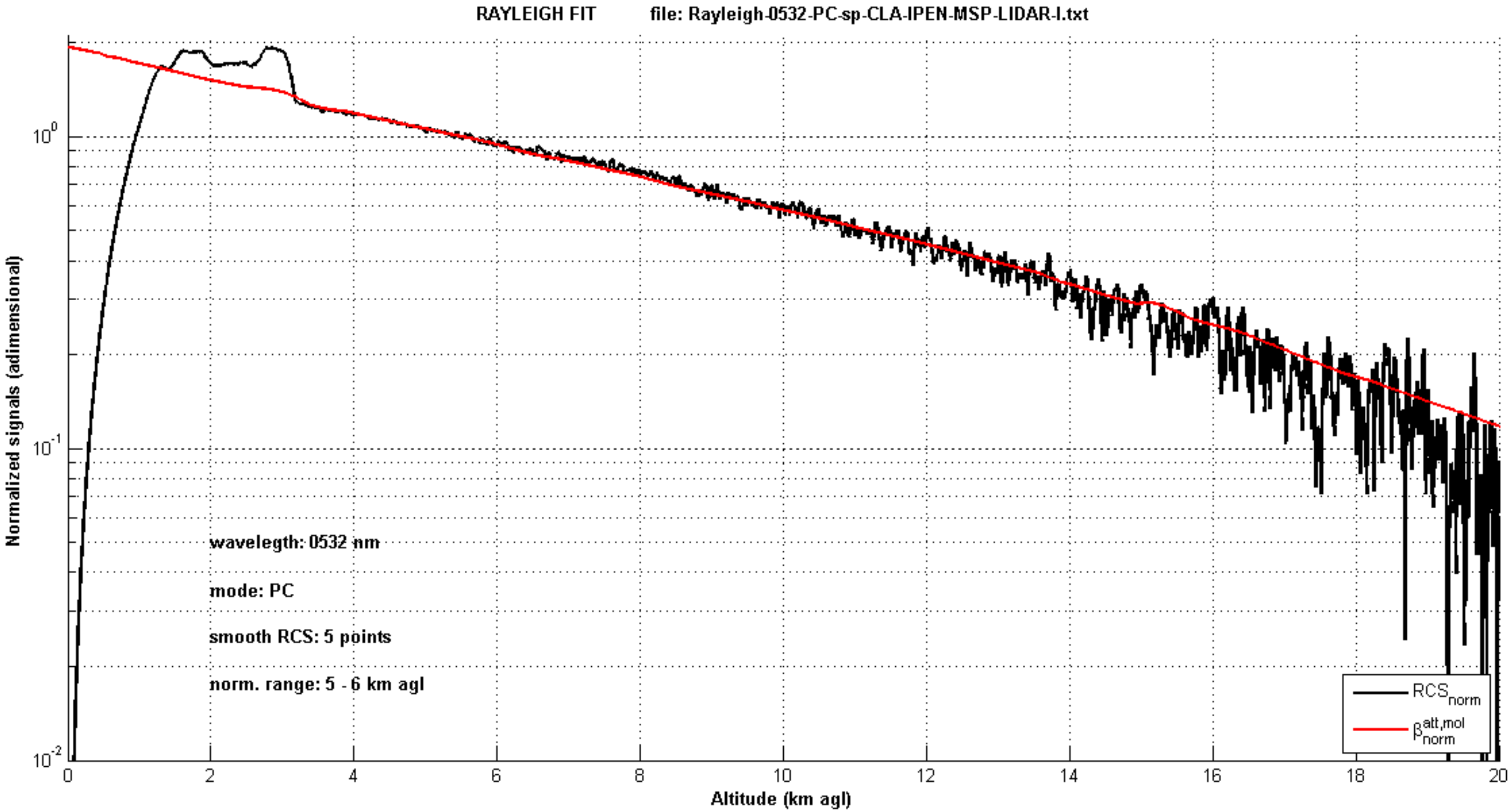

Similar trend above 3 km agl up to 15 km agl (approx.)

This height range can be used as z_{ref} for Klett-Fernald and Raman methods

ASCENDING OUTLINE

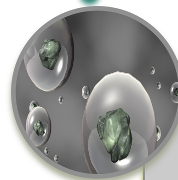

Aerosol-cloud interactions

Instrumental tests

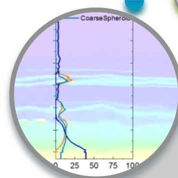

Microphysical properties

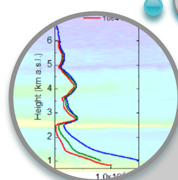

Optical properties

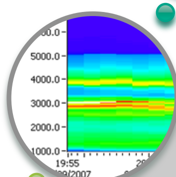

Geometrical properties

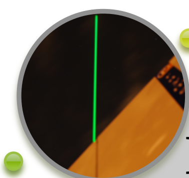

Fundamentals

Introduction

AEROSOL-CLOUD INTERACTIONS

Radiative forcing by components

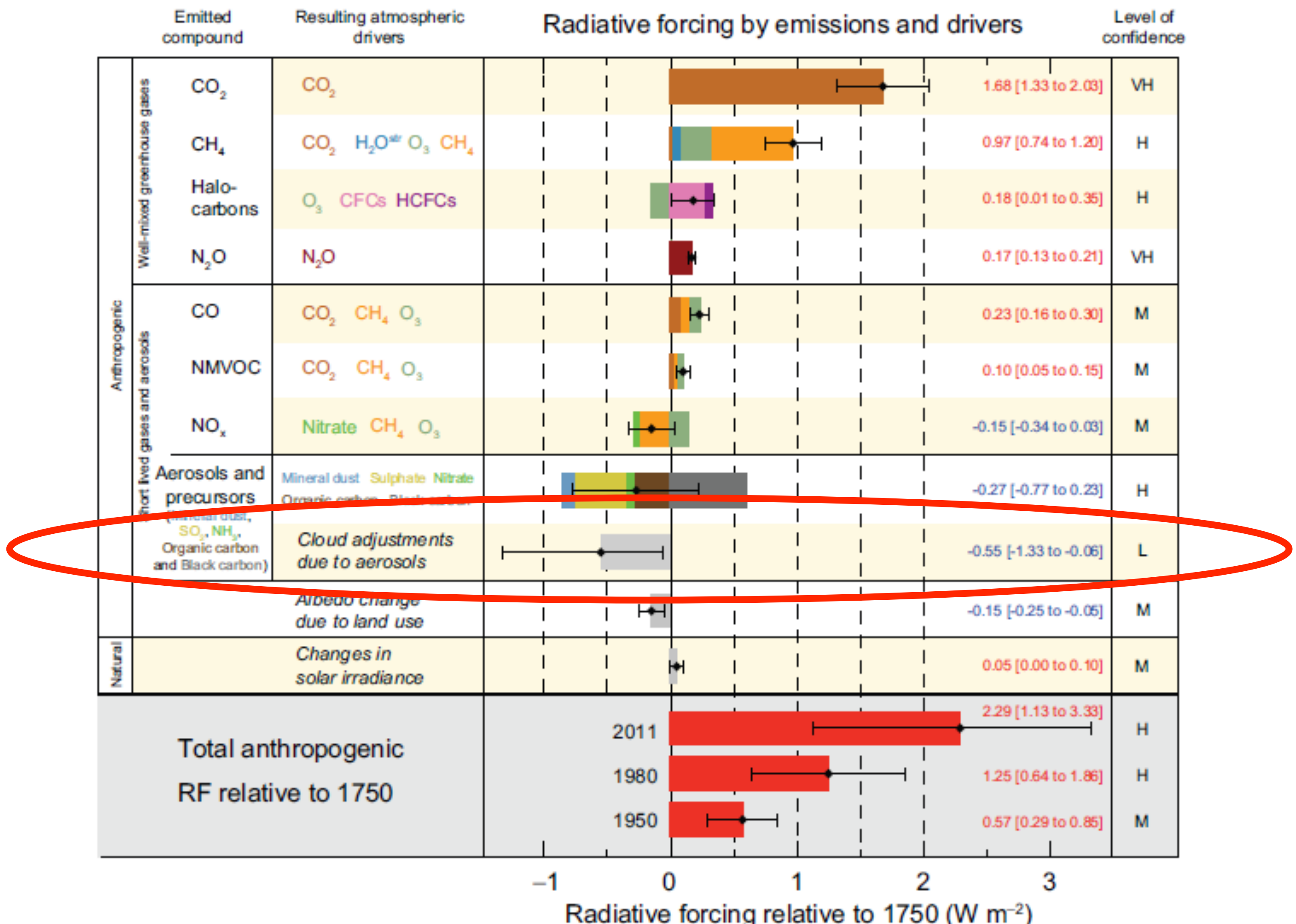

IPCC (2013)

IISTA

IFUSP

LIDAR APPLICATION: POLIPHON 1-STEP

$$\delta_p = \frac{\beta_{nd}^{\perp} + \beta_d^{\perp}}{\beta_{nd}^{\parallel} + \beta_d^{\parallel}}$$

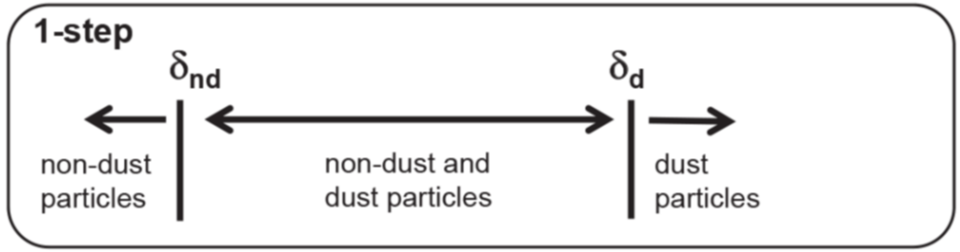

As shown by Tesche et al. (2009), the particle depolarization ratio can be expressed by:

$$\delta_p = \frac{\beta_{nd}\delta_{nd}(1+\delta_d) + \beta_d\delta_d(1+\delta_{nd})}{\beta_{nd}(1+\delta_d) + \beta_d(1+\delta_{nd})}$$

with the dust and non-dust depolarization ratios δ_d = 0.31 and δ_{nd}=0.05, respectively. After substituting β_{nd} with $\beta_p - \beta_d$, we solve the resulting equation to obtain a solution for β_d **(for $\delta_{nd} \leq \delta_p \leq \delta_d$)**

$$\beta_d = \beta_p \frac{(\delta_p - \delta_{nd})(1+\delta_d)}{(\delta_d - \delta_{nd})(1+\delta_p)}$$

$\beta_{nd} = \beta_p - \beta_d$

For $\delta_p < \delta_{nd}$ ➔ $\beta_{nd} = \beta_p$ (contribution by dust is negligible)

For $\delta_p > \delta_d$ ➔ $\beta_d = \beta_p$ (non-dust aerosol contribution is negligible)

LIDAR APPLICATION: POLIPHON 1-STEP

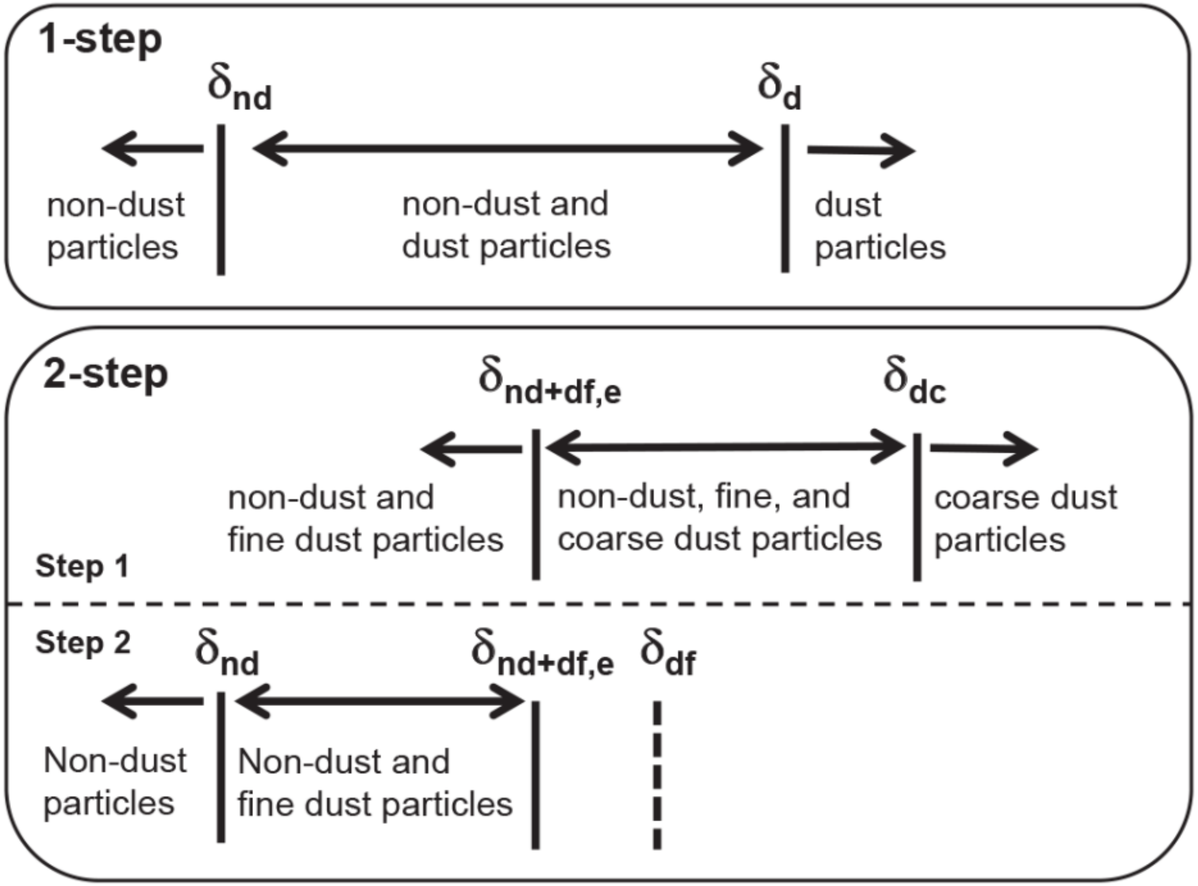

Illustration of the one-step and two-step POLIPHON methods to separate spherical particles from non-spherical dust particles (one-step method) and spherical particles, fine dust, and coarse dust particles (two-step method) by means of the particle depolarization ratio.

LIDAR APPLICATION: POLIPHON 2-STEP

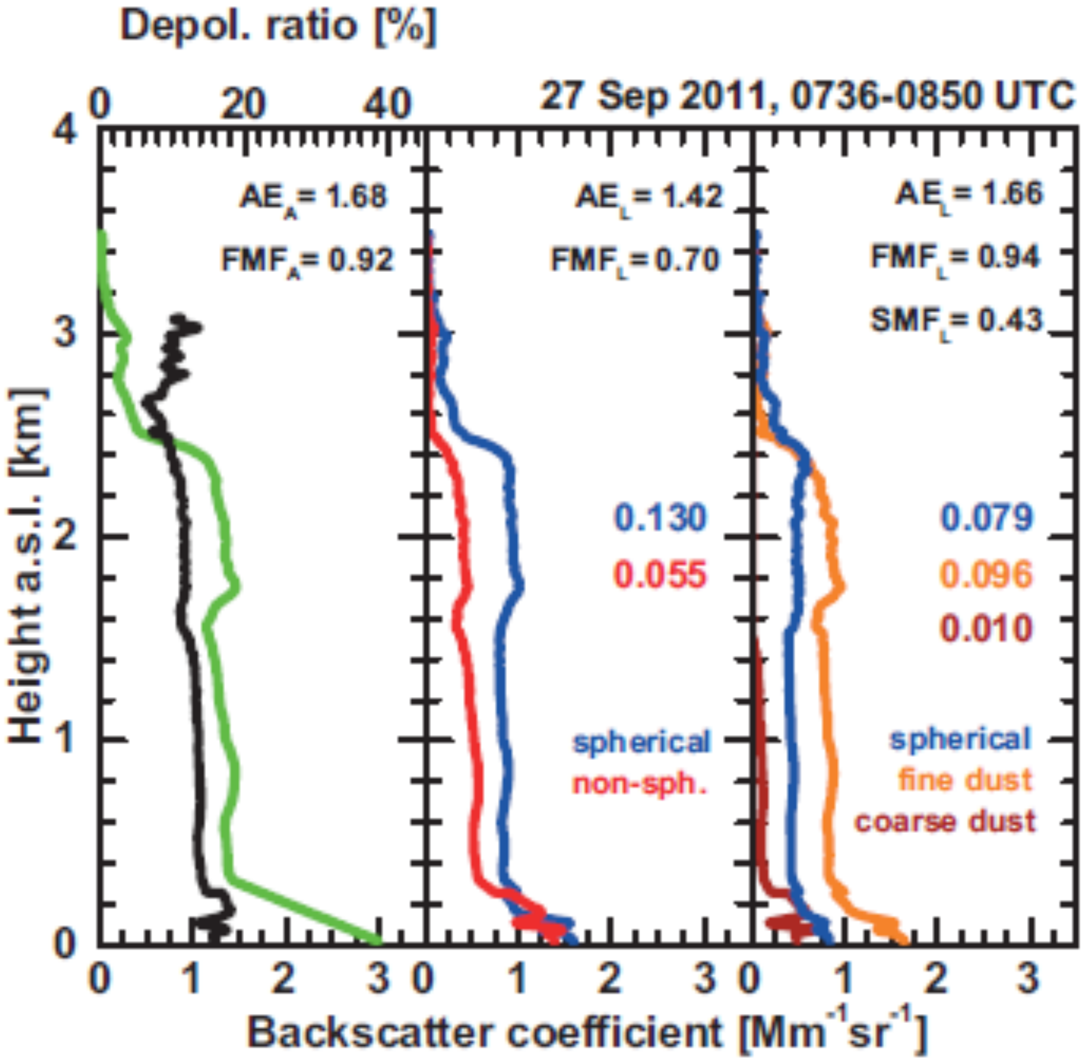

(Left) 532 nm particle backscatter coefficient (green) and particle linear depolarization ratio (black), (center) particle backscatter coefficients for 1-step method, and (right) particle backscatter coefficient for 2-step method

IISTA

USP

IFUSP

LIDAR APPLICATION TO ACI: INC PROFILES

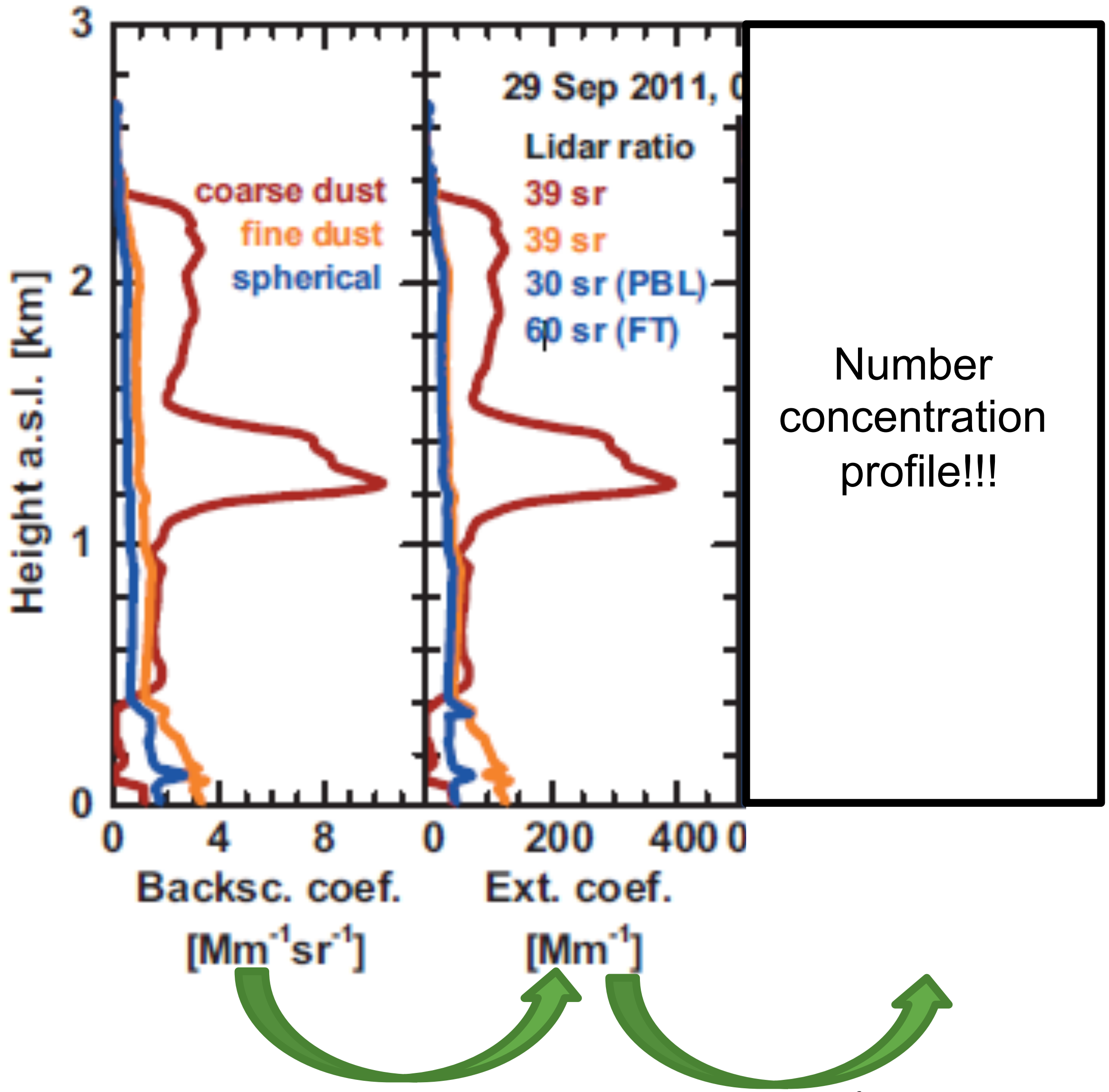

Lidar ratio   Conversion factor

$$n_{d,280}(z) = c_{d,280} \cdot \sigma_d(z)$$

LIDAR APPLICATION TO ACI: INC PROFILES

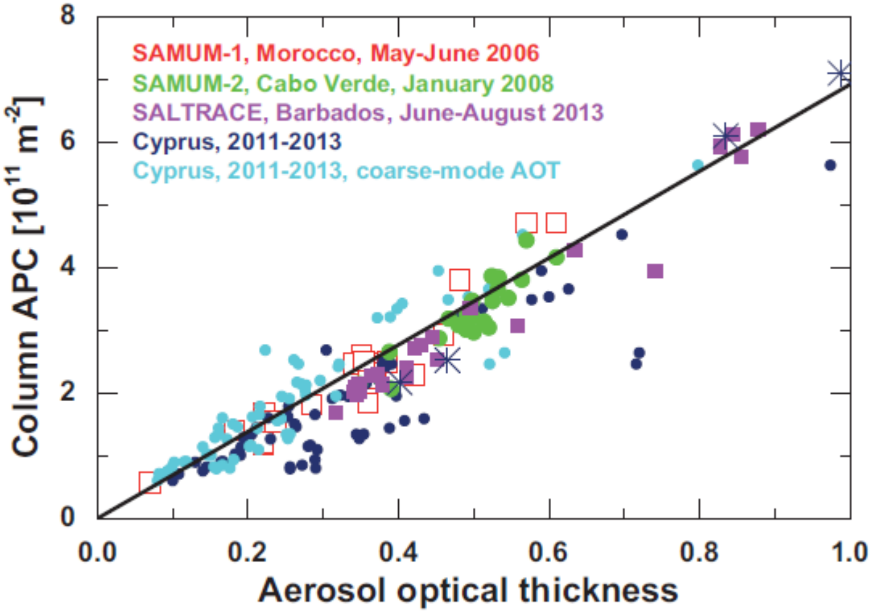

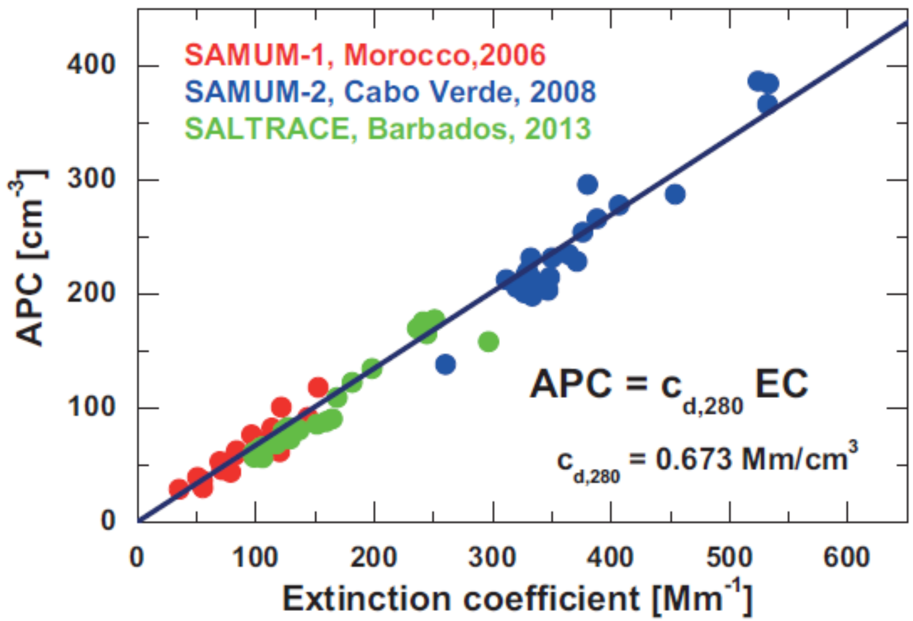

Correlation between aerosol optical thickness (500 nm AOT) (i.e. (column-integrated extinction coefficient) and column-integrated aerosol particle number concentration (column APC280) considering particles with r > 280 nm. Desert-dust-dominated observations from several field campaigns

To translate the column-related findings into scales of particle extinction coefficient (measurable with lidar) and respective particle number concentration, we simply used the layer depth information from the lidar

LIDAR APPLICATION TO ACI: ESTIMATION OF INC FROM APC280

The retrieval of APC_{280} from α_d is the basic lidar contribution to the estimation of the INC profiles

Next step is the link to the published INC parameterizations gained from comprehensive INC laboratory and field studies

The INC parameterizations introduced by DeMott et al. (2010, 2015) hold for standard (std) pressure (p_0=1013 hPa) and temperature (T_0=273.16 K) conditions so that we have to convert each profile value $APC_{280}(p_z, T_z)$ from ambient pressure p_z and temperature T_z at height z to $APC_{280}(p_0, T_0)$ by using the factor $(T_z p_0)/(T_0 p_z)$

LIDAR APPLICATION TO ACI: ESTIMATION OF INC FROM APC280

Global (aerosol-type-independent) INC parameterization (DeMott et al., 2010):

$$n_{\mathrm{IN}}(p_0, T_0, T_z) = a(273.16 - T_z)^b \times n_{\mathrm{a},280}(p_0, T_0)^{[c(273.16 - T_z) + d]},$$

$n_{a,280}$ (in std cm^{-3}) representing APC_{280}
n_{IN} (in std L^{-1}) representing INC
a=0.0000594
b=3.33
c=0.0265
d=0.0033
temperature T(z) in K (< 273.16 K)

Dust INC parameterization (DeMott et al., 2015):

$$n_{\mathrm{IN}}(p_0, T_0, T_z) = f_{\mathrm{d}} n_{\mathrm{a},280}(p_0, T_0)^{[a_{\mathrm{d}}(273.16 - T_z) + b_{\mathrm{d}}]} \times \exp[c_{\mathrm{d}}(273.16 - T_z) + d_{\mathrm{d}}],$$

f_d=3
a_d=0.074
b_d=3.8
c_d=0.414
d_d=-9.671

Finally, we transfer the obtained INC values $n_{IN}(p_0,T_0,T_z)$ to the ones for ambient pressure and temperature conditions, $n_{IN}(p_z,T_z)$, by multiplying $n_{IN}(p_0,T_0,T_z)$ with the factor $(T_0 p_z)/(T_z p_0)$

LIDAR APPLICATION TO ACI: ESTIMATION OF INC FROM APC280

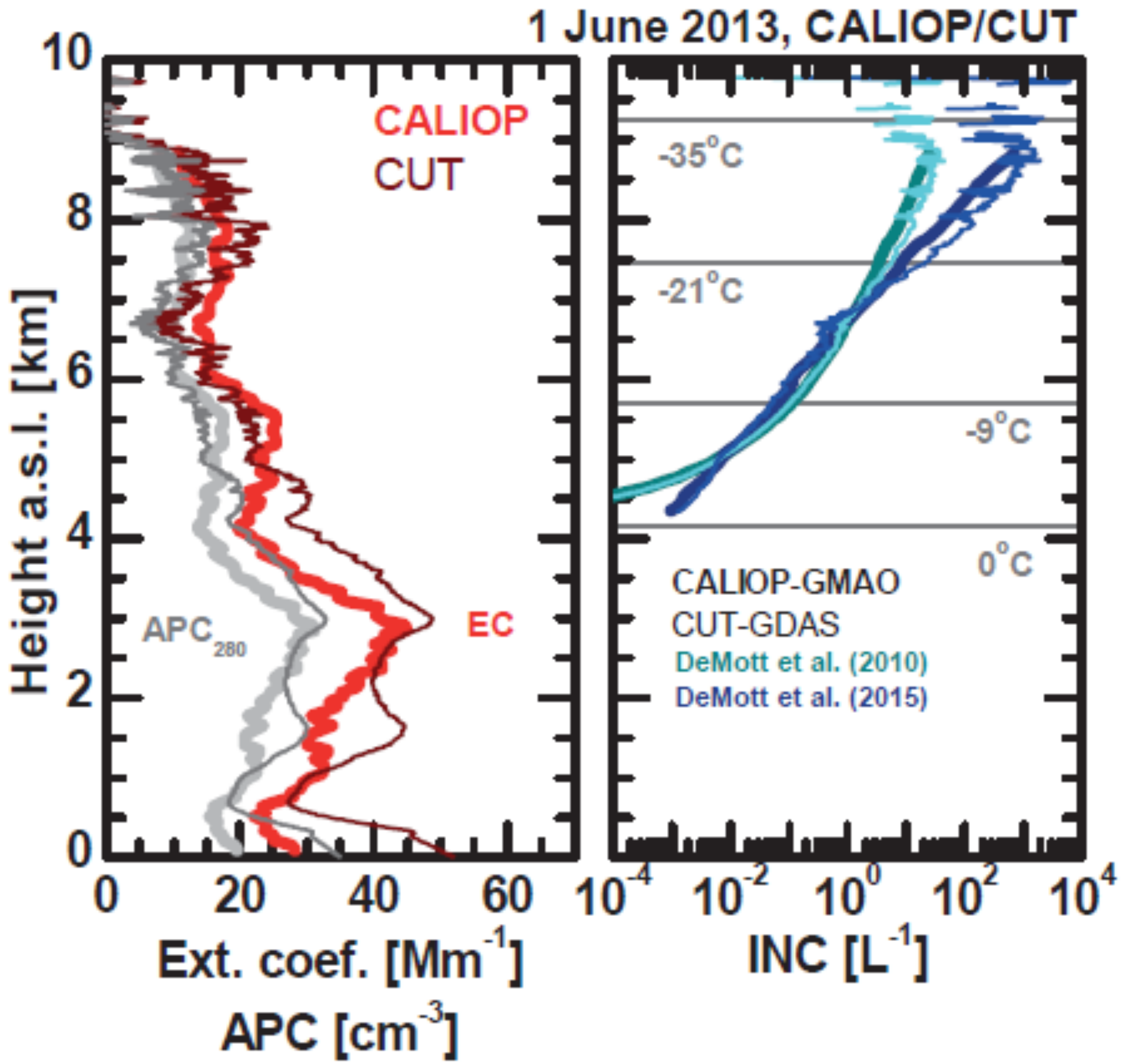

EARLINET

European Aerosol Research Lidar Network

spalinet

Spanish and Portuguese Aerosol Lidar Network

ACTRIS

***A**erosols, **C**louds, and **T**race gases **R**esearch **I**nfra**S**tructure Network*

Latin American Lidar Network

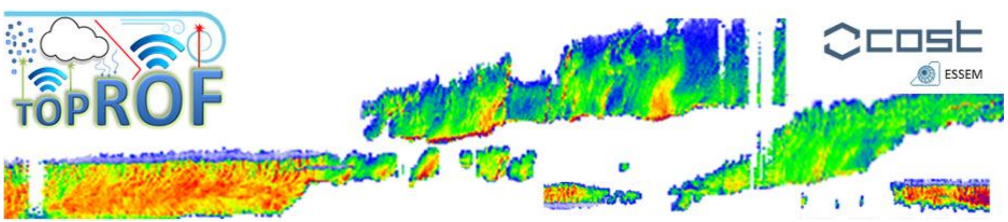

Towards operational ground based profiling with ceilometers, Doppler lidars and microwave radiometers for improving weather forecasts (COST ACTION ToProf ES1303)

IISTA

USP

IFUSP

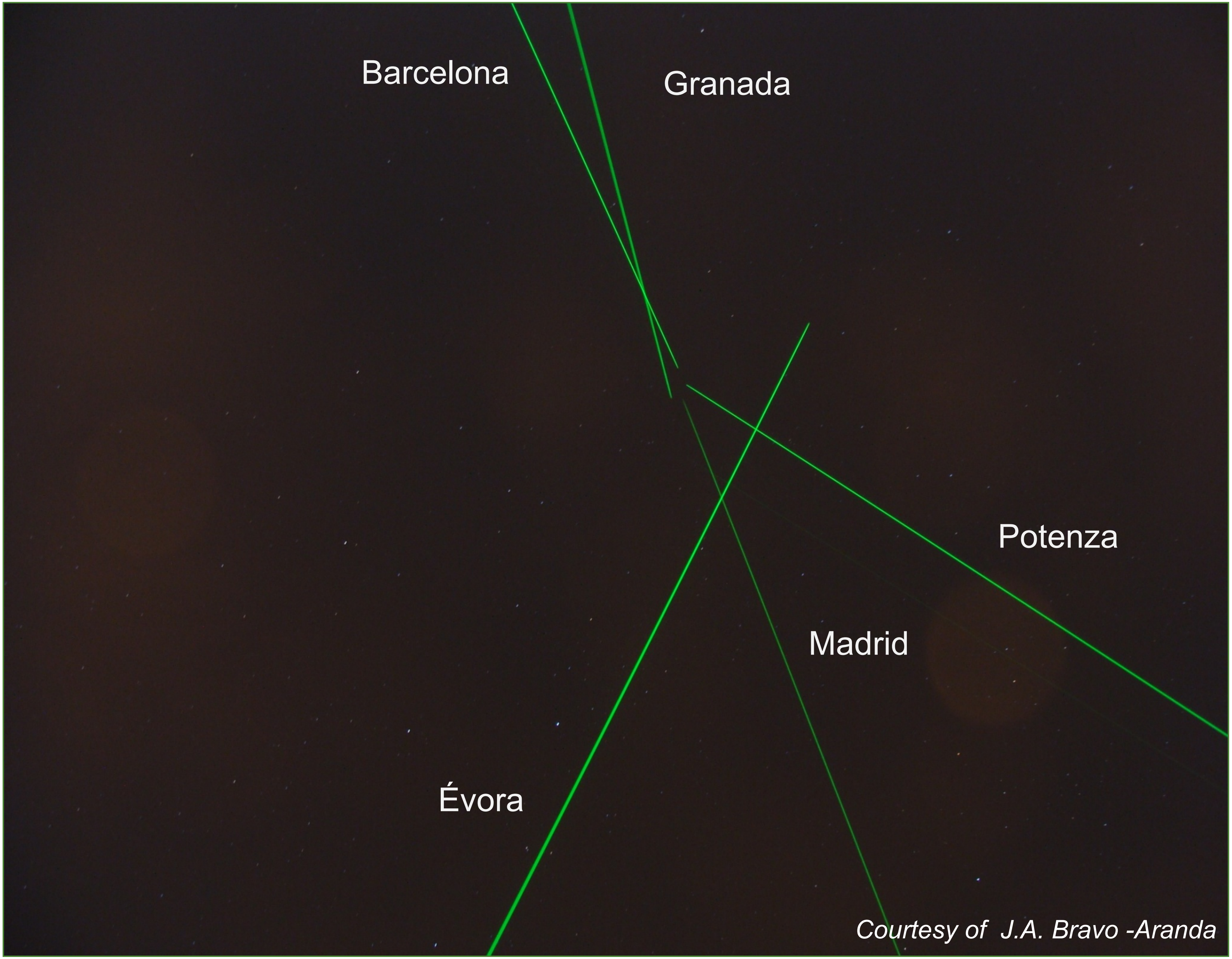

Courtesy of J.A. Bravo -Aranda